RHODES UNIVERSITY

Where leaders learn

Graphite:

Origin, Deposits and Economics

- An Exploration Study of the Orom Graphite Project

by

Jacobus Petrus van den Berg

A thesis submitted in partial
fulfilment of the requirements for the
degree of
MSc Exploration Geology

MSc Exploration Geology Program
Geology Department
Rhodes University
South Africa

March 2018

Acknowledgements

Firstly, I would like to thank Minrom Consulting services for providing me with the platform from which my exploration adventure was launched, particularly Oscar van Antwerpen, Minrom's director. I would also like to thank my colleague on the Orom Graphite exploration project, Ross Lewis, without whom the project would have been an un- successful and un-eventful event.

A special thanks to Prof R.E. Harmer for his patience, supervision and guidance during my dissertation and for his effort with the structuring of the exploration MSc course which already proved valuable.

I would also like to thank Ms Ashley Goddard, the Exploration Geology Secretary, for her unconditional administrative support during the course work, and for her organisational skills which provided memorable field trips.

Finally, I would like to thank my parents, without whom I would have never accomplished this MSc study. I would like to dedicate this study to my father who first suggested I pursue studies in geology.

Declaration

I, JP van den Berg declare this dissertation to be my own work. It is submitted in fulfilment to the Degree of Master of Science at Rhodes University. It has not been submitted before for any degree of examination on any other University or tertiary institution.

Signature of the candidate: 

Date: 16/03/2018

Abstract

Keywords: Graphite Exploration, Economics, Project management, Origins of Graphite.

Developing exploration projects successfully requires that the Reasonable Prospects for Eventual Economic Extraction (RPEEE) be confirmed and based on the global market perception and trend. The exploration methods applied in the attempt to establish this RPEEE must be based on a key management framework that assures the results, and eventually the conclusion, are obtained with best practical and technical approaches whilst managing the risks and capitalizing on each result.

The Orom Graphite project is located within the East African Orogenic belt, a suture zone between the Congo craton and the SLAMIN shield, formed during the formation of Gondwana during the late Proterozoic to early-Phanerozoic era. The closing of the Mozambique ocean, and the eventual collision between the craton and shield, occurred along the paleo-earths equator and migrated towards lower latitudes. This, along with the period's biodiversity boom, provided the perfect deposition environment for carbonaceous sediments which were later metamorphosed to amphibolite and granulites grade metamorphism, resulting in the carbonization and the eventual graphitization of these carbonaceous sediments. The project is located within a poorly developed part of Uganda with the closest port situated some 1 500 km to the east in Kenya. The poorly developed infrastructure along with probable high logistical cost assigns a low competitivity index if compared to the economic costs of peer projects. However, the potential resources of the Orom Graphite project suggest that the Life of Mine (LOM) can rival the largest resource currently reported within the market. The current market conditions suggest that a possible oversupply of graphite concentrate will dominate the market within the next 4 to 10 years. This suggests that new graphite projects such as the Orom Graphite project are likely to develop into the production phase once the global supply and demand stabilize. This requires the Orom Graphite project to develop from its current scoping study level to a project development study level associated with a definitive feasibility study. To date, the project developed through mapping, reconnaissance drilling, geophysical survey and trenching programs increasing the Net Present Value (NPV) considerably based upon a Cost-Based Valuation approach using Prospectivity Enhancement Multiplier (PEM). The metallurgical studies could however not produce a graphite concentrate product within industrial grade standards. The risk associated with developing the project further into the Mineral Resource Estimation (MRE) phase was quantified and risk was evaluated by implementing a point decision tree and calculating the Expected Monetary Value (EMV). Due to the unfavourable metallurgical results obtained to date, the risk associated with undertaking an additional metallurgical test is considerable with a slight chance of producing a negative project value estimated at 65%.

Overall, the Orom Graphite project contains favourable geological formations with a potential large resource. Market trends indicate that a considerable resource is currently being developed and can supply the global market for the next 4 to 10 years. The project's location within a landlocked country decreases its economic competitiveness with peer project and the unfavourable, but not conclusive, metallurgical results obtained during the scoping phase do not instil confidence that the project will develop into a productive mine soon. Managing the project development with future graphite demand in mind is the key to determining whether the project still has future value.

1. Contents

List of Figures

List of Tables

1 INTRODUCTION

1.1 Background (Exploration)

The search for mineral commodities is a costly and risky endeavour which can easily be side-tracked or mismanaged. The continued growth of the world markets requires the continued search for mineral resources which can replace currently exploited mineral reserves. The mineral exploration techniques used throughout the ages have revealed most of all the large near surface mineral deposits, resulting the new exploration techniques pushing the boundaries to discover deeper and more isolated mineralisation bodies. This resulted in exploration programs becoming increasingly more expensive with the associated risks also increasing. This trend can be observed within the gold exploration environment. Figure 1 reveals that 134 major discoveries were made within ten years (1990 – 2000) with an allocated exploration budget of 12.95 billion USD, whilst the next fifteen years only produced 106 major gold discoveries with an exploration budget of 38.5 billion USD. This suggests that the initial projects require on average 96.6 million USD to be discovered whilst the discoveries made from 2001 to 2015 required 363.2 million USD per discovery. Working in conditions that require ever increasing capital and a decreasing likelihood of success requires the basic exploration management principles and techniques to adapt accordingly.

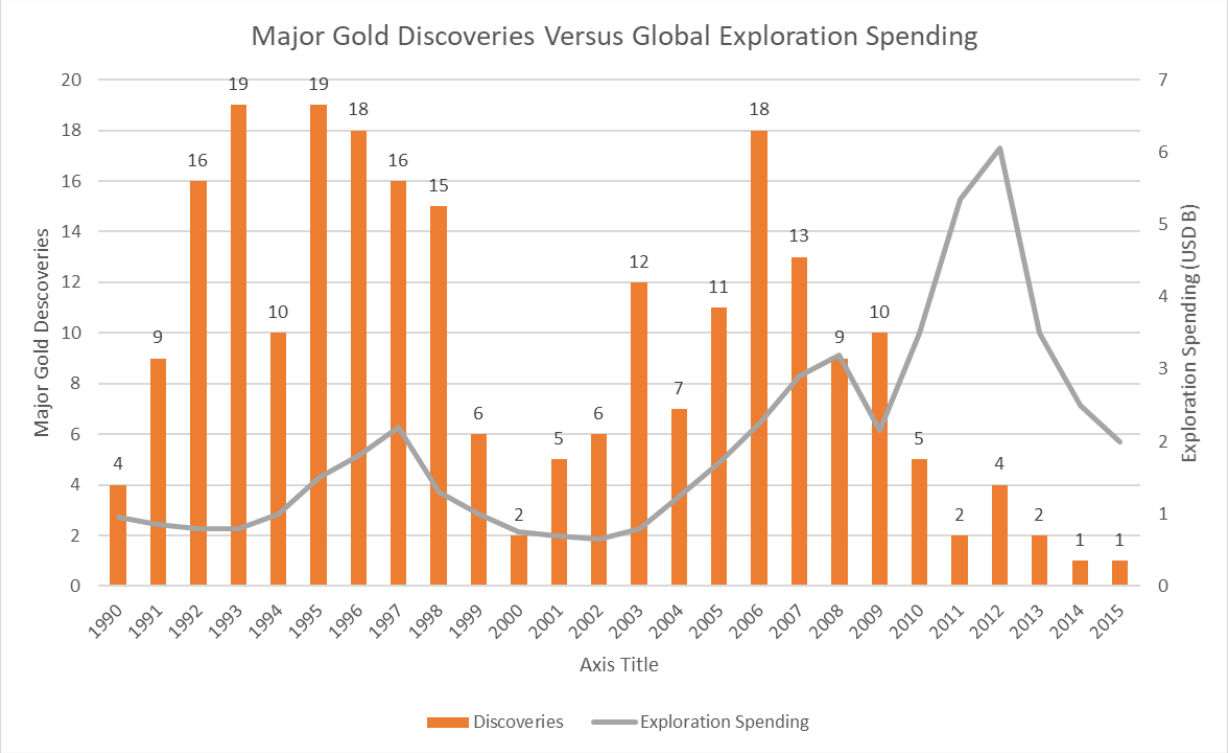

Figure 1 – Image illustrating gold exploration budget increase related to the amount of major new discoveries being made. Data obtained from Moore, (2016)

1.2 Objective and approach

The complex nature of developing an exploration project successfully requires a keen sense of understanding the commodity based on numerous fields. It should be noted that the sentence "developing an exploration project successfully" does not mean that the exploration project will develop into a productive mine. It rather means that the conclusion of an exploration project, whether it develops into a mine or whether it is abandoned due to poor results, is made at the earliest indication thus minimizing over expenditure and project mismanagement.

This study will endeavour to identify the primary fields associated with graphite exploration in an attempt to improve the management skills of future graphite exploration programs and implement the base principles within other exploration projects. The base principles include the following:

- Geology and mineralisation occurrences: Understanding the basic geological formations and conditions required to form a specific deposit. In this case it included identifying the origin of carbon within sediments, the likely conditions under which graphite formed and the most likely present-day locations which adhere to these geological and mineralisation conditions.
- Graphite market relationships and global market trends: The global mineral commodities demand is the primary drive for exploration. Identifying the possible market relationships and trends forms the base of each exploration project and will form the key criteria on whether a commodity can be extracted within economic parameters.
- Economics and financial aspects of graphite projects: Economic and financial parameters of peer projects can aid in evaluating and valuating an exploration project. Comparing both the economic (resource and grades) and the financial (Capex, Opex, etc.) parameters with those of peer projects can indicate whether the exploration project under investigation can compete in a competitive market.
- Project Management: The project's expectations and risks must be identified early in the project development phase in order to successfully manage the project's development and results. This requires that the principles listed form the parameters used to guide the project's development whilst managing the risks within a controlled environment.

1.3 Case Study

The Orom Graphite project is located in the north-eastern corner of Uganda, 110 km east of Kitgum. Graphite mineralisation was identified during numerous exploration programs conducted from 1962 to 1969 which investigating a zinc, nickel, copper anomaly found by regional soil sampling.

The project is located within the Northern Uganda Terrane containing the Mesoarchean Karuma- and Karamoja-Complex, Neoarchean Amuru Group and Neoproterozoic West Karamoja Group. The graphitic mineralisation occurs within the Orom Formation of the West Karamoa Group. This sedimentary sequence was subjected to upper amphibolite to granulite metamorphic conditions with local intrusions bringing an influx of heat.

The initial scoping study was initiated in 2015 and included mapping, pitting, trenching, drilling and geophysical programs. The mapping, pitting, trenching and geophysical programs were implemented in order to delineate the lateral extent of the graphite mineralisation. A total of 6 bore holes was drilled to a maximum depth of 120 m and established the weathering profile along with vertical mineralisation extents.

By using the principles listed in the previous section, the Orom Graphite project will be evaluated based on the geological environment, market requirements and project management needed to further develop the project successfully.

2 GRAPHITE CHARACTERISTICS AND ORIGIN

2.1 Graphite Characteristics

Carbon exists in nature as a number of allotropes and can be found in the earth's lithosphere, hydrosphere and atmosphere as solid, liquid, and gaseous state molecules and structures. These different carbon allotropes can migrate between these physical states when subjected to different chemical or physical conditions. Carbon is present in the atmosphere as carbon dioxide (CO_2). Atmospheric carbon dioxide reacts with water to produce bicarbonate (HCO_3^-) which is then used by plants, bacteria and algae as a source of energy in cellular reparation, and is later, at the time of their death, converted back into carbon dioxide. This is commonly referred to as the carbon cycle. In anoxic environments, organic carbon or bicarbonate are prevented from being oxidised to carbon dioxide. If anoxic conditions persist, sedimentation and diagenesis will eventually lock the carbon into the rock formation. If these carbon-rich rocks are subsequently subjected to high grade metamorphic conditions, the elevated pressures and temperatures will progressively change the structure of the carbon molecules in the carbonaceous sediments to lignite, anthracite, graphite and, at extreme P,T, diamond carbon structures (Pasteris, 1999).

Graphite is a grey-black opaque mineral with a metallic lustre and is relatively soft (1–2 on the Mohs hardness scale). Its distinguishing characteristics are its greasy feel, low density (2.09–2.23 g/cm^3), high resistance to thermal shock and high electric conductivity (Simandl, Paradis and Akam, 2015). These characteristics form the key ingredient in refractories, foundry, lubricants and in the electronic industry.

2.2 Geological Origins

The origin of the carbon molecules within graphite's atomic structure can be traced back to a reducing paleo-sedimentary environment producing carbonate or organic carbon rich sediments. In order for graphite to form, the sedimentary carbon must be subjected to conditions that remove impurities such as oxygen, hydrogen or sulphide, which are bound to the carbon molecules, thus allowing the carbon to be restructured into a platy molecular mass consisting of pure graphitic carbon.

2.2.1 Classification of Graphite Deposits

Graphite is a common accessory mineral within meta-sedimentary formations. In sufficient quantities, these meta-sediments can host three classes of graphite deposits. These three classes are primarily a function of metamorphic conditions under which the graphite formed (Figure 2) and are: 1) microcrystalline, 2) crystalline flake and 3) vein type graphite which includes lumps and chips (Simandl and Kenan, 1998a, 1998b, 1998c). Table 1 summarizes the key attributes of each deposit class.

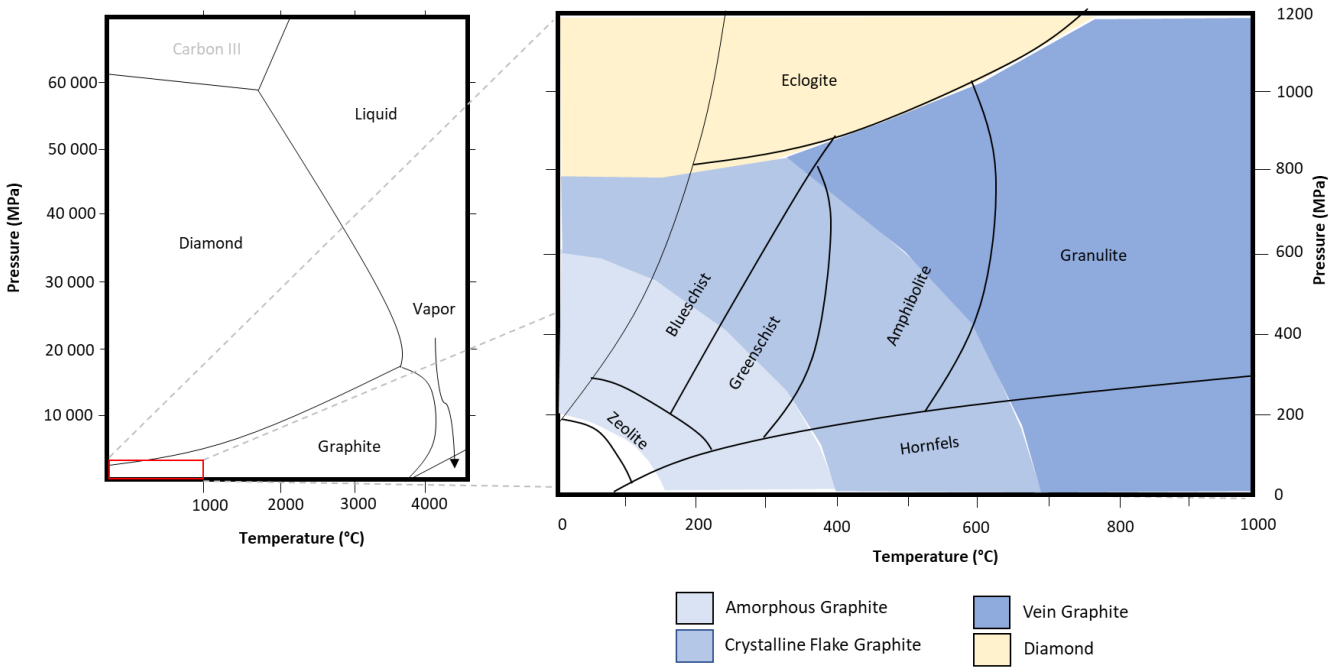

Figure 2 – LEFT: Carbon stability diagram illustrated on a pressure vs temperature diagram (Image obtained and modified from Bundy et al., (1996) . Right: Metamorphic facies diagram indicating possible graphite deposit type occurrences based on metamorphic grades (Metamorphic facies diagram modified from Punchuk, (2017)).

I. Microcrystalline (Amorphous) graphite deposits

Microcrystalline graphite, commonly known as amorphous graphite, is found within low greenschist metamorphic facies conditions usually associated with contact metamorphism or low grade regional metamorphism of carbonaceous rich sedimentary units.

Such deposits generally consist of fine stringers or bands of flaky graphite with numerous low grade metamorphic gangue minerals. These deposits can occur in a variety of shapes as commonly observed within deformation and metamorphic environments. Graphite mineralisation from these deposits is generally hand sorted and milled for use in applications which can tolerate higher ash (impurity) content (Simandl and Kenan, 1998b; Simandl, Paradis and Akam, 2015).

II. Crystalline Flake Graphite Deposits

Crystalline - or natural - flake graphite is found within metamorphic terranes that were subjected to upper amphibolite to granulite facies metamorphism and can occur in a diverse range of carbonaceous meta-sediments such as marbles, paragneisses, iron formations and quartzites. Some occurrences of crystalline flake graphite are also found within pegmatites, syenites and in some rare cases, serpentinized ultramafic rocks. Deposits of crystalline flake graphite occur as highly deformed, stratabound, continuous to lens-shaped mineralised bodies and are typically mined using open pit mining techniques. The graphite flakes are generally greater than 75 microns (µm) in size and can

reach sizes greater than 500 µm. Liberation of the graphite flakes from the gangue minerals involves numerous crushing, milling and flotation stages which, if implemented correctly, can produce up to 90% graphitic carbon grades at recoveries of 90% and greater whilst retaining the graphite flakes intact (Simandl and Kenan, 1998a).

III. Vein Graphite Deposits

Vein type graphite, also referred to as epigenetic graphite, is found within similar metamorphic environments as crystalline flake graphite but is associated with higher temperature conditions than the crystalline flake graphite. These deposits can resemble skarn-type assemblages in close proximity to igneous intrusions and can be found within igneous intrusions or in metamorphic zones with a retrograde overprint. This type of deposit is generally mined by means of low tonnage underground mining methods, following stockworks or anastomosing veinlets. The graphite product typically consists of graphite fragments between 0.5 to 0.8 cm in diameter and is referred to as lump graphite. The current known deposits supplying lump graphite are located in unstable social and political countries, resulting in the graphite industries favouring crystalline flake graphite over vein type graphite and modified industrial processes accordingly (Simandl and Kenan, 1998c; Simandl, Paradis and Akam, 2015).

Table 1 – Graphite deposit classifications and characteristics according to Simandl and Kenan, (1998a, 1998b, 1998c)

Deposit Classes	Microcrystalline	Crystalline	Vein
Tectonic Setting	Continental Margin and intracratonic basin	Continental Margin and intracratonic basin	High pressure and temperature metamorphic environment associated with igneous activity.
Geological Setting	Carbonaceous sedimentary rocks, sedimentary rocks with intercalated coal seams which have been metamorphosed by igneous intrusions or low grade regional metamorphism.	Metasedimentary belts of granulite or upper amphibolite facies metamorphism.	Meta-sedimentary belt with invading intrusive producing high-grade, dynamothermal metamorphic conditions.
Age of Mineralisation	Lower Carboniferous to Cretaceous or younger	Generally Precambrian	Generally Precambrian
Host/Associated Rock Types	Chlorite to muscovite schist, phyllites, quartzites, metagreywackes, limestones, sandstones and conglomerates. Coal seams or carbonaceous rich rock formations. Usually closely associated with igneous rocks.	Marble, paragneisses, quartzites, magnetite-graphite iron formations, clinopyroxenites, amphibolites and pegmatites. Associated rock formations include orthogneisses, charnockites, orthopyroxenites, amphibolites, granulites and various intrusive rocks.	Paragneisses, quartzites, clinopyroxenites, wollastonite-rich rocks, pegmatites.

Deposit Form	Stratiform or lens-shaped. Strike length can be meters to several kilometres.	Stratiform lens-shaped to saddle-shaped.	Vein can be millimetres to meters thick but generally less than 0.3 cm in thickness. Anastomosing, lens-, pod-, or saddle-shaped.
Textures/Structures	Schistose or massive.	Strong foliation, schistosity and lepidoblastic texture in paragneiss and schists. Granoblastic, equigranular or porphyroblastic texture in marbles.	Rosette, coarse flakes.
Associated Gangue Minerals	Meta-anthracite, anthracite, quartz, mica, coke, clay, pyrite and other sulphides, apatite, gypsum.	Carbonate-host rocks: calcite, clinopyroxene, pyrite and other sulphides with accessory minerals including dolomite, anorthosite, chlorite, clinozoisite, zoisite, garnet. In paragneisses: feldspar, quartz, biotite with accessory minerals including clinopyroxene, garnet, sillimanite, kyanite, sulphides, clinozoisite, scapolite and secondary gypsum.	Marble or Skarn: calcite with accessory minerals of wollastonite, hedenbergite, zoisite, clinozoisite, prehnite, quartz, titanite, sulphide, diopsides, scapolite. Meta-sediments: feldspar with accessory minerals of apatite, garnets, scapolite, biotite, sillimanite, secondary iron oxides.
Alteration Minerals	N/A	Chlorite, prehnite, zoisite and clinozoisite	No distinguishable alteration visible due to high nature of metamorphism required to form these vein-type deposits.
Ore Control	Carbonaceous sediments invaded by intrusive rocks imposing a greenschist metamorphic facies environment. Graphitization function of metamorphism with graphite grading into coal with distance from intrusion. Temperature required for graphitization lower under higher pressure such as in shear systems.	Low grade, large tonnage deposits generally hosted in paragneisses with higher grade portions structurally controlled, occurring in fold hinges.	Forms along joints, breccia zones, crests of folds, decollements along geological contacts and foliations.
Typical Grade and Tonnage	Average size and grade: 4 900 000 tonnes @ 55% to 80% carbon (Bliss and Sutphin, 1992)	Average grade and size: 2 400 000 tonnes @ 9% graphitic carbon (Bliss and Sutphin, 1992).	Varied tonnage data. Generally, high grades ranging between 40 to 90% graphitic carbon. (Bliss and Sutphin, 1992).

2.2.2 Depositional Environments

Sedimentary deposits rich in carbon can occur in a number of sedimentary environments including 1) carbonate platform and basin environments and 2) organic carbon sedimentary environments. These sedimentary environments are usually associated, but not limited, to passive continental margins with low energy, anoxic, fluvial or marine deposition mechanisms within a rich biological habitat. Carbonate

sediments usually occur as thick laterally extensive strata and are associated with tidal or evaporate sedimentary facies deposits, whereas organic rich sediments such as black shales dominantly occur in deep oceanic sediment facies deposits or fresh water braided river systems and swamps. The source of carbon in both carbonate and organic carbon sediments is highly dependent on biological activity. The Earth's biological history started in the Archean eon with the first known micro-organism fossils found in rock formations. However, the biodiversity boom related to the early Proterozoic eon is of more importance to identifying possible carbonaceous sediments as this period saw the largest increase in oxygen and bio-diversity levels (Figure 3). Combining the large biodiversity boom with a high sedimentary deposition rate provides adequate conditions for the formation of carbonaceous lithologies within a timeframe that can be metamorphosed.

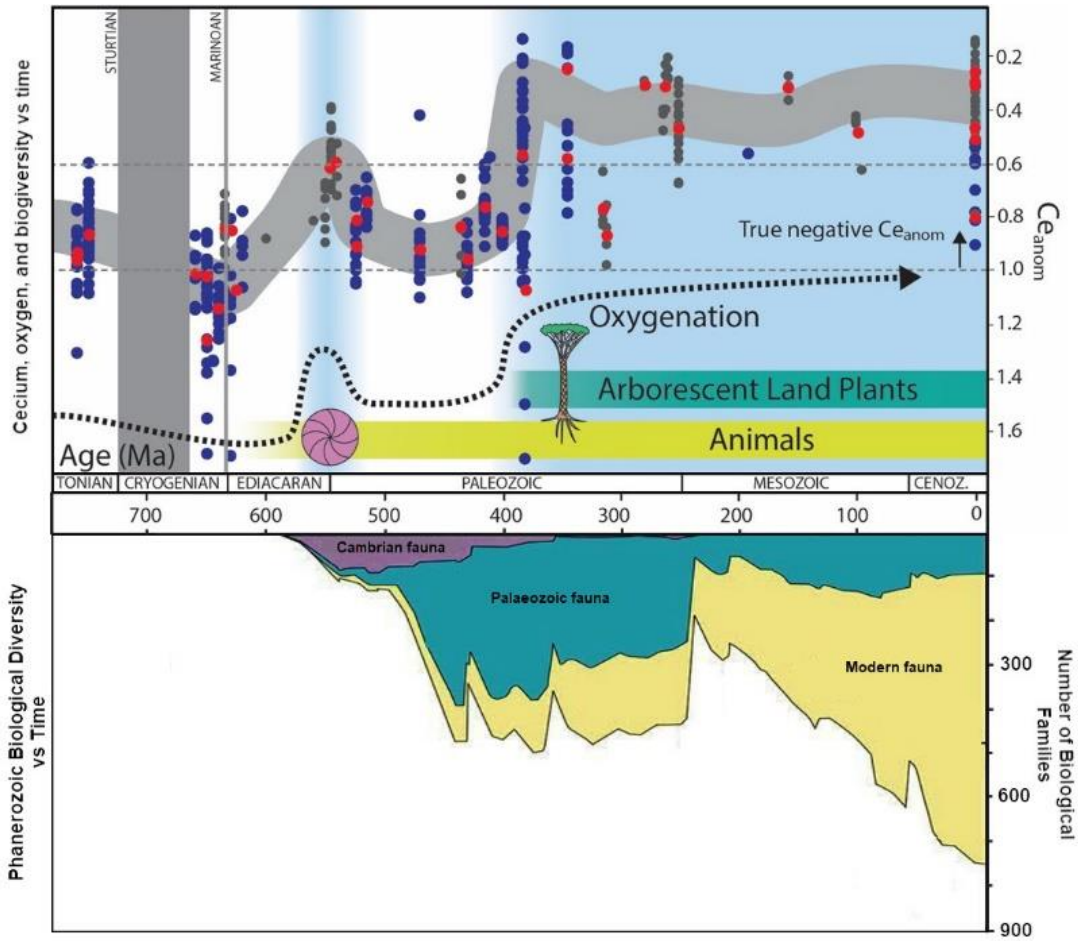

Figure 3 – Phanerozoic biological diversity, oxygen, ad cerium levels. TOP: Oxygen and cerium ion ratios compared to present day ratios indicating a major oxygenation event during the early Proterozoic eon. Image obtained from (Wallace et al., 2017). BOTTOM: Number of biological diverse families during the Proterozoic eon. Image obtained from (Barnosky et al., 2011).

I. Carbonate Carbon Deposition Environment

Carbonate sedimentary deposits can be found in a number of deposition environments where the calcium carbonate, originating from biological sources, accumulates into sedimentary strata. The

abundance of carbonaceous sediments is directly associated with the abundance of organisms and thus the conditions promoting organism growth such as water depth, temperature, salinity, nutrient availability and the supply of terrigenous clastic material. These sedimentary deposition environments usually contain a higher organic carbon to carbonaceous carbon ratio, whereas carbonaceous sediments formed from evaporites in more arid regions tend to contain a lower organic carbon to carbonaceous carbon ratio (Nichols, 2009). Sloss (1947) described the depositional environments according to two categories namely 1) Platform Carbonaceous Sediments and 2) Basin Carbonaceous Sediments.

i. Platform Carbonaceous Sediments

Carbonaceous sediments deposited within platform deposition environments form on peneplain passive continental margins within the shallow marine water, where the sedimentary transport rate is low, thus limiting the proportion of clastic sediments. The climate at which the deposition occurs greatly affect the formation of the grains with respect to the size and shape and determines the type of carbonaceous organisms which dominate the sedimentary environment. These factors will later affect the metamorphism, carbonization and graphitization of the carbonaceous sediments. These carbonaceous sedimentary deposits generally occur along coastal deposition environment such as beaches, beach barriers, lagoons and supratidal and intertidal zones. Shallow marine deposition environments include carbonate sand shoals, reefs, carbonate mud mount, and outer shelf and ramp (Nichols, 2009). These carbonaceous sediments generally contain a light colour, stratigraphically thin sedimentary secession covering a wide areal extent (Sloss, 1947).

ii. Basin Carbonaceous Sediments

Basinal carbonaceous sedimentary deposits can occur as platform evaporates and saline giant basins. Platform basinal depositions occur in arid regions where the circulation on the inner ramp/shelf can lead to the formation of platform ramp evaporate carbonaceous sediments. Saline giant basins refer to a body of water which has become isolated from marine waters. The salinity of the trapped body of water becomes saturated to the point where chemical precipitation of minerals occurs. These saline giant carbonaceous deposits can produce thick (1000 m thick) evaporate sedimentary deposits.

II. Organic Carbon Deposition Environment

Organic carbon rich sediment is deposited in a number of paleoenvironments ranging from braided river systems, continental basins and lakes, deltaic river systems and deep marine deposition environments. The source of the organic carbon can be from dead plants, animals and microbial organisms. For organic carbon to be trapped and stored in sediments, the paleoenvironmental conditions have to be of such nature that it promotes a slow decomposition rate, a high burial rate,

or a combination of the two. Continental deposition environments where oxygenizing conditions prevail require that the burial rate becomes the dominant factor for storing organic carbon in the sediments. In contrast, anoxic conditions require a slower burial rate than the pre-mentioned rate such as in deep lakes or glacial systems where low water circulation causes an anoxic layer to occur. The primary factor influencing the deposition of organic rich sediments in deep marine environments is due to poor circulation as a result of depth. These sedimentary depositions usually occur beyond the continental shelf within the abyssal marine realm and are associated with black shales which can contain 1 – 15% organic carbon (Arthur and Sageman, 1994).

2.2.3 Burial and Metamorphism

It has long been the consensus amongst geologists that syngenetic (microcrystalline and crystalline type deposits) and epigenetic (vein type deposits) flake graphite deposits were formed by either 1) maturation (carbonization) and metamorphism (graphitization) of organic or carbonaceous material or 2) graphite precipitation from C-O-H fluids as a result of changes in the pressure, temperature or chemical reaction of the carbon fluid with the host rock.

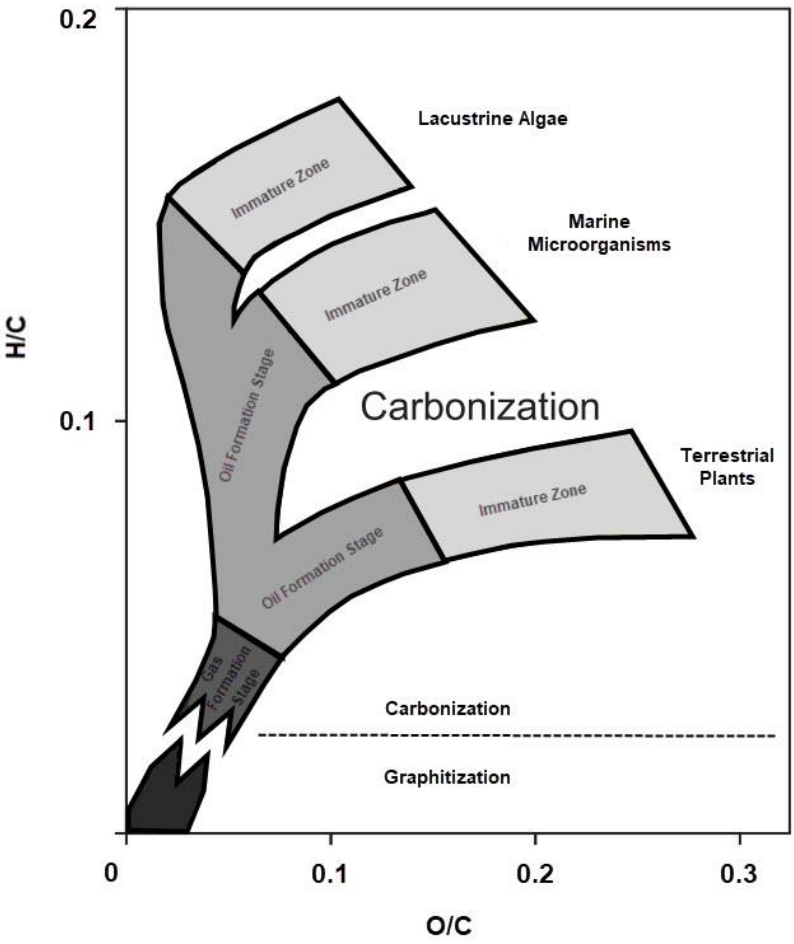

Figure 4 - Organic carbon material maturation and graphitization in term of H/C and O/C atom ratios. Modified from Simandl et al. (2015); based on data of (Grew, E, 1974)

Numerous hydrogen, oxygen and carbon isotope studies (Grew, E, 1974; Wopenka and Pasteris, 1993; Pasteris, 1999; Buseck and Beyssac, 2014) have defined the chemical and physical changes occurring during the metamorphism of organic material from numerous sedimentary deposition environments to graphite. These studies focused on lacustrine algae (H/C > 1.25), marine micro-organisms (1.1 < H/C <1.5) and terrestrial plants or coal deposits (H/C < 1), each containing different H/C and O/C atomic ratios. As the organic carbon sediments are buried, diagenetic processes (<200° and <3kb) (Figure 2) compact the carbon material

and force hydrocarbon oils and gasses from the carbon particles, leaving carbon-enriched residue within the compressed rock formation. A further increase in the pressure and temperature (>200°C and >3kb) associated with hornfels and greenschist metamorphic facies conditions can produce microcrystalline graphite deposits. As the pressure and temperature conditions reach amphibolite to granulite facies metamorphism, the hydrocarbon component is virtually completely removed from the organic carbon, with the carbon atoms rearranged into plate structures referred to as graphitic carbon. The process of hydrocarbons being forcibly removed from the organic material is referred to as carbonization whereas the restructuring of the carbon atomic into graphite is termed graphitization (Grew, E, 1974; Simandl, Paradis and Akam, 2015). As the organic carbon undergoes carbonization and eventually graphitization, the hydroxyl (OH) component is progressively lost. This results in the homogenisation of graphitic carbon with respect to the H/C and O/C ratio, effectively eliminating the ability to trace the origin of the carbon. This is well illustrated in Figure 4 .

Epigenetic graphite occurs notably within higher temperature and pressure environments resembling that of granulite facies metamorphism. These graphite occurrences indicate that graphite can migrate within a solution. Hahn-Weinheimer & Hirner (1981) and Weis et al. (1981) studied epigenetic graphite and the mobility of carbon in country rocks when subjected to increasing temperatures (700 – 900°C) and pressures. At these higher pressures and temperatures, a fluid/gas reaction occurs between the H-O-C molecules ($C + H_2O \rightarrow CO + H_2$) (Weis, Friedman and Gleason, 1981). CO then decomposes by the Boudouard reaction ($2CO \rightarrow C + CO_2$) at temperatures between 50 – 100°C and precipitates epigenetic graphite (Hahn-Weinheimer and Hirner, 1981).

Carbon's mobility in fluids can also be explained using C-O-H ternary diagrams (Figure 5 & Figure 6). These diagrams assume ideal mixing conditions with temperature, pressure and carbon concentration being

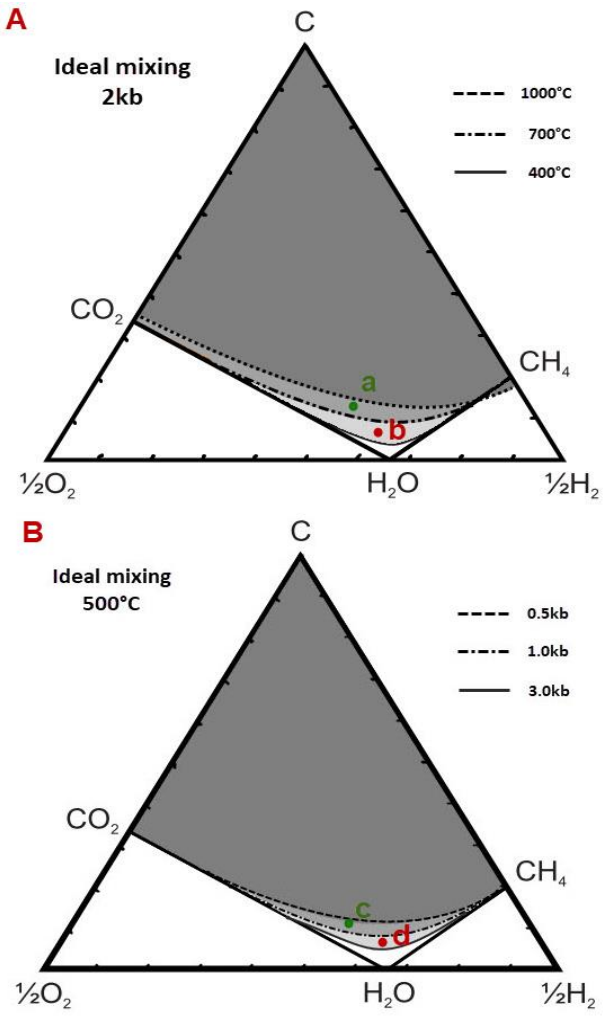

Figure 5 - Ternary C-O-H diagram. A: Graphite stability field in decreasing temperature from 1000°C to 400°C at a constant pressure of 2kb (assuming ideal mixing) with composition fluid composition "a" and "b". B: Graphite stability fields with decreasing pressures from 3.0kb to 0.5kb at constant temperature of 500°C (assuming ideal mixing) with fluid composition "c" and "d". Diagrams obtained from Ferry and Baumgartner, (1987)

the variable. At a constant pressure, the stability field of graphite increases with a decreased temperature. Figure 5A illustrates two fluids with different C-O-H compositions at constant pressure. As the C-O-H fluid cools, composition "a" will precipitate graphite at a temperature below 1000°C, whereas a fluid at C-O-H composition "b" will start to precipitate graphite at temperatures below 700°C. At constant a temperature (Figure 5B) graphite's stability field will increase with an increase in pressure. A carbon rich fluid (point "c" of Figure 5B) will start precipitating graphite at pressures greater than 0.5kb and at 500°C, whereas a slightly carbon poor fluid (point "d" of Figure 5B) will start precipitating graphite at pressures greater than 1.0kb at 500°C. Graphite precipitation can also occur with fluid mixing at constant temperature and pressure. Figure 6 illustrates the behaviour of a carbon containing fluid at 600°C and 5kb. A fluid with the composition at point A of Figure 6 will precipitate graphite along the tie lines. As graphite precipitates, the fluid composition will decrease in carbon until the fluid concentration reaches the graphite saturation curve and stops precipitating graphite. Further graphite precipitation can occur if the pressure increases, the temperature decreases or a fluid rich in carbon is mixed with the carbon poor fluid (or a combination of the factors mentioned above). Graphite precipitation can also occur with two C-O-H fluids which individually do not fall under the same temperature and pressure conditions - but do if mixed. For example, assume the composition of fluid C mix with fluid B (Figure 6). The composition of the mixed fluid will migrate towards the graphite saturation curve and precipitation of graphite will occur. The precipitation of graphite will continue as long as the carbon concentrations remains within the graphite stability field (Ferry and Baumgartner, 1987).

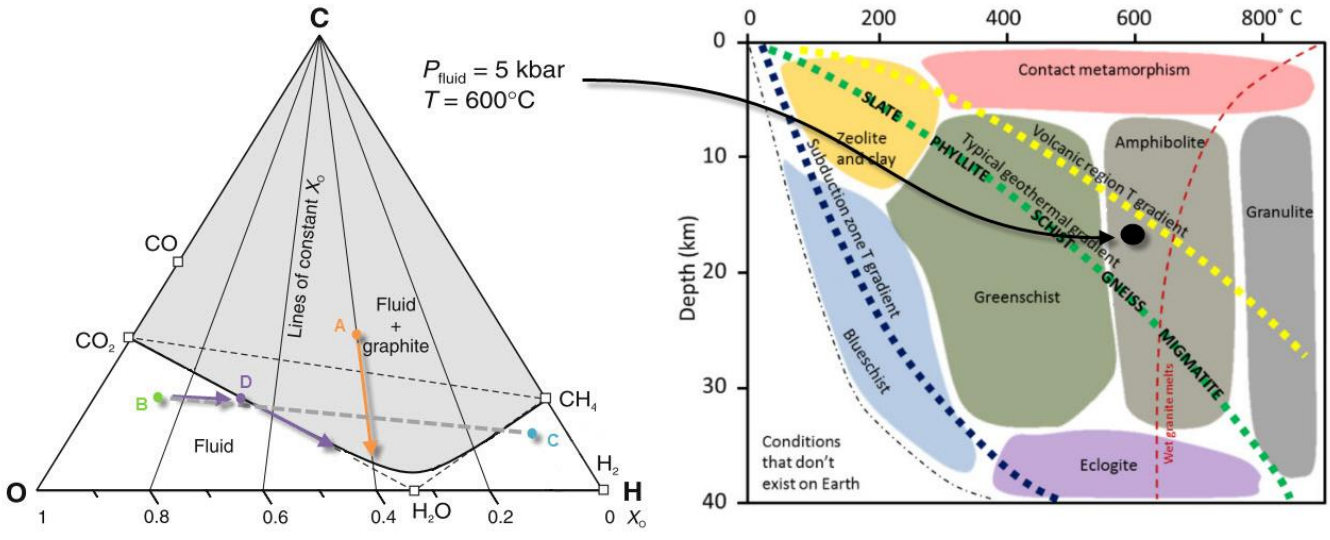

Figure 6 – Ternary C-O-H diagram at 600°C and 3.5kb amphibolite metamorphic facies conditions. Fluids A illustrates the precipitation of a carbon rich fluid whilst fluids B and C contain different compositions and illustrate the mixing reaction and its effect. Modified from Ferry and Baumgartner (1987)

3 GLOBAL GRAPHITE MARKET AND USES

The following chapter deals with the ever-changing graphite market and focusses on the graphite's applications, historical and future supply and demand. As such, the sources of the data are generally obtained from market reviews (Hykawy and Chudnovsky, 2014; Scogings and Chesters, 2014; Scogings, Chesters and Shaw, 2015; Basson, 2017), opinions (Kramer-miller, 2015; Scogings, 2016; Jeff Desjardins, 2017; Struthers, 2017) and presentations (Shaw, 2015). The historical global graphite supply data was primarily obtained from the USGS webpage under the graphite section (*USGS Minerals Information: Graphite*). The resource and economical statements used in this section were compiled from data obtained from technical reports (if available) and company presentations made available to the public. It should be noted that the section does not include all the global graphite resources but rather a set of resources representing the graphite projects developed at the time of this dissertation's compilation and completion. As such, a number of resource updates and new discoveries could have occurred which can influence the data considerably. The list of company reports, announcements and presentations from which the resource data was sourced is recorded within the appendix section rather than being presented as citations. In addition, the predicted market trends are also based on market opinions and are presented in this dissertation as scenarios from which a platform can be based for future graphite exploration programs.

The industrial demand for graphite started over 100 years ago, finding application as a lubricant. The increase in construction and in steel demand during the early 1900s further intensified the demand for graphite due to its applications in the refractory industry and for steel production. This growth was directly related to the expansion of the global steel industry fuelled by both World Wars followed by the economic and infrastructure growth of the USA and Western Europe from the 1950s into the 1970s. During the 1980s and 1990s the graphite market continued to grow as a consequence of the Asian economic boom. Figure 7 illustrates how the demand for graphite is proportional to the global steel production. This suggests that the base demand for graphite will continue to follow global steel production whilst new graphite applications will increase the demand. This increase in demand is likely to grow in the technological industry due to the global quest for a cleaner and "greener" solutions to generating energy and efficiently storing it. This stimulated the research and the development of effective bulk energy storage media, specifically the development of the Li-ion battery which uses graphite as its main anode material. A unique feature of the graphite market is that one graphite application does not supersede another, thus demand builds as new applications for graphite are developed.

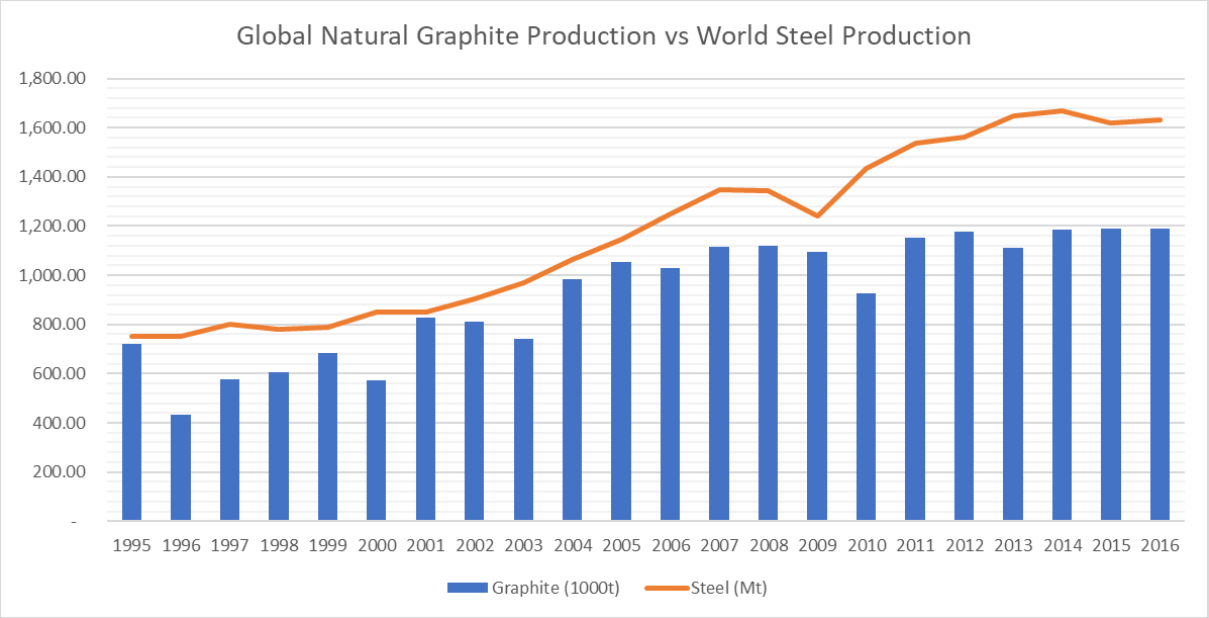

Figure 7 - World natural graphite production relative to world steel production. Source: USGS and Basson (World Steel Association" (2017)

3.1 Global Graphite Uses and Demand

In industry, graphite is generally used either as an essential part of an end product, or as a secondary ingredient used in the processing of another. Each of these products or production processes require graphite with specific characteristics such as purity (graphitic carbon vs organic carbon), flake size, moisture content and ash (impurity) content. This has created a market comprised of a number of sectors each requiring a different graphite product - as illustrated in Table 2. Commodities such as copper, gold and iron ore are marketed as uniform entities and thus contain a uniform price regardless of the location of the commodity. Flake graphite on the other hand, contains different graphite flake sizes and carbon purities which determine the price of the commodity.

The market price for these different graphite flakes is highly variable due to a relative closed market which is not controlled by a central dealing agency but is rather driven by seller-buyer contracts. The general consensus is that the graphite flake size has the largest impact on selling price, followed by the purity or contained graphitic carbon content of the individual flakes. Thus, larger flake graphite competes better in the graphite market than smaller flake graphite due to the greater range of industrial applications which can be serviced, as larger flakes can be reduced in size if required.

Table 2 - Graphite properties required by industrial Applications

Applications	Finished Grade (GC – Graphitic Carbon)	Flake sizes (Mesh)	Flake Size (Microns)
Refractory and Crucible Product Specs			
Refractories	85-90%GC	-50 +100	300 - 150 µm
Crucibles	85-90%GC	-100 +200	150 - 75 µm
Lubricants	95%GC	-50 +500	300 - 30 µm
Brake Linings, Gaskets, and Carbon Brushes Specs			
Brake Linings	95 - 98%GC	-200 +250	75 - 63 µm
Carbon Brushes	95 - 99%GC	-200 +250	75 - 63 µm
Gaskets	80 - 99.9%GC	-200 +250	75 - 63 µm
Powdered Metallurgy			
Powdered Metallurgy	95 - 99%GC	-10 +50	2000 - 300 µm
Battery Product Specs			
Alkaline	90 - 99.9%GC	-150 +250	95 - 63 µm
Lead Acid	90 - 95%GC	-250 +300	63 - 50 µm
Lithium Ion	99 - 99.9%GC	-300 +500	50 - 30 µm
Spherical Graphite [1]	99.9%GC	-100 +150	150 - 95 µm
Fuel Cells	99.9%GC	-100 +350	150 - 40 µm
Special Product Specs			
Expandable Graphite	90 - 99.9%GC	-50 +100	300 - 150 µm
Graphite Foils	85 - 94%GC	-50 +100	300 - 150 µm
Polymers	50 - 60%GC	-2500 +1000	5 - 15 µm
Graphite Ropes and Packing Materials	85 - 94%GC	-100 +150	150 - 95 µm
Graphite Parts	85 - 94%GC	-50 +100	300 - 150 µm
Graphite Blocks	85 - 94%GC	-150 +250	95 - 63 µm
Pencils	85 - 94%GC	-50 +100	300 - 150 µm
New Material Specs			
Nuclear Reactors	93 - 95%GC	-50 +100	300 - 150 µm
Construction Building Material	98 - 99%GC	-50 +100	300 - 150 µm
Graphene	98 - 99.9%GCC	-30 +50	600 - 300 µm

[1] Spherical Graphite processing can utilize all flake graphite sizes. The 100 to 150 mesh size is currently the preferred size used to produce spherical graphite due to the economic advantages rather than the physical properties.

3.1.1 Refractories

Graphite is used in refractories as an add-in product in the manufacturing of refractory stones such as magnesia-carbon and alumina-carbon bricks, as well as in crucibles. The thermal conductivity characteristics of graphite increase the thermal conductivity of these products and decrease the thermal gradient between hot and cold faces, thereby reducing the expansion of the products. Natural graphite used in this process usually consists of -50 to -150 mesh flakes having a graphitic carbon purity ranging between 94% to 98%.

3.1.2 Foundries

Graphite's unique thermal and cohesive characteristics makes it a required ingredient in water-based paints used on foundry facings. These unique characteristics aid in the hot metal mouldings and separation of the mould from the hot metal once cooled.

3.1.3 Lubricants

Graphite containing lubricants are used in both very high and low temperature applications, as for example in die forging, as an anti-seizing agent in gear lubricant in large machinery, as well as to lubricate locks.

3.1.4 Recarburising

Carbon is used in the manufacturing and production of steel alloys as a hardening agent. These steel alloys can contain from 0.3% carbon in low carbon steel products, to 0.6% in high carbon steel products. Natural graphite is used as a carbon supplement along with metallurgical coke and calcined petroleum. Although a number of carbon products can be used in the steel alloy manufacturing process, natural graphite has the advantage of having high carbon purity.

3.1.5 Batteries

The battery industry is recently welcomed renewed interest and investment due to ineffective energy storage capacity worldwide. Recent technology improvements have seen the electricity market shifting from a primary sodium-sulphur consuming industry to a market which is more focussed on lithium-ion batteries. The primary reason for this shift is due to the lower cost associated in producing lithium-ion batteries. Figure 8 illustrates the current and future predicted cost for lithium-ion, lead-acid, sodium sulphur and sodium metal halide batteries. Furthermore, lithium-ion batteries also outperform their competitors with respect to their usable capacity (kWh) and endurance (cycles). This means that lithium-ion batteries are more efficient and effective in storing and discharging energy and continue with this cycle for longer. Table 3 below illustrates the calculated cost for both lead-acid and lithium-ion based on the usable capacity and cycles of each. Lithium batteries can further be

subdivided into 6 subcategories based on their cathode and anode material (Table 4). Of these 6 subcategories, only one battery system does not contain graphite as a component. This suggests that along with lithium, the primary component of these batteries is graphite.

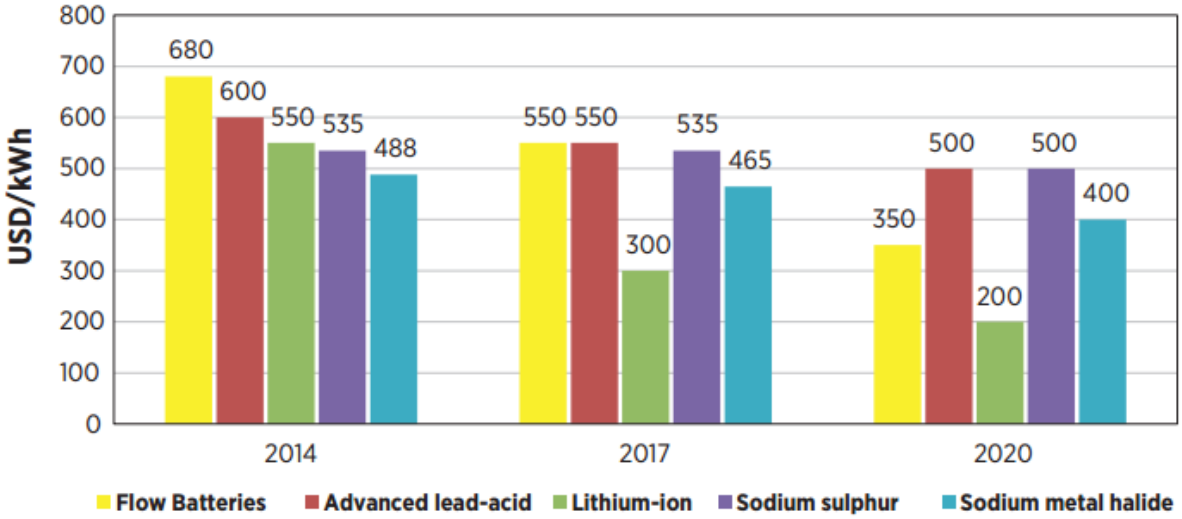

Figure 8 – Current and future battery production price per kilowatt hour. Image obtained from Grothoff, (2015)

Table 3 – Lithium-ion and lead-acid battery cost. Sourced from Grothoff, (2015)

	Lead-acid	Lithium-ion
Battery power	5	5
Battery capacity (kWh)	14.4	8
Usable capacity (kWh)	7.2	8
Cycles	2800	6000
Price (EUR)	8900	18900
EUR/kW	1780	3780
EUR/kWh	618	2363
EUR/Usable kWh	1236	2363
EUR/Useable kWh/Cycle	0.44	0.39

Graphite's high conductivity, large surface area and layered crystalline structure makes it a highly effective anode material if combined with lithium. Producing the graphite used in these batteries requires coated or uncoated spherical graphite, a morphed product of natural or synthetic graphite. Both natural flake graphite which has a higher capacity and synthetic graphite which has a better rate capacity, can be used to produce spherical graphite. Although natural flake graphite is cheaper than synthetic graphite, their physical characteristics when mixed produce the desired product. The spherization process of uncoated graphite includes the micronizing, rounding and purifying of synthetic or natural graphite. This spherization process can utilize all sizes of graphite flakes but economic factors have led manufacturers to adapt processes to primarily use -100 to -150 mesh size fractions due to the availability of this size fraction at lower cost relative to the larger flake sizes. The

first step in the spherization process is micronizing which reduces the flakes down to 40 µm and which after rounding produces snowball like pellets. The size of these rounded graphite flakes is dependent on the application they will be used for and can be from 5 to 20 µm in size. The purification process traditionally involved chemical processes with hydrofluoric and sulphuric acid as the primary purifying agent. Environmental concerns stimulated the development of an alternative high energy thermal purifying process which removes impurities and increases the grades from approximately 94%CG to 99.95%GC. Producing coated-spherical graphite includes complicated processes that coat the rounded grains with pitch or asphalt. These coated grains are then baked at 1 200°C, producing a hardened carbon shell which effectively protects the spherical graphite from exfoliation and increases the battery life. This process of spherization uses up to 3 tons of natural graphite to produce 1 ton of spherical graphite. While complex, the spherization process results in a significantly higher value product: uncoated spherical graphite trades at approximately US$ 3 000 per ton whereas coated spherical graphite sells for US$ 4 000 to US$ 6 000 per ton for natural, and US$ 8 000 to US$ 12 000 for combined natural and synthetic graphite ('About Spherical Graphite'; Rapp *et al.*, 2016).

Table 4 – Lithium-ion battery subcategories and capabilities. Sourced from Grothoff, (2015)

Lithium-ion battery subcategory	Cathode	Anode	Electrolyte	Energy Density (Wh/kg)	Cycle Life	2014 price per kWh (USD)
Lithium iron phosphate	LiFePO	Graphite	Lithium Carbonate	85-105	200-2000	550-850
Lithium manganese spinel	LiMnO	Graphite	Lithium Carbonate	140-180	800-2000	450-700
Lithium titanate	LiMnO	LiTiO	Lithium Carbonate	80-95	2000-25000	900-2200
Lithium cobalt oxide	LiCoO	Graphite	Lithium Carbonate	140-200	300-800	250-500
Lithium nickel cobalt aluminium	LiNiCoAl	Graphite	Lithium Carbonate	120-160	800-5000	240-380
Lithium nickel manganese cobalt	LiNiMnCo	Graphite, silicon	Lithium Carbonate	120-140	800-2000	550-750

3.2 Historical Global Production

Global graphite supply increased by 65% over the past two decades from an estimated 720 000t in 1995 to 1 189 000t in 2016. The graphite supply was primarily from the top three natural graphite producing countries namely China, India and Brazil (Figure 9) which together have supplied 83% of the global natural graphite produced since 1995. China dominates, having produced 61% of the natural graphite supply since 1995. Figure 9 illustrates the major natural graphite producing countries which

produced more than 900 000 tons per year, with Figure 10 representing the minor producing countries which together produce less than 45 000 tons per year. The number of countries producing graphite has notably increased since 2002. However, the data seems to be fragmented with some counties not consistently producing graphite each year and some reporting a decreasing production. This can be the result of geopolitical circumstances where some counties do not report their yearly graphite production and are thus excluded from this data pool. The global demand for graphite prior to the recent technology boom could also have played a pivoting role in the data collection as graphite minerals were not regarded as a strategic mineral. These factors resulted in a generally poor yearly graphite market census and in the development of a mineral commodity traded system functioning on a willing-seller-willing-buyer contract platform rather than within a set market platform which can be regulated. The data provided by the USGS indicates that some production numbers are speculative and based on external factors such as the production of graphite consuming commodities (Oldon, 2017).

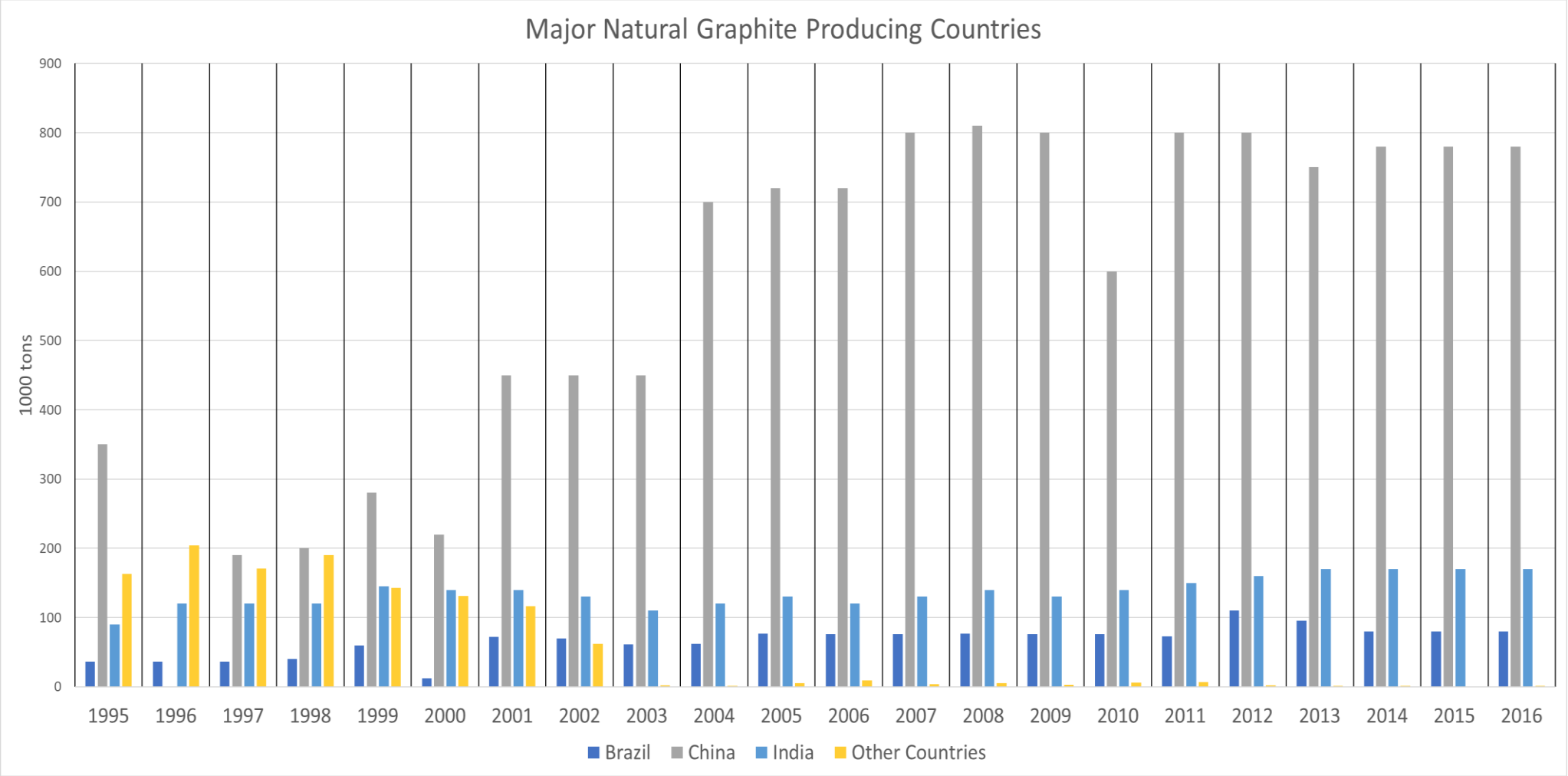

Figure 9 – Major (<900 000t/y) Natural Graphite Producing countries from 1995 – 2016. Source: (Olson, n.d.; Oldon, 2017)

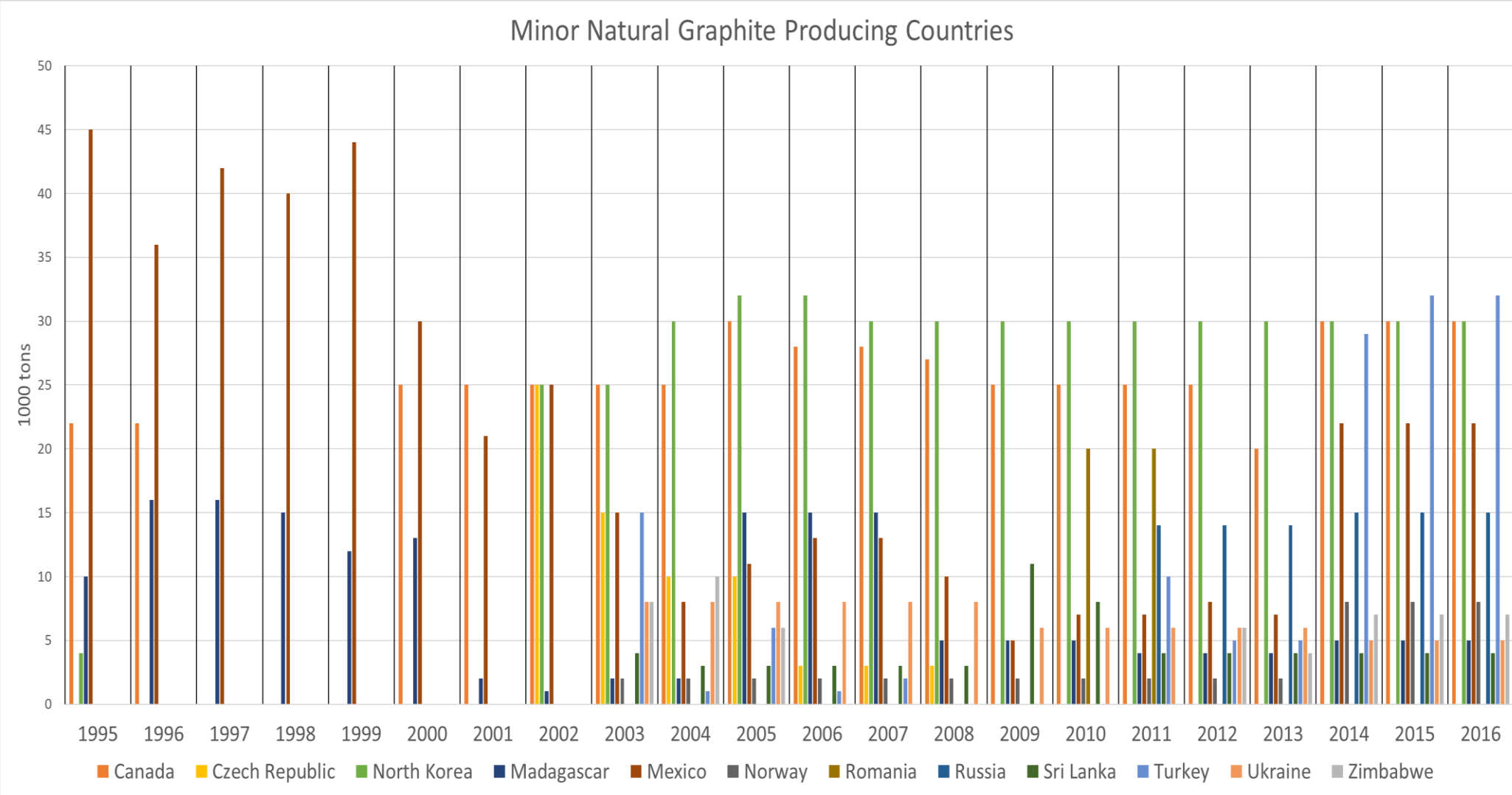

Figure 10 – Minor (<45 000t/y) Natural Graphite producing countries from 1995 to 2016. Source: (Olson, n.d.; Oldon, 2017)

3.3 Global Graphite Resources

In 2017, USGS reported the Global natural graphite resources to be an estimated 800 million tons of recoverable graphite. Since 2012 this resource estimation has seen an increase due to a renewed interest in the global graphite market with numerous companies evaluating natural graphite deposits in Africa, Australia and the north-Americas. Figure 11 illustrates the resources[2] reported by these companies whereas Figure 12 illustrates the graphitic carbon grades with relative graphitic flake size distribution. This resulted in a collective resource report of 4.4 billion tons which includes a diverse range of graphitic carbon grades and flake sizes.

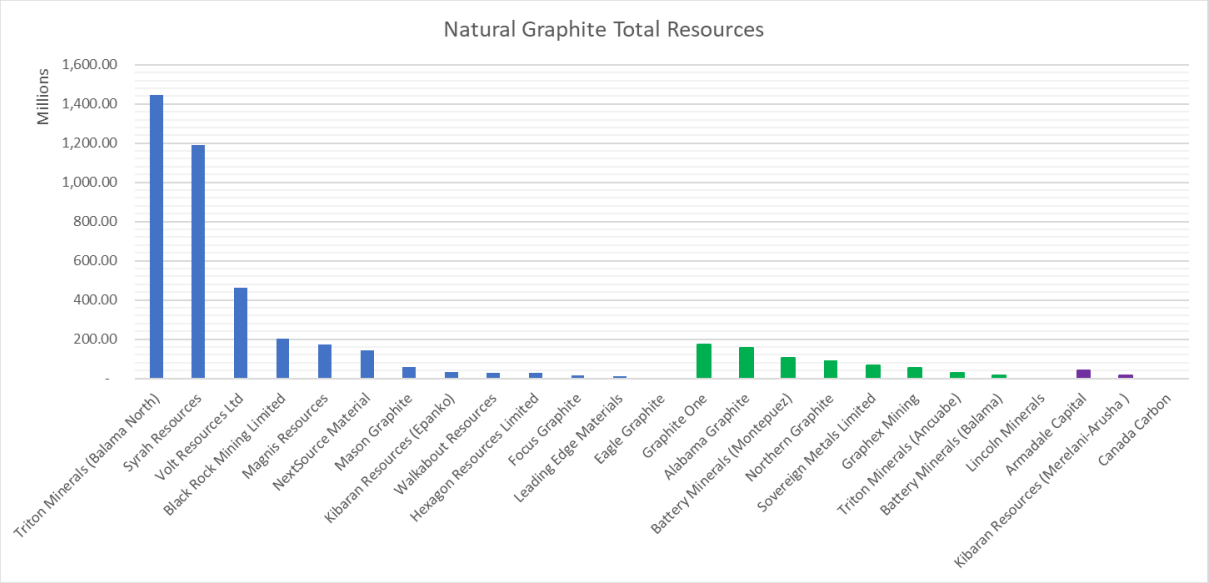

Figure 11 – Global Natural Graphite Resources reported for Exploring or Producing companies based on the highest reported resource criteria. Blue – Measured, Indicated, and Inferred resources; Green – Indicated and Inferred resource classification; Purple – Inferred resource classification.

[2] Resource is defined as a mineral concentration within the earth's crust of suspected economic value where the geology and grade are known to an increasing degree from inferred to indicated to measured.

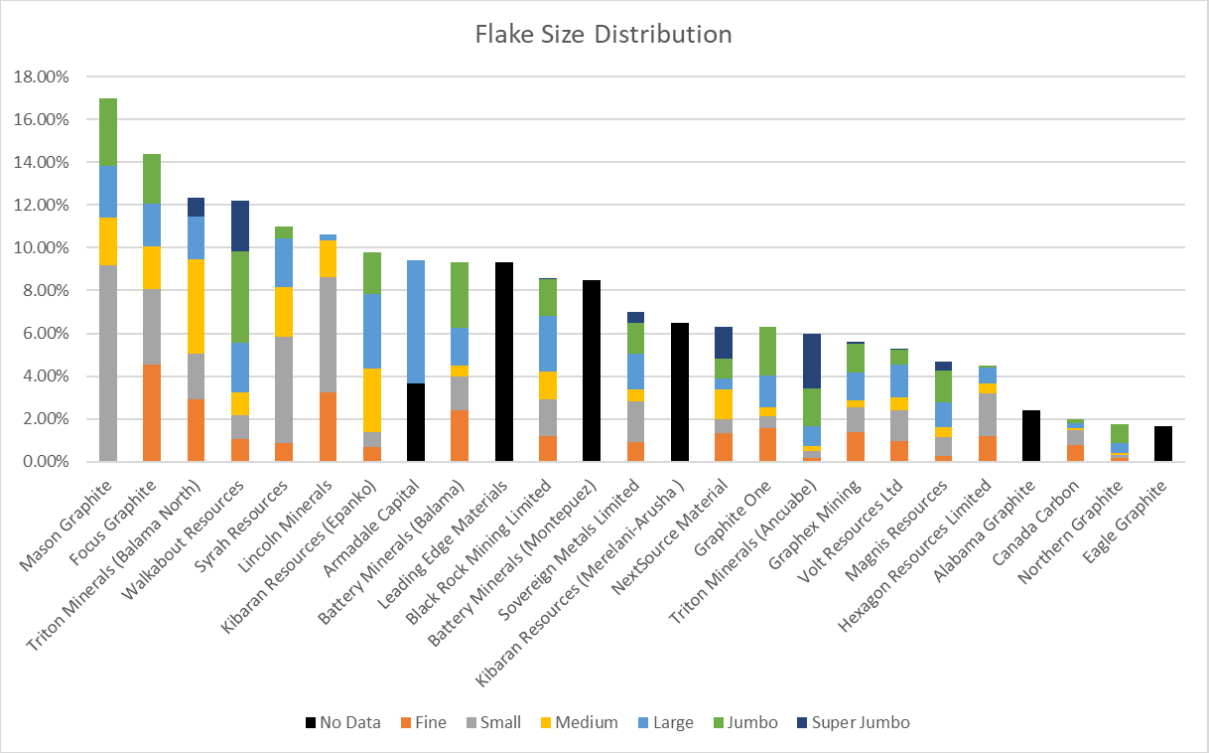

Figure 12 – Graph illustrating the Total Reported Graphitic Carbon percentage of the reported resource with the relative Flake Size Distribution based on the reported metallurgical analysis.

3.4 Global Supply and Demand Forecasts

Three primary industries - the refractory, foundries, and battery sectors - currently dominate global graphite demand, with the refractory industry currently being the largest consumer. The growth in these primary graphite consuming industries will determine the global graphite demand growth for natural graphite. As growth in these industries, especially the refractory industry, is directly proportional to the Global GDP (Hykawy and Chudnovsky, 2014), future growth in demand for graphite will be controlled by GDP. Over the last two decades, the global GDP has grown at an average rate of 5% per year which suggests that graphite demand is likely to follow the same trend.

The development of the battery as the primary energy storage medium will develop the energy industry and its continued momentum suggests that it can develop as the primary graphite consuming industry.

The shift of the global energy industry from a primary energy supplying service to an energy storage and supplying service has been the one of the primary focusses of graphite's future demand (Stern and Cleveland, 2004; Carley *et al.*, 2011). Along with this shift in the energy sector, global pressure to reduce carbon emissions has also propelled the development of Electric Vehicle (EVs), which primary component includes batteries. These developments and changes instil positive future growths in the

graphite demand with Shaw (2015) predicting an annual growth of approximate 14% in the natural graphite demand.

The research to increase the efficiency of batteries used to power these initiatives created a new demand base for graphite, lithium and numerous other critical metals. Although a number of battery technologies are rotating within the market, the lithium-ion battery has seen the largest growth. The growth in this sector is largely due to the effectiveness of the lithium-ion battery design which outperforms its competitors' with respect to battery usable capacity and cycle life versus cost (Grothoff, 2015). This increased use of lithium-ion batteries is clearly revealed in the battery installed capacity during the period from 2013 – 2014 as illustrated in Figure 13. Although Li-ion batteries can be used within a number of environments such as off-grid power storage media in renewable energy generation, the Li-ion battery applications for EVs have captured investors' and market speculators' interest. Some estimations predict that the demand for graphite can increase with as much as 524% compared to the current global graphite demand, in a 100% EV market (Jeff Desjardins, 2017), although it is highly unlikely that the EV will dominate the vehicle market in the near future. However, due to lack of a better estimation, a hypothetical 100% EV market will be used as the "best case scenario".

Obtaining accurate historical global graphite demand statistics is somewhat arbitrary with the only reasonably reliable statistics obtained from the reported global supply as mentioned in section 3.2. From 2014 to 2016 the global graphite supply has stagnated at approximately 1.19Mt per year. Assuming that the global demand for graphite reflects the global supply during this period, then an increase in the demand can be estimated, assuming the global vehicle market migrates to a hypothetical 100% EV market in either 20 years or 40 years. By calculating an exponential growth curve representing future demand over both 20 or 40 years, two scenarios were created which can be used in future predictions (Figure 14). The first scenario estimates an exponential increase in EVs of 4% per year for 40 years resulting in a global graphite demand of 5.04Mt by 2057. The second scenario estimates an 8% yearly increase in EVs for a period of 20 years resulting in a 5.04Mt global graphite demand by 2037.

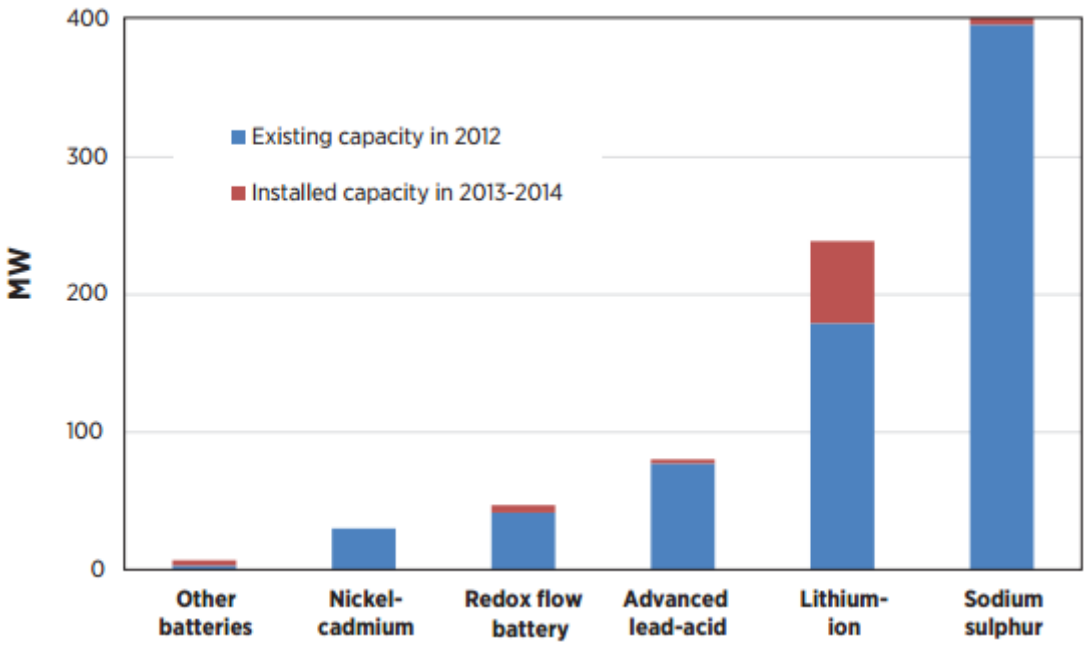

Figure 13 – Battery capacity and commissions (MW) installed during the period from 2012 – 2014 clearly show the large growth in the Lithium-ion battery sector. Image obtained from Grothoff, (2015).

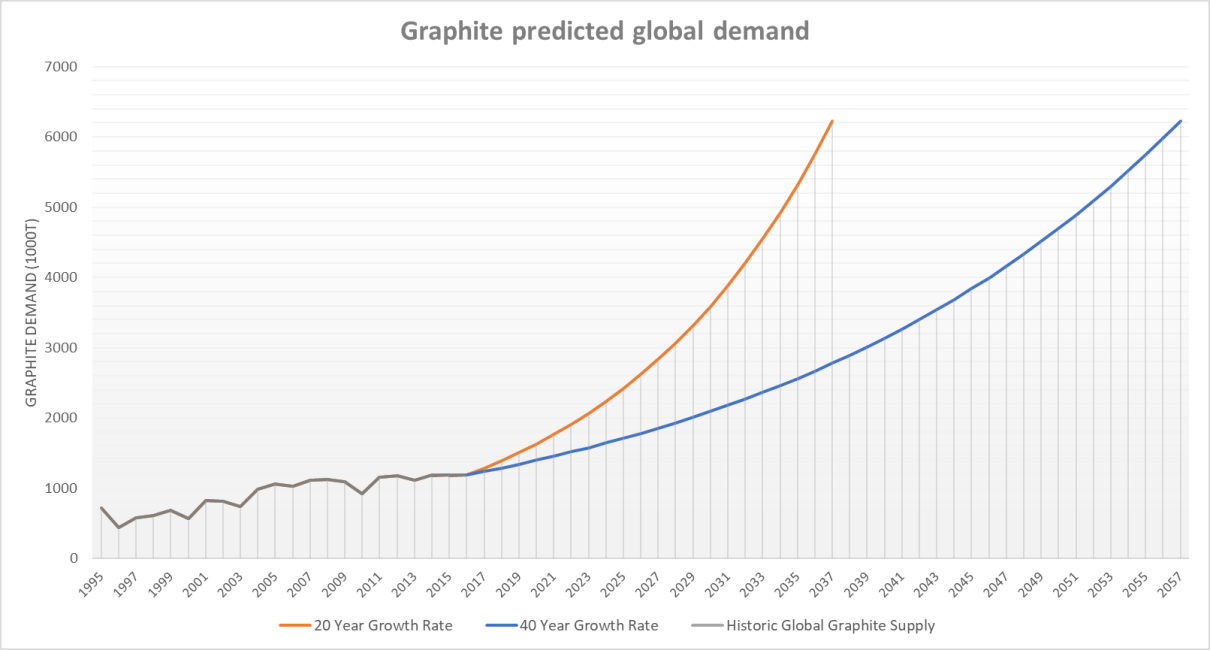

Figure 14 – Global graphite demand forecast based on a 524% increase in graphite demand within a 100% EV market scenario. Exponential curve represents two scenarios whereby the 100% of the global vehicles market are EVs within 20 (Orange Curve) or 40 (Blue Curve) years. Data obtained from Jeff Desjardins (2017) related to the impact of electric vehicles on the technology minerals.

The reported increase in new graphite resources over the last decade is significant, with the largest discoveries made in eastern Africa. These resources are currently under different economic delineation and evaluation stages, with numerous companies declaring potential production numbers

based on identified reserves. If these targets are met, an additional 607 900 tons of natural graphite production could be achieved by 2019 (Table 5). Other projects which have not reported possible production dates but have reported proposed production figures in their feasibility studies, would provide an additional 718 300 tons of natural flake graphite to the market. Assuming these exploration projects (Table 5) begin production within the next 10 years, then the global graphite demand for the next 5 to 17 years can be met; however, additional sources of graphite will be needed to supply the demand beyond that. Figure 15 illustrates the relationship between the demand and supply of the two scenarios (20 and 40 year) based on the 524% increase in graphite demand as predicted by Jeff Desjardins (2017). If the four companies, that is Eagle Graphite (10 000t/y), Mason Graphite (51 900t/y), NextSource Material (16 000t/y) and Syrah Resources (355 000t/y), start production in 2018 followed by Volt Resources (170 000t/t) in 2019, a predicted oversupply of natural graphite will dominate the market until 2022 for the 20-year scenario, whereas the oversupply will likely last until 2027 for the 40-year scenario. Although the remaining nine companies did not indicate a production date, the combined graphite which can be supplied to the market at any given time amounts to 718,300t/y, seven times the present global graphite demand.

Table 5 – Graphite production. Information obtained from companies' web-pages. See appendix for list of companies and source of data.

Company	Graphite Production (tpa)	Year
Leading Edge Materials	10,000.00	2014
Eagle Graphite	10,000.00	2015
Mason Graphite	51,900.00	2018
NextSource Material	16,000.00	2018
Syrah Resources	355,000.00	2018
Volt Resources Ltd	170,000.00	2019
Battery Minerals	100,000.00	Not Specified
Black Rock Mining Limited	52,000.00	Not Specified
Focus Graphite	44,300.00	Not Specified
Graphex Mining	70,000.00	Not Specified
Hexagon Resources Limited	88,000.00	Not Specified
Kibaran Resources	60,000.00	Not Specified
Magnis Resources	220,000.00	Not Specified
Sovereign Metals Limited	44,000.00	Not Specified
Walkabout Resources	40,000.00	Not Specified
TOTAL	1,328,700.00	

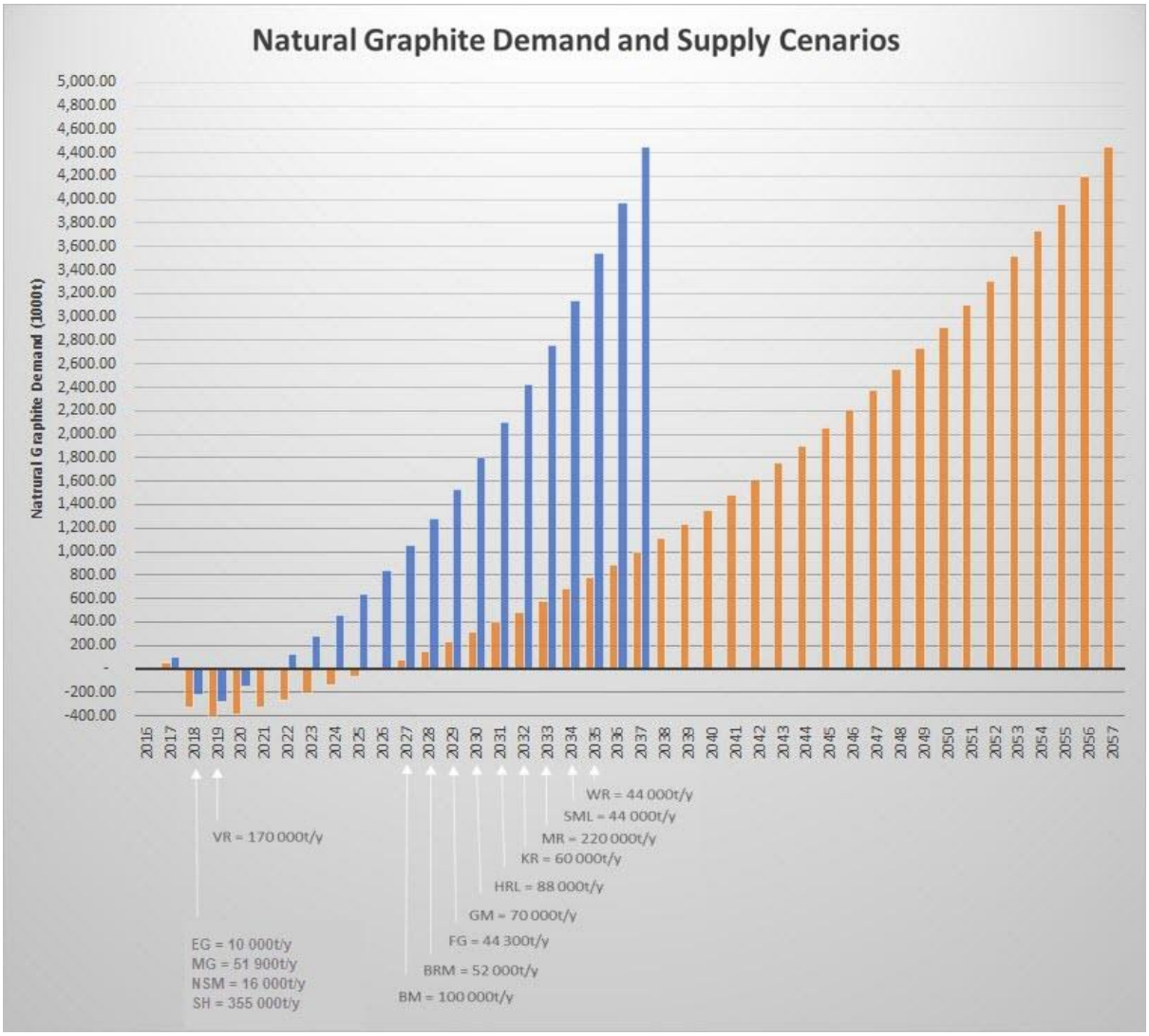

Figure 15 - Figure illustrating Yearly Global Graphite Demand minus known and predicted graphite supply. Orange bars indicate graphite demand growth for a 100% EV market within a 20year period. The Blue bars indicate the graphite demand growth based on a 100% EV market over 40 years. The company and reported annual graphite supply illustrates the impact these graphite supply will have on the graphite demands or both the 20year and 40year scenario. Abbreviations: EG = Eagle Graphite; MG = Mason Graphite; NSM = NextSource Material; SH = Syrah Resources; VR = Volt Resources Ltd; BM = Battery Minerals; BRM = Black Rock Mining Limited; FG = Focus Graphite; GM = Graphex Mining; HRL = Hexagon Resources Limited; KR = Kibaran Resources; MR = Magnis Resources; SML = Sovereign Metals Limited; WR = Walkabout Resources. (See appendix for list of companies and source of data)

4 GRAPHITE CASE STUDY – OROM GRAPHITE PROJECT, UGANDA

The data and conclusions stated in this chapter are in concordance with a scoping study level conducted on the Orom Graphite project (hereafter referred to as "the project") in Uganda. The author of this dissertation is part of the project management team currently evaluating the graphite deposit and was responsible for planning, executing and managing the field data gathering and geological interpretations. This section will also draw on information and work performed by external consultants and includes metallurgical, geophysical and mineralogical studies conducted under the geological management team's supervision.

The data, as stated below, includes the conclusions and opinions associated with a scoping study and is expected to be refined and improved as the project develops to a Pre-feasibility study and/or a bankable feasibility study.

4.1 Project Description and Accessibility

The study area consists of Exploration Licence 1025 located in the Orom Sub County, Kitgum district of northern Uganda. The project area can be accessed from Kampala vie the Kampala-Gulu Highway for approximately 330 km. The recently constructed 100 km Gulu-Kitgum Road provided access to Kitgum. In order to access the project site from Kitgum, one must take the Kidepo-Gulu gravel road some 110 km east past the town of Orom.

4.2 Physiography

Uganda lies between the eastern and western sections of Africa's Great Rift Valley. The country shares borders with Sudan to the north, Kenya to the east, Lake Victoria to the southeast, Tanzania and Rwanda to the south and the Democratic Republic of Congo (DRC) to the west. Whilst the landscape is generally quite flat, most of the country is over 1 000 m in altitude with the western border consisting of the Ruwenzori Mountains reaching peaks of 5 109m. The lower regions are generally marked by lakes occurring within the Rift valley and has an elevation of approximately 900 m above sea level.

The project site's topography can be described as undulating flatlands with a series of prominent steep hills with rounded crests consisting of weathering resistive granite rocks piercing the general topography. The Orom Mountain is a prominent landmark rising approximately 1 000m above the surroundings with steep to vertical slopes and rounded crests. The vegetation is generally thick and dense with the local fauna and flora being proportional to the mountain elevations with dense forests occurring along the steep slopes and crests, and savanna grasslands and thorn trees and shrubs dominating the low-lying plains (Figure 16).

Figure 16 – Local Physiography. LEFT: Savanna plains with thorn trees and shrubs (picture taken by author). RIGHT: Dense Forest slopes and peaks with granulite and granitoid rounded crests (Picture provided by Geophysics helicopter pilot).

4.3 Climate

The relative elevation and geographical location of Uganda assures a relatively uniform warm climate year-round with the average yearly temperatures in the mid-twenties. The project site experiences similar climate trends but with local micro-climate fluctuations due to the geographical location and topography. The closest town (Orom Town) located on the eastern side of the Orom mountain experiences more moderate annual temperatures in the mid-twenties with an average variation of 3.4°C. The average rainfall reported for this town is 1000 mm per year with the rain season starting in March and lasting until October (Figure 17). The project site, located on the western slopes of the Orom mountain, experiences fluctuating temperature changes and generally higher annual precipitation evident from the lush vegetation. No temperature nor precipitation data is however available for the project site.

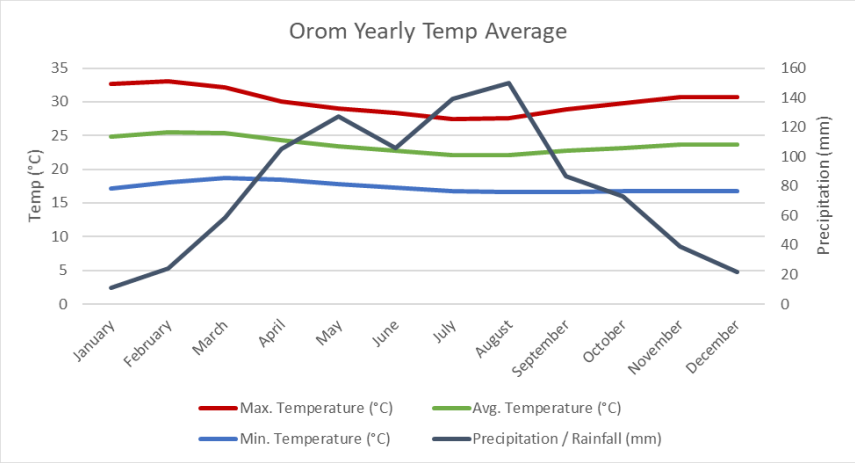

Figure 17 – Orom town Yearly temperature and precipitation average. Data obtained from "Climate Rom: Temperature, Climograph, Climate table for Rom - Climate-Data.org, no date".

4.4 Local Resources and Infrastructure

The north-eastern part of Uganda is rural with poorly developed resources and infrastructure. Decades of civil unrest has mainly reduced north-eastern Uganda to self-sustaining farming communities with their primary source of income and provisions being provided by humanitarian organisations and tourism to the Kidepo National Park located approximate 30km north-east of the project area. The local population is poorly educated with most of the population above 25 years of age being illiterate.

The Kidepo National Park has an airfield for fixed wing aircrafts with charter flights available from Uganda's national airfield in Entebbe. The nearest town providing basic consumables is Kitgum with the provincial town of Gulu providing the basic infrastructure and equipment needs for northern Uganda. Power supply is currently being installed from Kitgum to the Kidepo National Park and is expected to be completed by 2019. The overall power supply is, however, subject to seasonal fluctuations with frequent power outages occurring and lasting for days. Local water supply is accessible by means of seasonal streams draining from the Orom mountain fountains. Local water bore holes provide an additional source of potable water for the local villages.

4.5 Historical Exploration Work

In 1969, W. H. Morton released a report titled "*Mineralisation in the Rom Mountain Graphitic Gneisses*" whilst employed by the Ugandan Geological Survey and Mines Department. The report described the extent of exploration conducted in the Orom mountain range since 1964.

The purpose of the report was to combine the results of numerous small exploration programs aimed at delineating and identifying the source of the geochemical anomalies located during a regional mapping and soil sampling program conducted in 1962. No specific report or data identifying these

anomalies could not be obtained but reference are made to Hawkes and Webb (1962). According to Morton, (1969) the area proved to be anomalous in Zinc and to a lesser extent Cobalt, Nickel, Copper, and Chromium. These anomalies were first investigated by Nash (1964) by means of a geochemistry sampling and pitting program. This was followed by ground geophysics, which according to a unpublished report by Evans (1965) did not produce any compelling evidence to mineralisation, siting the graphitic gneiss as over-shadowing any possible sulphide anomalies. A unpublished report (Nash, 1966) confirmed anomalous zinc values of 600 – 1000 ppm with accessory copper and nickel values of 200 ppm and 190 to 290 ppm respectively. Both Nash (1966) and Baldock *et al.* (1969) concluded that the graphitic gneiss members are metamorphosed carbonaceous or black shales with the base metal anomalies most likely a result of syngenetic mineralisation.

Later work conducted by Westerhof *et al.* (2014) reinterpreted the regional geology into modern lithological sequences.

4.6 Regional Geology

The regional geological features associated within the project area form part of the Eastern Africa Orogen Belt, formed during orogenic from approximately 750 Ma to 500 Ma. (Shiraishi *et al.*, 1994; Grantham, Maboko and Eglington, 2003; Meert, 2003; Collins and Pisarevsky, 2005; Guiraud *et al.*, 2005) and are related to the formation of the super continent known as Gondwana. The meta-sedimentary formations along with intrusive suits are remanence of a suture zone signifying the convergence, collation and amalgamation of lithosphere forming part of the most recent Wilson Cycle/Supercontinent cycle (Wilson, 1966).

The East African Orogenic Belt marks the suture zone between Western and Eastern Gondwana forming the supercontinent Gondwana. Some of the major theories regarding the assembly of Gondwana includes a series of collisional events spanning over 250 Ma between different crustal blocks (Grantham, Maboko and Eglington, 2003; Meert, 2003; Meert and Lieberman, 2008) or a single collision event following progressive crustal thickening from the west to east (Windley *et al.*, 1994; Collins, Razakamanana and Windley, 2000). The foundations of these theories are based on Neoproterozoic paleomagnetic data collected form the numerous amalgamated blocks as well as geochronological data collected form the geological formations. Meert (2003) uses these datasets to reconstruct the conglomeration of Eastern Gondwana and later the supercontinent Gondwana with Meert and Lieberman (2008) having further developed on this concept by incorporating biological and climatological data, reconstructed from fossil evidence.

The development of the East African Orogenic Belt is related to the a series of smaller orogenic events dated between 820 Ma to 650 Ma (Meert, 2003). The first collisional event occurred with the

amalgamated SLAMIN Terrane, a conglomerate of crustal blocks including the present-day Eritrea, Somalia, Ethiopia, Seychelles, Madagascar, India and Sri Lankan, with the amalgamated Congo and Kenyan Craton (North-Central East Africa crustal blocks). This converging and collisional event resulted in the closure of the Mozambique Ocean and the wedging of the Arabian – Nubian Shield island arcs between the two-crustal block dated approximately at 750 – 820Ma (Figure 18 – Cross Section a). The second collisional event occurrent with the convergence and collision of the amalgamated SLAMIN Terrane and the Australian/Mawson Continent (Present day Antarctica) resulting in the closing of the Mawson Sea dated approximately at 650 – 620Ma (Figure 18 – Cross Section b) (Meert, 2003). The final orogenic event related to the amalgamation of Gondwana is referred to as the Kuunga orogeny. This orogenic event, dated at 550 Ma to 530 Ma, resulted in the convergence of the Laurentia continent with the amalgamated Eastern and Western Gondwana resulting in the closure of the Damara Belt in Namibia and is interpreted to be the cause of the transcurrent tectonism in the region which is currently Kenya, all the way to the Arabian – Nubian shield and is likely a result of the Aswan Shear stretching from the southeast of Uganda to the northwest (Grantham, Maboko and Eglington, 2003; Meert, 2003).

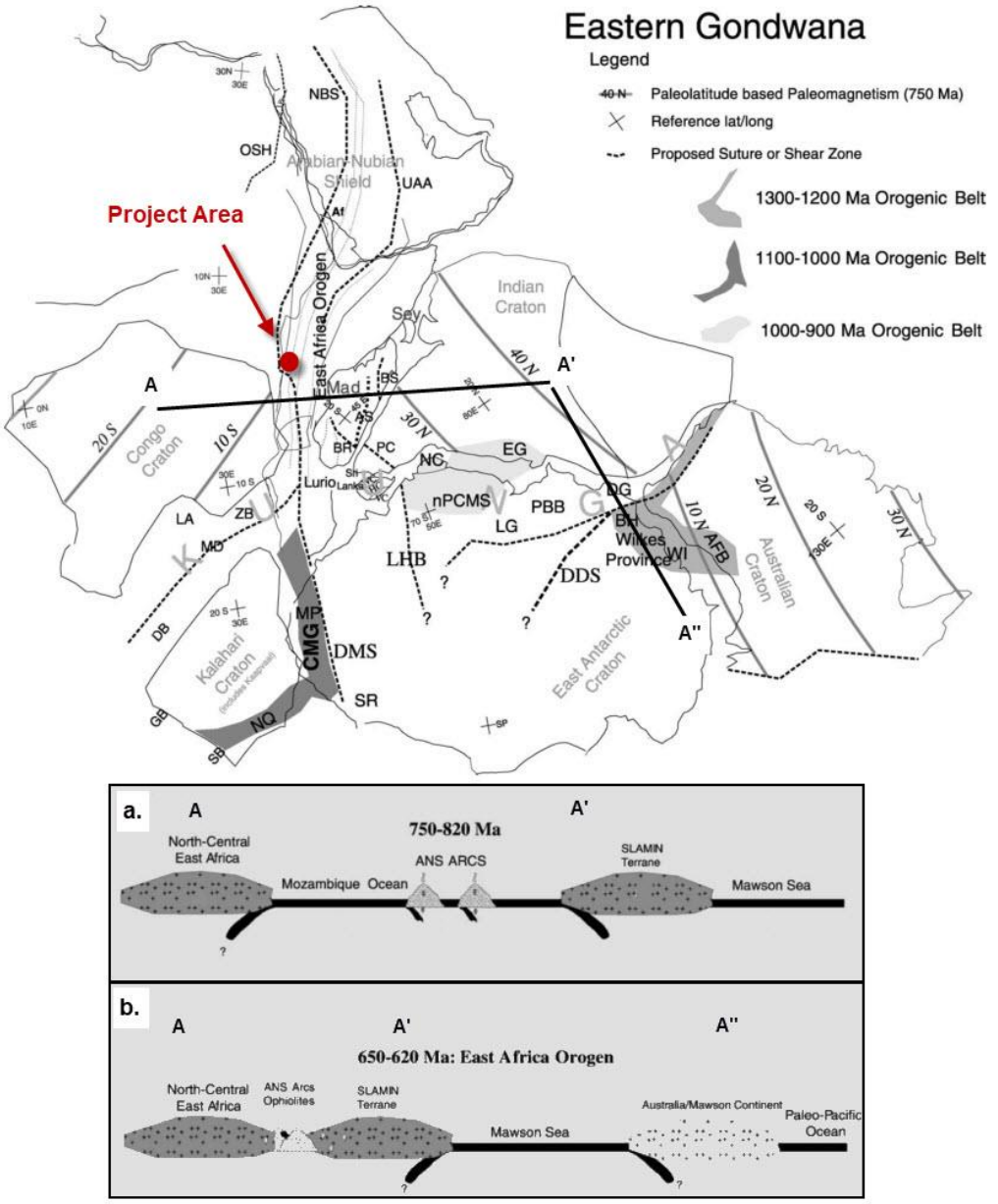

Figure 18 – Map illustrating the different crustal blocks forming eastern Gondwana reconstructed using geochronological and paleomagnetic data. Sections illustrating the collisional events during the East African Orogen. Abbreviations for the plan view map: Af = Afif terrane (Saudi Arabia); AFB = Albany–Fraser Belt (Australia); ANS ARCS = Arabian-Nubian Arcs; AS = Angavo shear zone (Madagascar); BH = Bunger Hills (Antarctica); BR = Bongolava–Ranotsara shear zone (Madagascar); BS = Betsimisaraka suture zone (Madagascar); CMG = Coats Land – Maudheim–Grunehogna (Antarctica); DB = Damara Belt (Africa); DDS = Darling – Denman suture (Antarctica–Australia); DG = Denman Glacier (Antarctica); DMS = Dronning Maud suture (Antarctica); EG = Eastern Ghats (India); GB = Gariep Belt (Africa); HC = Highland Complex (Sri Lanka); LA = Lufilian Arc (Africa); LG = Lambert Graben (Antarctica); LHB = Lutzow – Holm Belt (Antarctica); MD = Mwembeshi Dislocation (Africa); MP = Maud Province (Antarctica); NBS = Nabitah Suture (Arabia); NC = Napier Complex (Antarctica); nPCSM = Northern Prince Charles Mountains (Antarctica); NQ = Namaqua Belt (Africa); OSH = Onib – Sol Hamed suture (Arabia); PBB = Prydz Bay Belt (Antarctica); PC = Paughat – Cauvery (India); SB = Saldania Belt (Africa); SR = Shackelton Range (Antarctica); UAA = Urd Al Amar suture (Arabia); VC = Vijayan Complex (Sri Lanka); WC = Wanni Complex (Sri Lanka); WI = Windmill Islands (Antarctica); ZB = Zambezi Belt (Africa). Figures modified from Meert (2003).

4.7 Local Geology

The oldest rock formations encountered in Uganda form part of the Archean Basement which can be subdivided into the Lake Victoria Terrane (LVT), West Tanzania Terrane (WTT), West Nile Block (WNB), Rwenzori Terrane (RW), and the North Uganda Terrane (NUT) (Figure 19 - A). The NUT covers approximately 60% of Uganda. It is separated from the West Tanzania Terrane (WTT) which is located in the east by what is termed a “major mid-crustal dislocation”. The NUT’s western margin consists of the 1.0 Ga old Madi-Igisi Belt and West Nile Block which is bound to the north and north-east by the Neoproterozoic Pan-African fold belts . The major building blocks of the NUT consist of the Mesoarchean Karuma- and Karamoja-Complex and the Neoarchean rock unit of the Amuru Group, consisting of highly deformed and metamorphosed granitoids, gneisses and migmatites of igneous or sedimentary origin.

The graphite mineralisation targeted within the Orom mountanous region was indentified by Morton (1969) and interpreted to be hosted within the Neoproterozoic West Karamoja Group which consists predominantly of mafic granulites, garnetiferous granulites and graphitic granulites (Table 6). The paleosedimentary enviroment is interpreted to have involved accumulations of sediment in shallow to deep oceanic sedimentary basins or intracontinental oceans. These sediments were consequently subjected to diagenesis followed by regional upper amphibolite to granulite grade metamorpic conditions associated with collisional tectonics. The collisional event related to the formation of the East African Orogenic Belt formed large scale crustal thrust structures displacing the Neoproterozoic West Karamoja Group on top of the Neoarcheaen Amuru Group. Syn- to post- orogenic intrusives, scattered throughout the project area, are grouped within the Okaka and Lamwo Suites (Westerhof *et al.*, 2014).

The migmatitic garnetiferous gneisses of the Orom Formation mostly occur in flat areas as scarce outcrops in the Kitgum, Patongo and Kitido District. The Orom Formation reflects different deposition environments with variation in arenitic and pelitic proportions, resulting in psammitic metagreywackes, banded biotite-garnet gneisses and diatexitic gneisses. According to Morton (1969), the graphitic member of the formation is most likely the result of a metamorphosed black shale protolith. Granulite-grade metamorphism however, destroyed all chemical and sedimentary structures, giving the formations a migmatitic appearance and making it difficult to separate the psammitic and more pelitic members. Major minerals of these migmatitic gneisses are plagioclase, quartz, K-feldspar, garnet and biotite with accessory minerals being hercynite, sillimanite and cordierite. Abundant garnets usually occur on compositional boundaries and are a by-product of dehydration melting during granulite- to amphibolite- grade metamorphism.

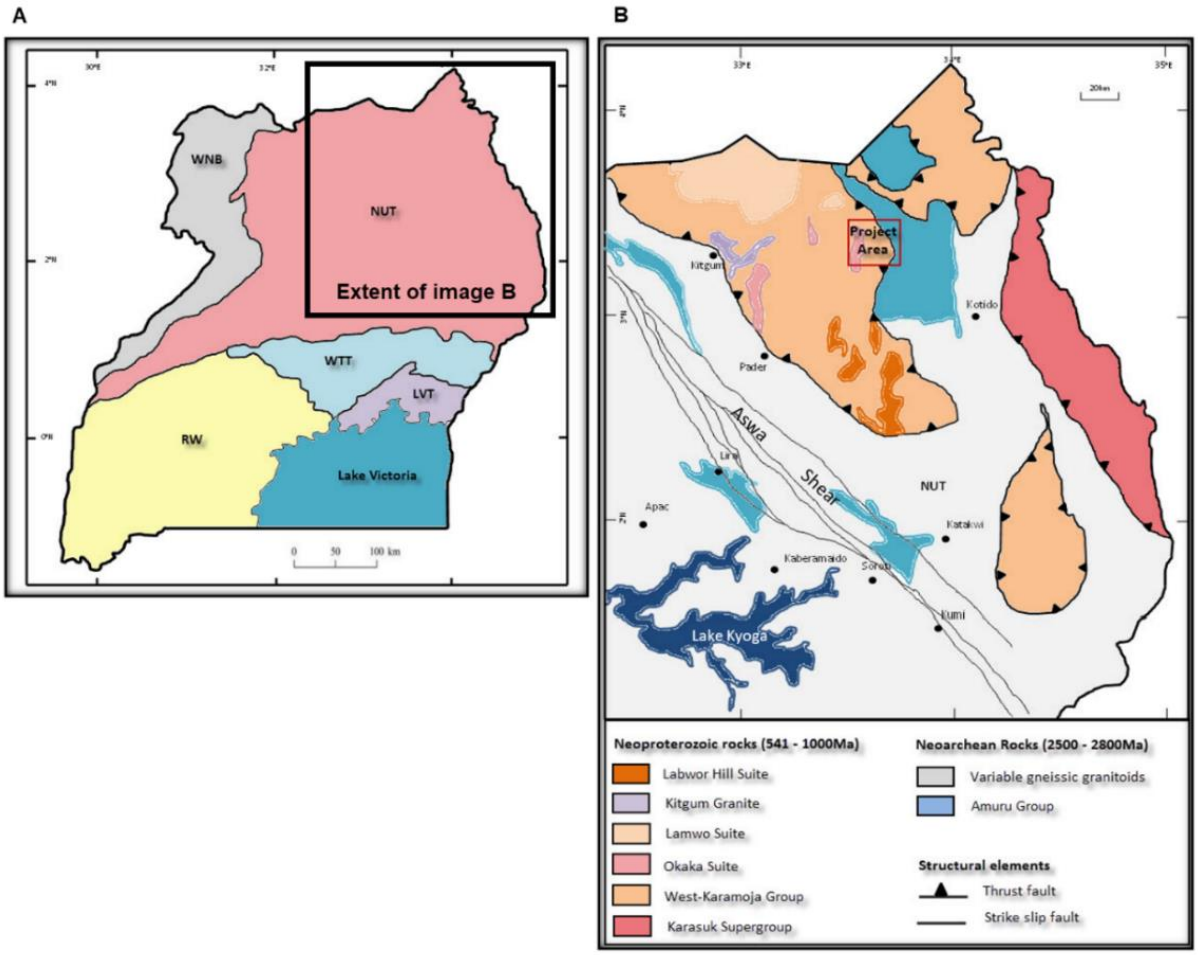

Figure 19 – A: Geological Terranes of Uganda. Abbreviations: Lake Victoria Terrane (LVT), West Tanzania Terrane (WTT), West Nile Block (WNB), Rwenzori Terrane (RW), and the North Uganda Terrane (NUT). B: Local geological features assocaietd with the Orom Graphite Project. Map modified after (Westerhof et al., 2014)

Table 6 – Stratigraphy of the West-Karamoja Group

Group	Formation	Lithology	Description
West Karamoja Group	Obwar	Granulite	Homogeneous, equigranular, medium grained, massive or weakly foliated mafic granulites, charnockites, and Migmatitic garnetiferous gneisses.
	Kaket	Felsic granulite	Heterogeneous, foliated leucrocratic quartz, plagioclase, and K-feldspar dominated gneisses with anatectic granitic veins. Granulite grade metamorphism destroyed all sedimentary remanence and textures.
	Orom (Graphite host)	Migmatitic garnetiferous gneiss	Migmatitic graphitic and garnetiferous gneisses with arenitic and pelitic components.
	Ogili	Intermediate granulite	Pyroxene granulites formed during granulite facies metamorphism. Bedding observed in pyroxene, quartz and plagioclase textures.

Group	Formation	Lithology	Description
	Lakwor South	Amphibolite	Texturally concordant to banded, fine0 to medium-grained amphibolite. Primary mineralogy consisting of amphiboles, pyroxenes, and plagioclase.
	Agoro	Calc-silicate rock	Epidote-amphibolites composed of quartz, plagioclase, epidote, garnets, hornblende, diopside, and occasional magnetite.
	Lakwor	Sericite quartzite	Fine- to medium-grained, schistose quartzite with sericite as the distinctive mineral assemblage.
	Kalapata	Mafic granulite	Mafic granulites consisting of pyrexene granulites and gneisses (Williams, 1966; Baldock *et al.*, 1969)
	Kalere	Ultramafites	
	Pire	Garnet-biotite gneiss	Banded garniferous biotite gneisses and mafic granulites and charnockites. Highly deformed (MacGregor, 1962)
	Napararo	Banded granulite and charnockite	Banded granulites and charnockites with local graphitic-rich bands (Cawley, 1962).
Intrusive Rocks	The intrusive rocks found in the study area are divided into the West Karamoja Complex and in-situ intrusions of the West Karamoja Belt. The intrusive rocks of the West Karamoja Complex consist of charnockites and some granitoids and are considered an intrinsic part of the overthrust structures/Klippes that form part of the West Karamoja Group. This intrusive Suite is interpreted to predate the structural deformation and thrusting related to the Pan African orogeny and are not considered to be in-situ intrusives, but like their granulite country rocks, were emplaced tectonically in their current position. The West Karamoja Complex includes the Okaka Suite consisting of charno-enderite, charnockites and anorthosites. The Labwor Hills Suite consists of granites and Otukei charnockites. The intrusive rocks of the West Karamoja Belt are regarded to be in-situ Pan-African plutonic intrusives, most likely related to the subduction, collision and amalgamation of the eastern Gondwana. This intrusive suite consists of biotite, charnockites and coarse porphyritic granites of the Lamwo Suite and younger Kitgum granites.		

4.8 Exploration Results (Project Scoping)

4.8.1 Geological Mapping

Prior to 2015, the earliest mapping data obtained was from work produced by Morton (1969) which investigated the copper anomaly identified by regional soil sampling in the Orom area. The results of Morton's mapping included graphitic gneiss units which at the time were of no economic interest. The reconnaissance mapping program conducted in 2015 was implemented with the aim to delineate these mapped graphitic bearing units as identified by Morton (1969) and was conducted by traversing all possible accessible pathways through the thick vegetation cover. Local farmers proved a valuable source of information with regards to the location of graphitic units as some elders had been involved in Morton's mapping and pitting program. This traverse mapping revealed a clear trend in the

orientation of the graphitic gneisses wrapping around the Orom mountain (Figure 20). Three broad lithological units were identified during the mapping exercise and included graphitic gneisses, graphite-barren gneisses and amphibolites.

- Barren Gneiss
    - Quartzo-feldspathic Gneiss

Poorly foliated, granoblastic polygonal textured, medium grained quartz and feldspars with minor ferromagnesian minerals and graphite flakes. Thin stringers of well foliated ferromagnesian and minor graphite occur within this lithology but are usually less that 1 cm in thickness (Figure 21 - A & C).

    - Coarse grained quartzo-feldspathic Gneiss

This poorly foliated, inequigranular granoblastic polygonal, coarse-grained quartzo-feldspathic unit contains quartz and white to cream coloured feldspar crystals exceeding 1 cm in size, with some displaying radiating textures especially in sections containing pegmatitic characteristics.

- Graphitic Gneiss
    - High to medium grade graphitic gneiss

Typically composed of alternating layers of light and dark medium- to coarse-grained minerals. Dark bands contain dominantly ferromagnesian minerals with graphite and are well foliated, with thin graphitic stringers clustered into bands displaying lensoid structures wrap around nodules of coarse-grained quartz and feldspar resembling augen gneiss. Light bands are primarily composed of medium- to coarse-grained quartz and feldspar with minor medium- to fine-grained ferromagnesian minerals displaying a granoblastic polygonal texture (Figure 21 - D).

    - Medium to low grade graphitic gneiss

Similar banding is observed as in the higher-grade graphite gneisses but with a lower content of graphite flakes and more ferromagnesian minerals. Bands alternate between light, medium grained quartz and feldspar, dark medium- to fine-grained ferromagnesian dominant with varied amount of graphite and dark greenish, fine grained, poorly-foliated amphibole and pyroxene dominant bands (Figure 21 - B).

- Amphibolite
    - Garnet Amphibolite

Fine- to medium- grained, pinkish purple garnets occur within a greenish poorly foliated, fine grained amphibolite and pyroxene rich matrix alternating with light quartz and feldspar rich layers. Garnets

generally occur as small, well-rounded crystals displaying porphyroblastic and poikiloblastic textures. Garnet clusters larger than 1 cm in diameter are common.

- Amphibolite

Medium grained poorly foliated, greenish grey bands of dominantly amphiboles (hornblende and actinolite). Minor quartz, feldspars and epidote can also be observed with some fine-grained graphite flakes occurring as accessory minerals (Figure 21 - A &C).

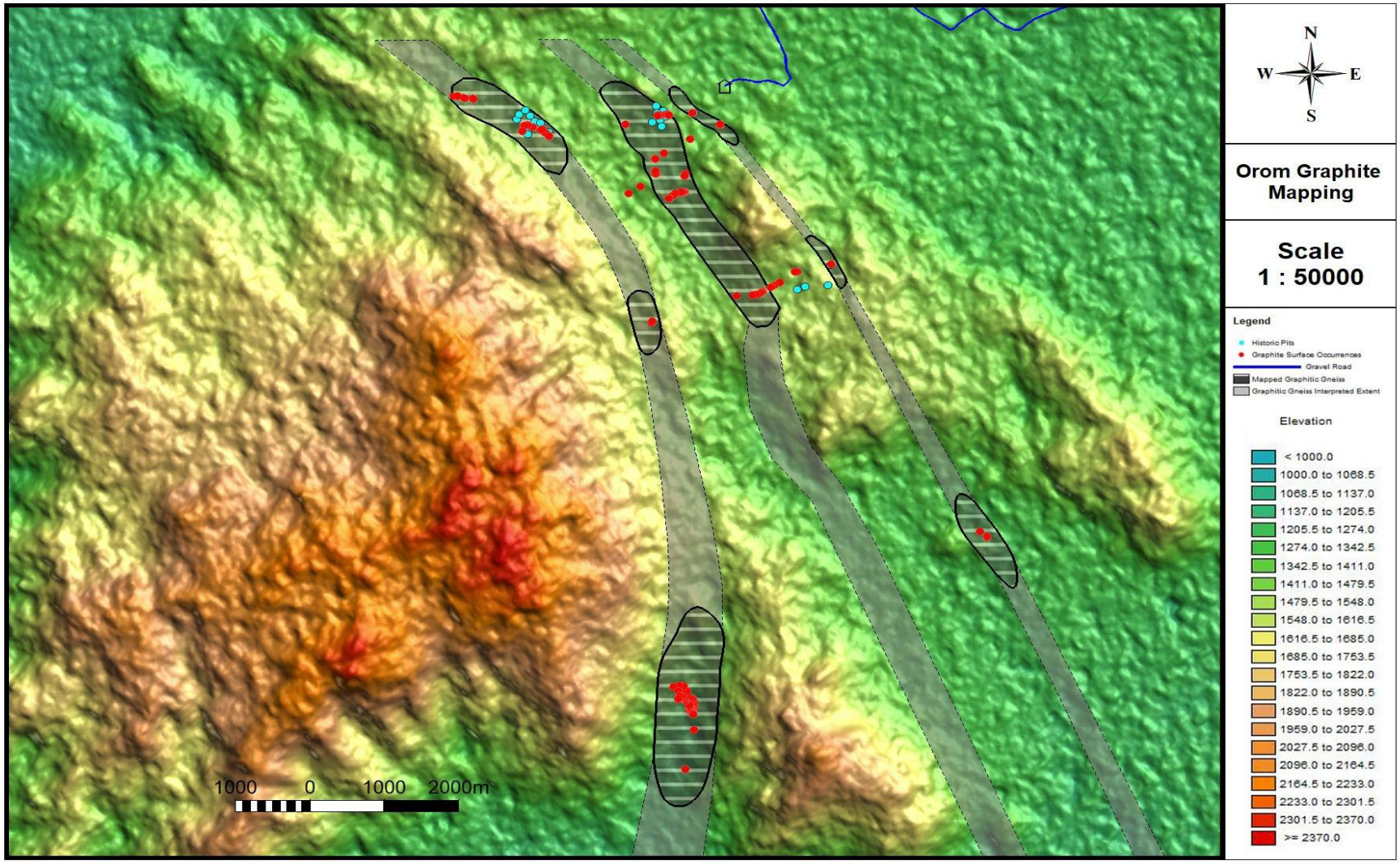

Figure 20 - Local map of the Orom Graphite project area identifying the graphitic bearing gneiss unit (Dark grey hatched areas) with extrapolated strike (light grey areas), draped over a DEM. Historical excavated pits (Blue circles) identified the extent of the graphite gneisses. The red circles indicate extensive graphite surface lithologies identified.

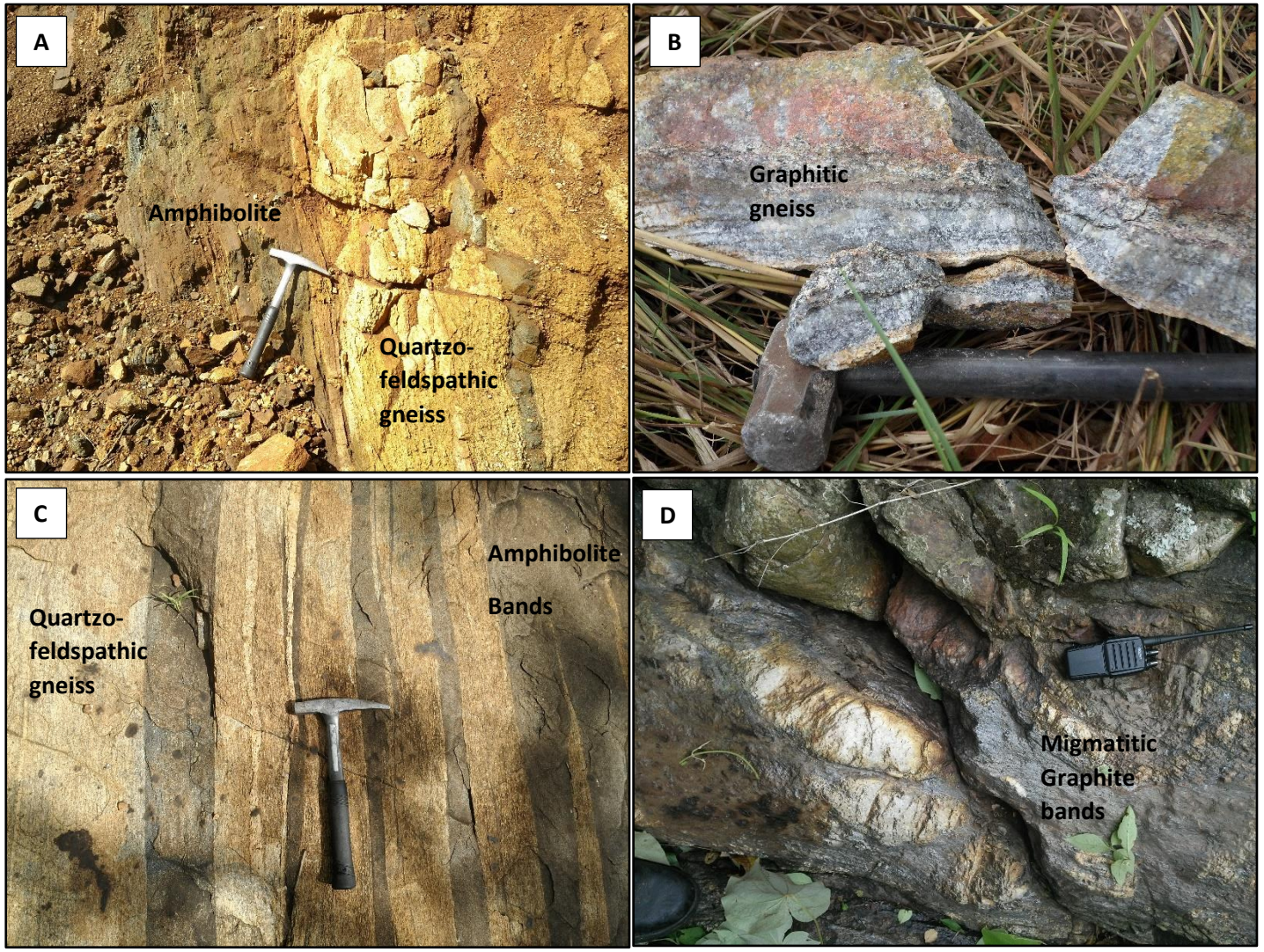

*Figure 21 – **A**: Vertical to sub-vertical dipping quartzo-feldspathic bands interbedded with hornblende and actinolite amphibolite bands. **B**: Low grade graphitic gneiss. Quartz and feldspar stringers with foliated graphite and biotite bands wrapping around the elongated porphyroblastic angulating quartz and feldspar grains. **C**: Steeply dipping banding. Dark bands consist dominantly of linear pyroxenes and amphiboles. Orange grey bands consist of elongated quartz and feldspar with biotite. Thin light-coloured stringers dominantly consist of quartz and minor amounts of feldspars. Display almost migmatitic deformation. **D**: Pure graphite veins wrapped around clasts of quartz and feldspar in graphitic augen gneiss units (high grade).*

4.8.2 Geophysics

The conductive quality of graphite makes time-domain electromagnetic (EM) techniques the most accurate and useful geophysical exploration tools in identifying blind graphite mineralised deposits. The method uses a continuous varying primary electric field which induces a primary magnetic field. The primary magnetic field induces a secondary electric field in the conductive body, which in turn generates its own secondary magnetic field. This secondary magnetic field is picked up by the receiver and can be manipulated to produce a 3D model of the conductive ore body. The effectiveness of the EM method is due to the low resistivity of graphite of between 10^{-6} – 10^{-2} Ωm compared to theoretical background resistivity values of the hosting igneous and mafic formations of between 10^{3} – 10^{5} Ωm (Dentith and Mudge, 2014).

In May 2016, a helicopter-borne EM geophysical survey was conducted over the project area using the versatile time-domain electromagnetic (VTEM) plus system with Full-Waveform processing. Measurements consisted of vertical (Z) and In-line horizontal (X) components of the EM fields using induction coil and a caesium magnetometer. The parameters of the survey consisted of east-west orientated traverse lines spaced 200 m apart with tie lines flown perpendicular to the traverse lines at a spacing of 2000 m, covering a 237 km^2 area (Figure 22). The helicopter altitude for the period of the survey averaged at 98 m above ground, at a constant speed of 80 km/hour. The Transmitter-receiver loop averaged at a terrain clearance of 67 m with the magnetic sensor at 85 meters.

The data obtained from the VTEM survey was screened to identify electromagnetic anomalies, conductive zones and chargeable zones. Electromagnetic anomalies (EM anomalies) were identified using all time domain channel profiles. These anomalous targets where correlated with the mapping results and confirmed a perfect correlation between the EM anomalies and graphite mineralisation. Bedrock conductivity was also modelled with the aim of identifying and possibly delineating a depth extent to the conductive rock formations.

The VTEM results provided an accurate profile of the conductive bedrock which were used to update the lithological trends identified in the mapping exercise and these improved maps formed the base of the future exploration programs.

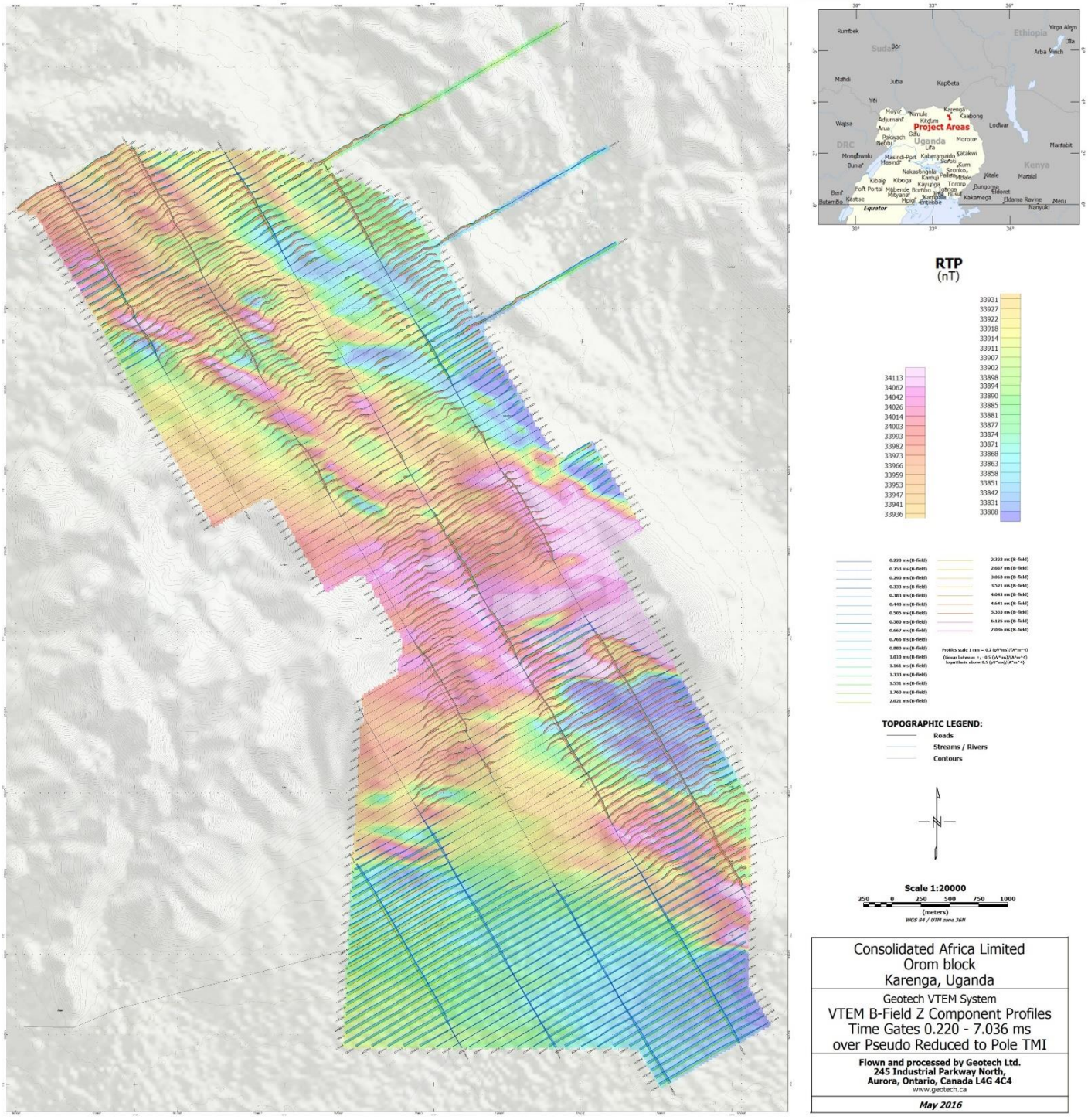

Figure 22 - Electromagnetic VTEM results displayed on a plan view map with flight paths, topography, B-field linear results and grid data reduced to poles (RTP) – A mathematical adjustment that converts the data to resemble perpendicular magnetic fields as observed at the poles (Baranov and Naudy, 1964; Ansari and Alamdar, 2009).

4.8.3 Trenching

I. Trenching Program

The trenching program was designed using the combined mapping and geophysical data. Trenches covered Targets 1 and 2 and were focussed on delineating the lithological and weathering characteristics of the graphitic gneiss units. The entire program consisted of three trenches dug perpendicular to the strike of the graphitic gneisses. A major problem was encountered with the topography which consisted of steeply dipping slopes with highly vegetated low-lying rivers and gullies and required some changes to the final position of the trench lines as shown in Figure 23.

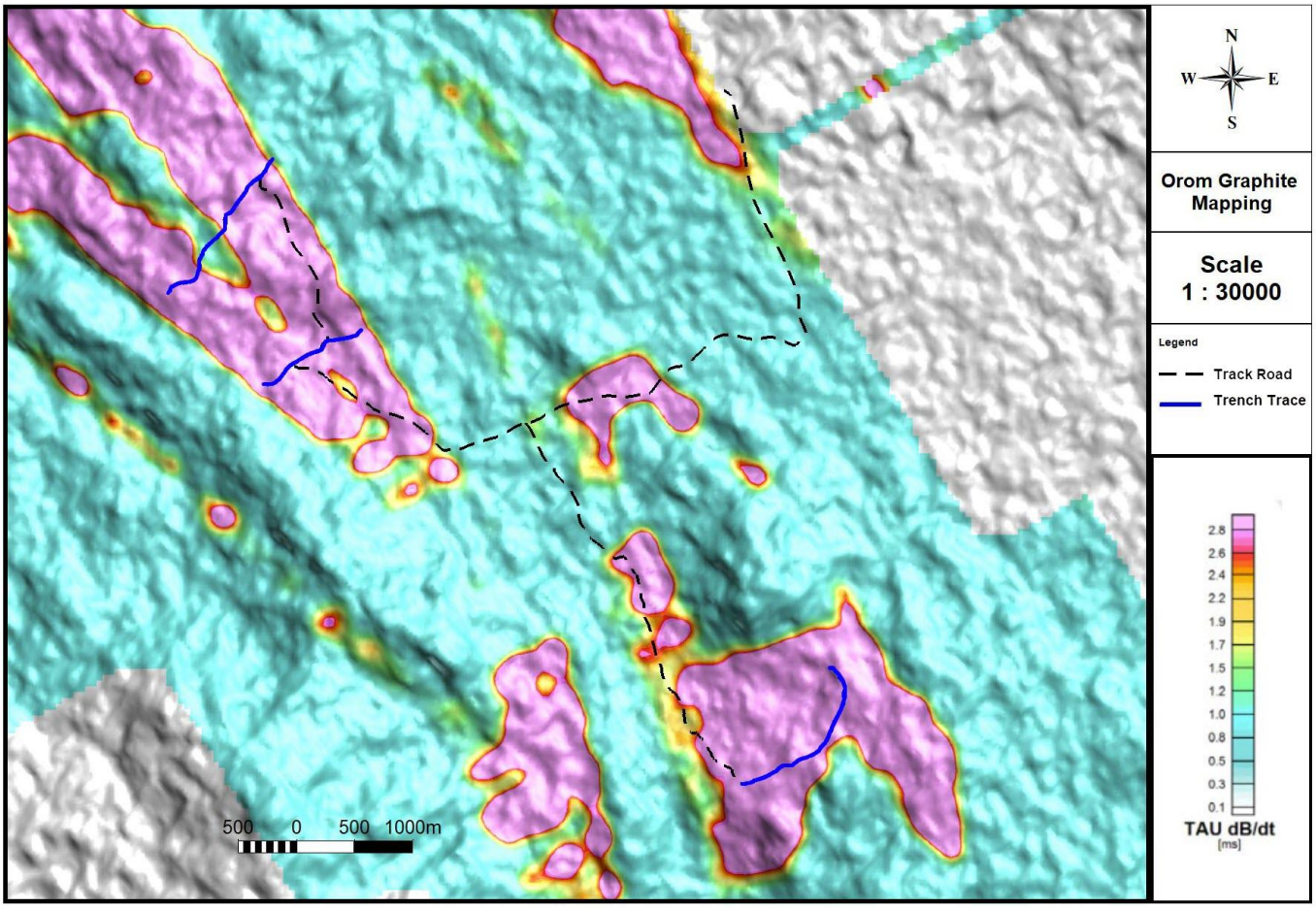

Figure 23 - Plan view illustrating trench locations and trends draped over the local DEM with geophysical high conductive zones.

II. Trenching results

The lithological units identified during the mapping program were used as lithological standard within the trench mapping program. Additional identified lithological units were added to the local stratigraphy for future reference. As seen in Figure 24, Figure 25 and Figure 26 the location of the graphitic gneiss correlates well with the interpreted conductive zones. However, the trenching revealed that the zones do not represent continuous graphitic gneiss units but rather bands of graphitic gneiss interbedded with quartzo-feldspathic gneiss. Amphibolite units are generally barren. On average, graphitic gneiss bands were intersected over 54%

of the trench lengths. Structural measurements obtained from the bedding planes and lineations show that the Target 1 anomaly represents an isoclinal synform plunging towards the north-west at approximately 20°. The north-eastern limb of the synform has an average dip of 67° on 238° (i.e. south-westward) whereas on average the south-western limbs dip 68° towards 037°.

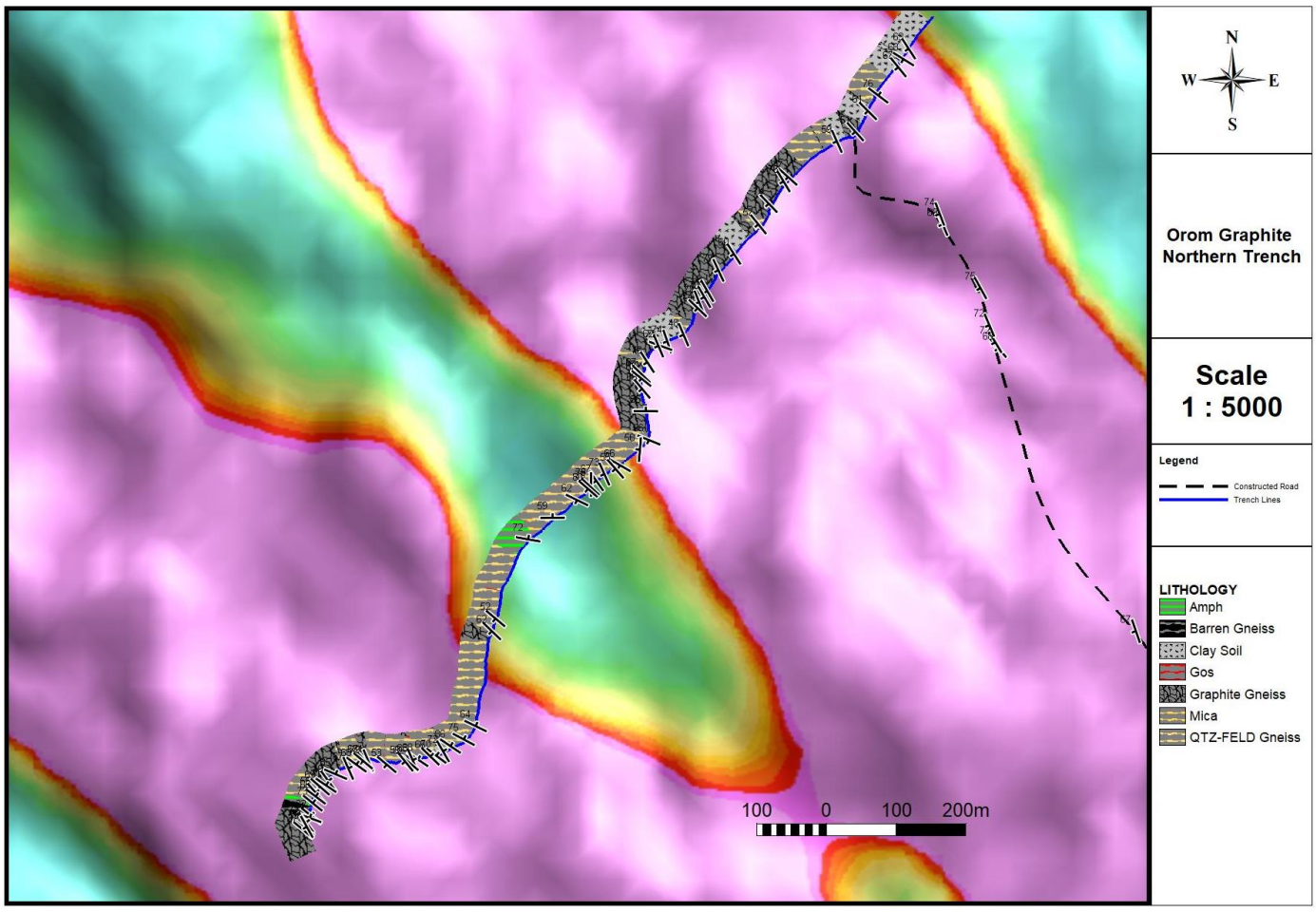

Figure 24 – Lithological unit intersecting the Northern trench

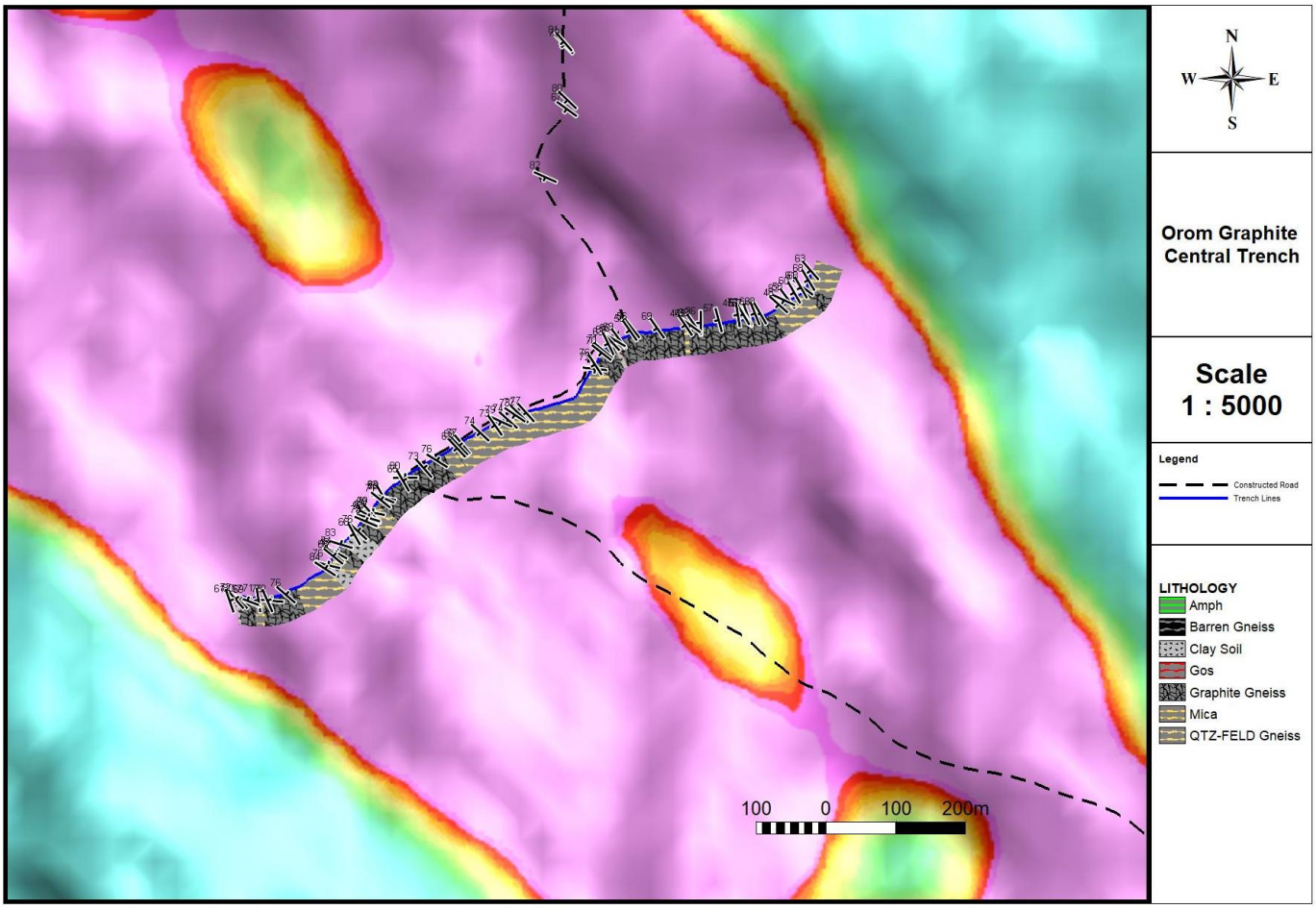

Figure 25 – Central trench lithological intersections.

I. Additional Results

Additional geological features observed during the trenching program included numerous highly oxidised ferrous gossan material trending with the host lithology. These gossans are dominantly associated with the amphibolite lithologies but does occasionally occur within the graphitic gneisses. Samples of these oxidised ferrous material were collected but not analysed due to the client's budget constraints.

The occurrence of these gossan material along with the indicated copper anomaly indicated by the historical regional sampling, warrant further investigation. These occurrence and samples were presented to the client but analysis is still pending.

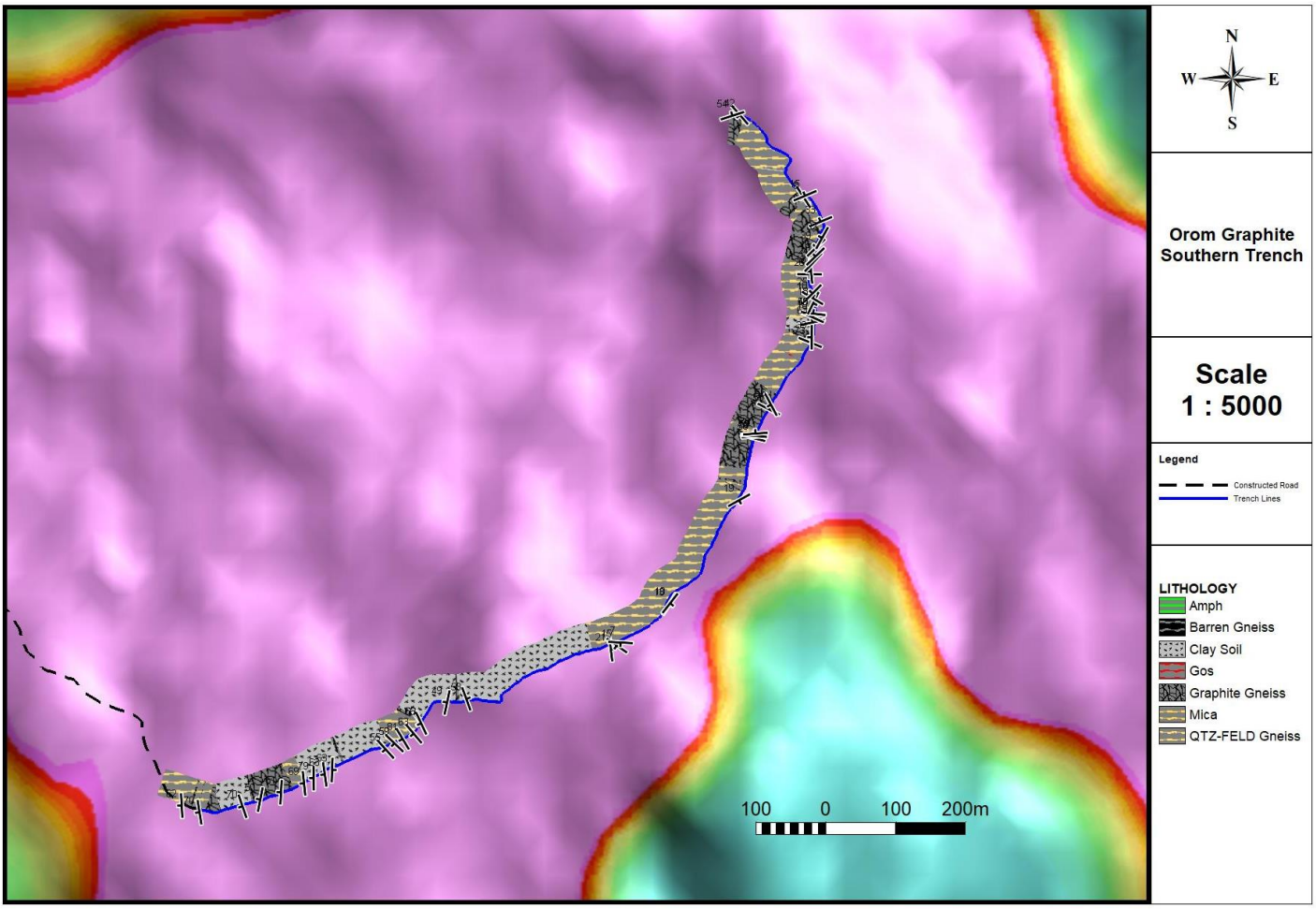

Figure 26 – Southern Trench lithological intersections.

4.8.4 Reconnaissance/Exploration Drilling

The exploration drilling program conducted in 2015 consisted of approximately 600 m of diamond core drilling divided into a total of 6 bore holes (Grouped in 2 zones - 3 bore holes per zone as seen in Figure 27).

All bore holes were inclined with the azimuth of the holes orientated perpendicular to the lithologies as determined by the mapping campaign. The aims of this program were to establish the depth extent of mineralisation, to define the weathering profile and to recover sufficient unweathered material for a representative metallurgical sample. The intention of the drilling program was not to delineate a resource within the license area but rather to assess the possible viability of mining and extracting the graphite from the graphite mineralised body. Each of the zones contained two bore holes drilled in a heel-to-toe configuration which delineated the depth extent of the graphitic gneiss units. The third bore hole was placed further down the lithological strike with the aim of delineate the lateral continuity of the graphitic bands. This implemented method allowed the drilling team to optimize the budget in such way that the largest

possible portion of the budget was allocated towards data collection from drilling, rather than on road and supporting infrastructure needed to access the drilling location.

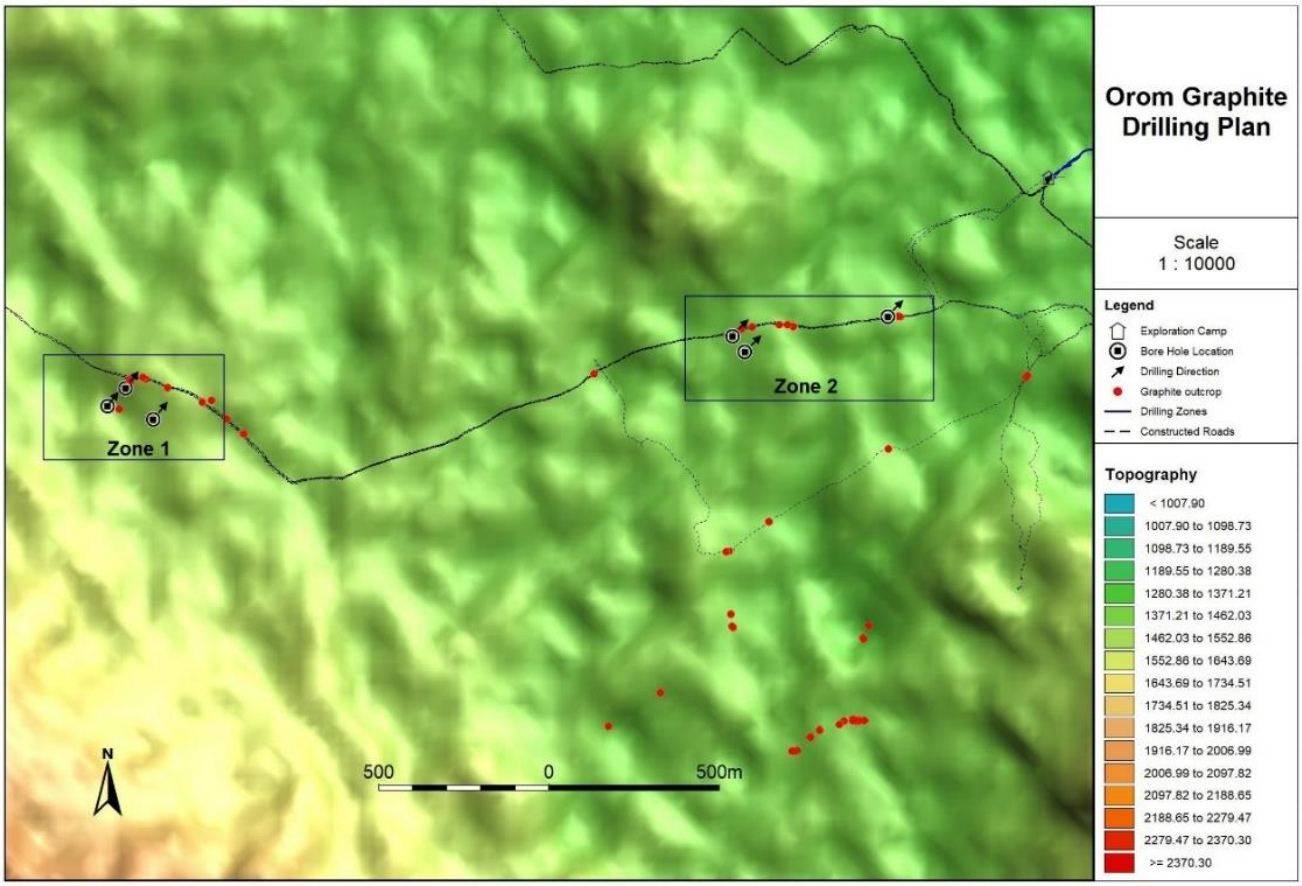

Figure 27 - Drilling campaign bore hole locations. Two zones identified based on surface mapping.

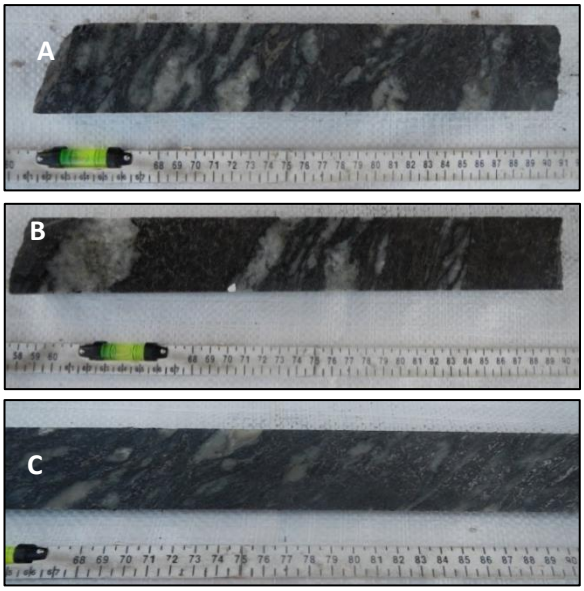

Figure 28 - Unweathered core of the graphitic gneiss member.
A:High grade well foliated graphitic gneiss displaying characteristic lens-shaped textures around elongated pinching coarser grained quartz and feldspars. Sulphides (pyrite) occur on foliation surfaces and within fracture zones. Browning biotite does occure with graphite along foliation planes.
B: Medium grade graphite gneiss. Bands of dark foliated ferromagnesian and graphite, alternating with thin bands of white to creamed coloured quartz and feldspars.
C: High grade graphite gneiss with lens-shaped nodules of coarser grained quartz and feldspar. Minor disemminated sulphides present.

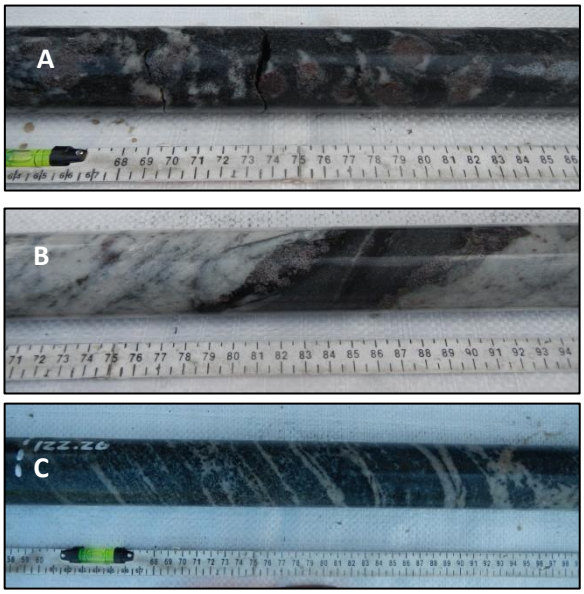

Figure 29 – Amphibole and pyroxene dominated members alternating with quartzo-feldspathic members, accessory minerals of garnet within amphibolite member.
A: Large aggregates of pinkish purple garnets within medium grained amphibolite matrix displaying lens-shaped textures with garnet porthyroclast with asymmetric tails of leucosomes (High temperature deformation).
B: Band (5 cm thick) of fine- to medium-grained amphibolite with pinkish aggregates of small garnets concentrated on the contact boundary between the amphibolite and quartzo-feldspathic rock.
C: Medium to coarse grained, poorly foliated, banded, dark green amphibolite with thin (<1 cm thick) quartz and feldspar dominant stringers.

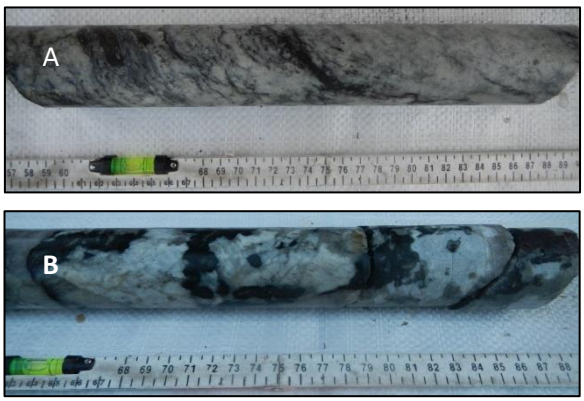

Figure 30 – Quartzo-feldspathic members intersected.
A: Medium grained quartz and feldspar dominant lithology with thin stringers of well foliated micas and minor amount of graphite. Sulphides do occur on foliation surfaces and within fractures.
B: Minor lithological unit comprising dominantly of quartz and feldspars reaching up to 5 cm in diameter, with large aggregates of amphiboles and pyroxenes scattered through the lithological unit. Large reddish pink garnet can be seen on the right-hand edge of the core.

The primary lithologies intersected included graphitic gneiss, amphibolite and quartzo-feldspathic gneisses as illustrated within the halved core intersections seen in Figure 28, Figure 29, and Figure 30. The weathering profile observed in the core suggested deeper weathering within the low-lying areas (average depth of 50m) relative to the hill crests and slopes which is typical of topical to sub-tropical regions with an average rainfall form 270 – 2000mm per year (Berry and Ruxton, 1959).

The drilling results suggest that the local uniformity of the graphitic units is highly complex with graphitic bands anastomosing within the quartzo-feldspathic gneiss. This results in highly irregular grades which can vary considerably from a couple of meters to centimetres as illustrated in Figure 31 and in Table 7. The combination of data from the drilling, mapping, and trenching programs revealed a graphitic lithological unit that is continues with strike and depth. Further drilling is however required to increase the geological confidence of this graphitic unit.

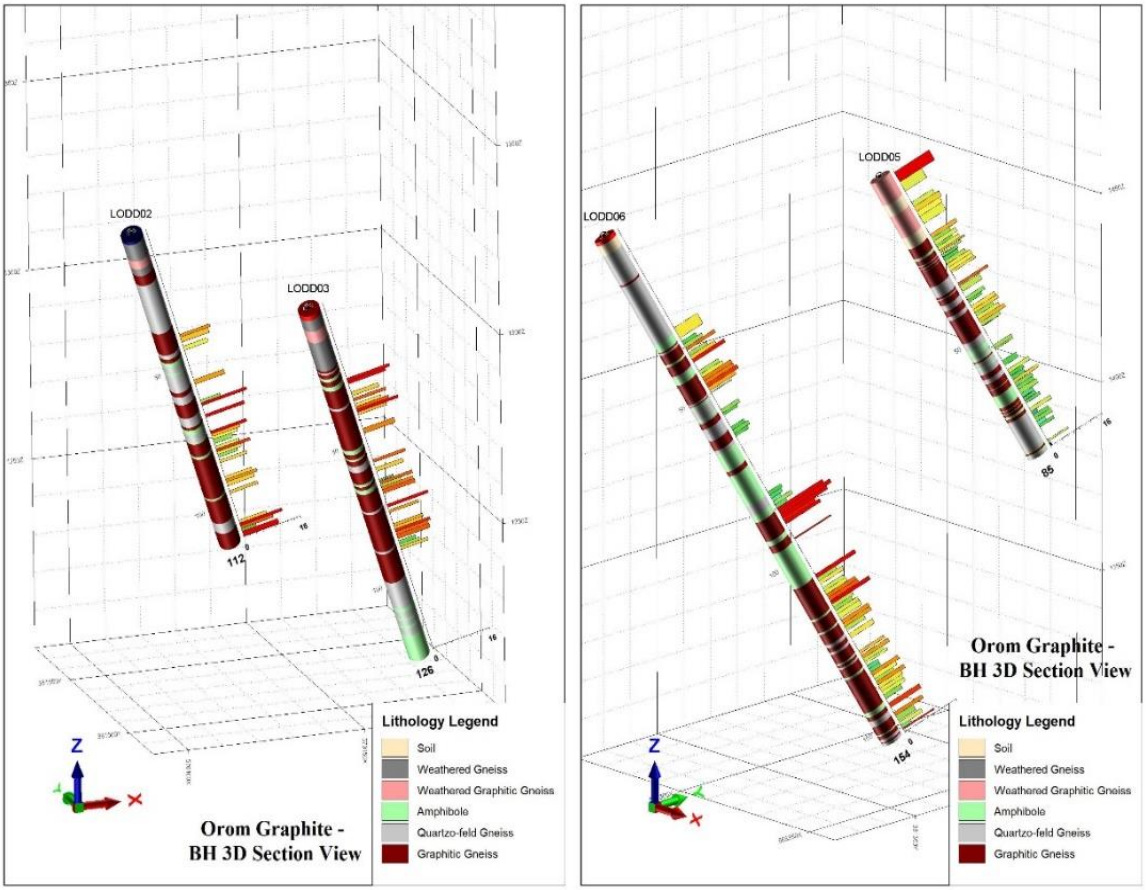

Figure 31 – 3D sections of four bore holes illustrating the lithological intersections as well as the Graphitic Carbon Grades. Grade scale indicated at the bottom of the bore hole.

Table 7 – Significant intersections and graphitic grade distribution of bore holes LOFF 06 and LODD 03. Gr Gn = Graphitic Gneiss; Gr Gn/Amph = Graphitic Gneiss with thin stringers of amphibolite; L = Low Grade; M = Medium Grade; H = High Grade. Grade determined by logging procedure (See section 4.8.5).

Hole_ID	Sample_ID	From	To	Interval	Lithology	GRAP_C
LODD06	M6078	80.66	81.66	1	Gr-Gn/Amph (L-M)	4.08
LODD06	M6079	81.66	82.66	1	Gr-Gn/Amph (L-M)	3.47
LODD06	M6080	82.66	83.55	0.89	Gr-Gn/Amph (L-M)	2.65
LODD06	M6081	83.55	84.55	1	Gr-Gn/Amph (M)	5.54
LODD06	M6082	84.55	85.6	1.05	Gr-Gn/Amph (M)	3.39
LODD06	M6083	85.6	86.6	1	Gr-Gn (H)	14.10
LODD06	M6084	86.6	87.6	1	Gr-Gn (H)	15.90
LODD06	M6086	87.6	88.6	1	Gr-Gn (H)	14.20
LODD06	M6087	88.6	89.6	1	Gr-Gn (H)	9.88
LODD06	M6088	89.6	90.47	0.87	Gr-Gn (H)	11.00
LODD06	M6089	92.82	94.11	1.29	Gr-Gn (H)	0.00
LODD06	M6091	94.75	95.07	0.32	Gr-Gn (H)	11.50
LODD06	M6092	105.94	106.94	1	Gr-Gn (M-H)	12.30
LODD06	M6093	106.94	107.94	1	Gr-Gn (M-H)	5.79
LODD06	M6094	107.94	108.94	1	Gr-Gn (M-H)	7.35
LODD03	M6175	23.92	25.77	1.85	Gr-Gn (M)	0.00
LODD03	M6176	27.38	28.38	1	Gr-Gn (M-H)	12.00
LODD03	M6177	28.38	29.38	1	Gr-Gn (M-H)	10.60
LODD03	M6178	29.38	30.38	1	Gr-Gn (M)	0.00
LODD03	M6179	30.38	31.38	1	Gr-Gn (M)	0.00
LODD03	M6180	31.38	32.38	1	Gr-Gn (M)	0.00
LODD03	M6181	32.38	33.73	1.35	Gr-Gn (M-H)	7.64
LODD03	M6182	34.65	35.65	1	Gr-Gn (M-H)	9.14
LODD03	M6183	36.65	37.65	1	Gr-Gn (M-H)	7.29
LODD03	M6184	37.65	38.65	1	Gr-Gn (M-H)	9.19
LODD03	M6186	38.65	39.65	1	Gr-Gn (M-H)	11.60
LODD03	M6187	39.65	40.65	1	Gr-Gn (M)	8.12
LODD03	M6188	40.65	41.65	1	Gr-Gn (M)	0.00

4.8.5 Project Standard Operating Procedures

The standard operating procedures (SOP) are based on the Australian-JORC and Canadian-NI43 101 Standards and Guidelines. These SOP were implemented during the mapping, trenching and drilling sampling campaigns.

I. Logging

The core obtained was subjected to three separate stages of logging, each implemented to collect different data. These logging categories include 1) core loss/gain, 2) lithology/geological and 3) geotechnical/structural logging.

The core loss/ gain logging stage started off by orientating the core so that the bedding plane is as close to perpendicular as possible to the length of the core box. Each third meter of core was pieced together at natural breaks in order to assure the core is orientated with increasing depth from top-left to bottom-right of the core box. At the end of each core run, the natural breaks were checked for "bottom breaks". This indicates that the core had a clean break at the bottom of the drill bit and is marked by a slight increase in the core diameter. These bottom breaks were used as start points for meter marking. Following the orientation and management of the core, core loss and gain were measured for each core run as drilled by the drilling team. The percentage of core recovered, and losses could be obtained by dividing the total recovered core by the total length of the core run. It should be noted that in this case, core refers to any piece of cylindrical rock mass which contains geological data. Irregular rock pieces and unconsolidated soil material did not add to the core recovery.

The geological logging implemented, gathered all relevant geological data such as the following:

- Lithological Data
    - Colour
    - Mineral Assemblages
    - Rock type
    - Grain Size
    - Contact type,
    - Texture
    - Fabric
    - Alteration type
    - Alteration style
- Mineralisation
    - Type of Mineralisation
    - Mineralisation %
    - Sulphide %

An additional column was provided for any comments or interpretations made by the logging geologist. This interpretation section was highly encouraged as the data available for the area was sparse.

The geotechnical logging provides information as to the rock-quality designation (RQD) and identifies zones with high fractures and joints. The data collected included the flowing:

- Joint numbers and spacing
- Bedding and fracture plane orientation
- Joint fill type
- Joint infill thickness
- Abrasiveness of natural core breaks
- Rock-quality Designation: $\frac{\sum core\ pieces > 100\ mm}{length\ of\ drill\ run} \times 100$

II. Data Management

Data was managed by the on-site and project geologist. The logging procedures mentioned above were gathered on hard copy paper, with the logging geologist responsible for capturing the data on an Excel template document. Each logging template contains a column which the site geologist must sign in order to identify the responsible person and thus assures a chain of custody is maintained. Once the project was completed, all hard copy files were scanned and added to the database for future reference. In addition to the core logging sheets, each core tray was photographed and uploaded to the database.

III. Quality Assurance and Quality Control

The quality control was implemented on two levels. The first consisted of field duplicate, blank and certified reference material (CRM or standards) being inserted into a 20-sample batch. The primary function of these quality control samples is to audit the sample preparation facility and the sample analysis laboratory for possible sample contamination, analysis repeatability as well as the instrument and analysis method accuracy. This assures that the results received are both accurate and precise. The second level of quality control was implemented by the analytical laboratory. Each laboratory inserted their own duplicate and CRMs which were monitored by the analytical staff as each sample batch was analysed.

IV. Security

Sample and core security was controlled by the site geologist from the drill to the shipment facility in Kampala. The core was transported by the logging geologist from the drilling site to the exploration camp where logging and sampling occurred. Core handling was conducted under the supervision of the site geologist during logging and sampling. This assured that a limited amount of personnel had access or control of the core during the handling, logging and sampling period thus prohibiting core and sample manipulation. The halved core is stored in Kitgum in a container on a secure facility whilst all the samples reject material is stored in a container in South Africa for future reference.

4.8.6 Initial Metallurgical Tests

During the course of the exploration program, a number of samples were submitted to two different laboratories namely SGS South Africa and SJT MetMin for metallurgical analysis, grade distribution analysis, flake liberation studies and mineralogical investigation. The author, along with members of the exploration team, planned and managed these analytical studies with the physical work and interpretations being conducted by qualified external consultants and contractors. This section will draw on the data and results as provided by the responsible contractors and consultants.

The metallurgical studies were conducted to establish whether the graphite can be liberated and upgraded, and if any of the gangue minerals would have a significant impact on the mineral processing. This process was aimed at determining the Reasonable Prospects for Eventual Economic Extraction (RPEEE) required to eventually report the mineralisation body within a Resource category for graphite as an industrial commodity. The metallurgical tests were conducted on both the weathered and unweathered zones as each contains different physical and chemical properties and will react differently within a processing circuit.

I. Graphite Grade Analysis (Weathered and un-weathered material)

Graphite grade analyses were conducted on pit, trench and rock samples collected during the mapping and trenching programs (classified as weathered samples) and in-situ samples collected during the drilling program (classified as unweathered samples). The majority of the weathered trench samples were collected from the three trenches intersecting the mineralised band of target 1 and 2 and delivered a total of 12 bulk samples. The results of these samples delivered a grade distribution across the intersecting mineralised lithology. The reject material discarded after the grade analysis was kept for further metallurgical studies which will be fully discussed in the following sections. Similar analysis was conducted on the unweathered samples collected from the core during the drilling campaign with the reject material stored for further metallurgical analysis. The grade analysis conducted on the unweathered samples provided a grade distribution with depth.

The analytical method used during the different exploration programs was kept identical in order to eliminate analytical bias that can develop from different analytical techniques. The results reported both total carbon and graphitic carbon percentages and were obtained by combustion analytical method known as LECO. The results for the weathered and unweathered samples suggested that the weathered samples contained on average a higher grade but wider variability than the unweathered samples which contain a lower averaged GC grade but less variability. A summary of the grade results is illustrated in Table 8 with the sample grade distribution histogram illustrated in Figure 32.

Table 8 – Statistical summary of the head grade chemical analysis obtained from weathered and un-weathered samples.

	Weathered Samples				Un-weathered Samples	
	Pit Sample Grades n = 48		Trench Composite Sample Grades n = 12		Core Sample Grade n = 222	
	C (Total %)	C (Graphite) %	C (Total %)	C (Graphite) %	C (Total %)	C (Graphite) %
Min	0.48	0.38	3.85	3.08	0.73	0.55
Max	29.60	26.20	9.71	9.15	16.70	15.90
Mean	12.12	10.71	6.66	6.08	8.34	7.86
Range	29.12	25.82	5.86	6.07	15.97	15.35
Var	45.60	36.21	3.97	4.62	8.86	8.04
StDev	6.75	6.02	1.99	2.15	2.98	2.84
CoV	0.56	0.56	0.30	0.35	0.36	0.36
Mode	12.10	10.00	#N/A	#N/A	14.30	6.73
Median	12.35	10.20	6.47	5.65	7.97	7.60

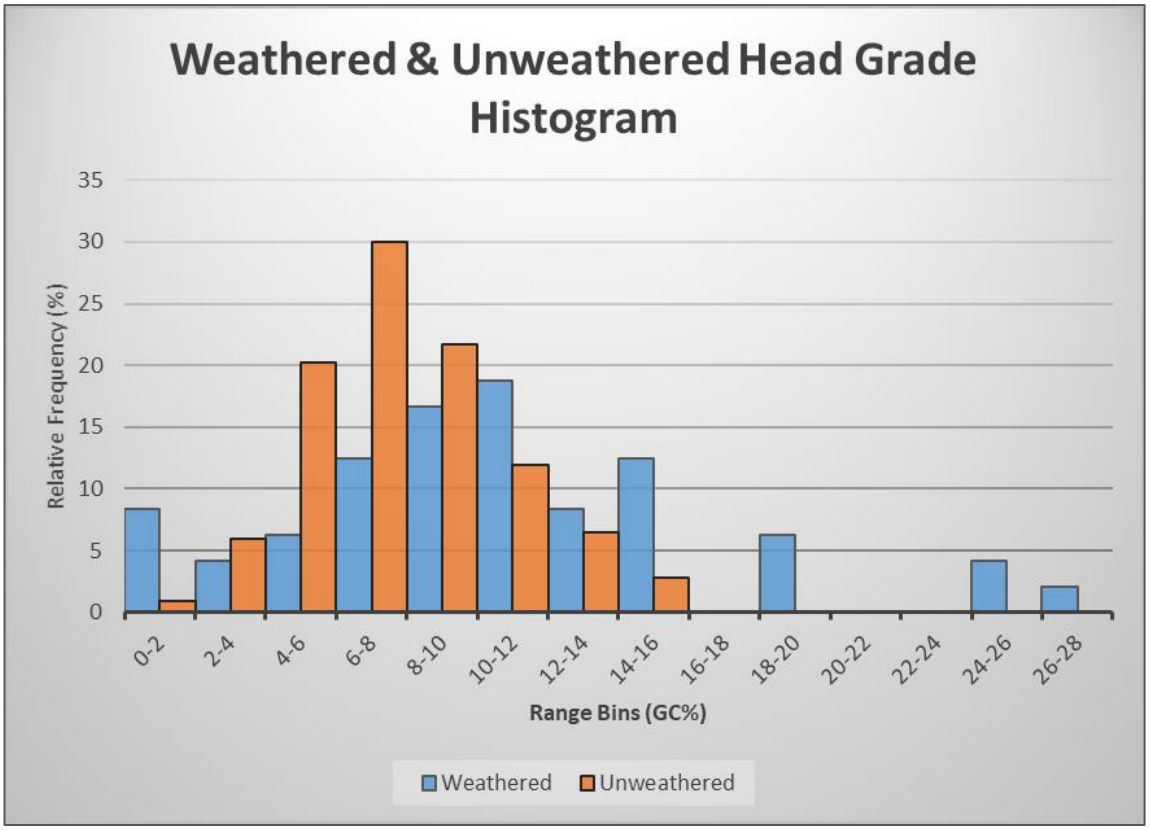

Figure 32 - Weathered and unweathered head grade distribution histogram illustrating the graphitic carbon grade population. GC% = Graphitic Carbone Percentage

II. Flake Size distribution analysis (Weathered and unweathered material)

The graphite flake size distribution was studied by SGS laboratories in South Africa. The method used to estimate the graphite distribution included counting 150 grains from each sample thin sections and measuring the flake length and width. The recoded graphite dimensions were used to calculate the area occupied by the flakes and to categorize them into predetermined flake length groups. Each size distribution group was then analysed in order to obtain a representative graphitic carbon grade. The grade distribution analysis of the weathered material obtained during the reconnaissance program was composited a homogenised into one sample with a head grade graphic carbon content of 12.5GC% (Table 9). The overall trend observed from the weathered graphite size distribution indicates that the small to large graphite flakes contains the highest graphitic carbon grades, with the highest upgradeability occurring within the +250 µm to -1500 µm size fraction represented by the graphitic carbon distribution curve (Figure 33).

Table 9 – Graphite flake size and grade distribution of the collective un-weathered graphite flakes.

Weathered Graphite Flake Size Fraction Distribution					
Microns	**Size Class Terminology**	**Mass**		**Graphitic C**	
		g	**%**	**%**	**Distr %**
-45 µm	**Fine / Amorphous**	126.90	12.54	5.8	5.8
+45 µm	**Fine / Amorphous**	50.90	5.03	9.45	3.79
+75 µm	**Fine / Amorphous - Small**	89.33	8.82	11.5	8.1
+125 µm	**Small**	169.88	16.78	15.1	20.23
+250 µm	**Medium- Large**	196.80	19.44	16.3	25.3
+500 µm	**Large - Jumbo**	208.08	20.55	13.8	22.64
+1000 µm	**Jumbo**	141.24	13.95	10.5	11.69
+1500 µm	**Jumbo**	29.21	2.89	10.6	2.44
Total		**1012.34**	**100**	**12.53**	**100**

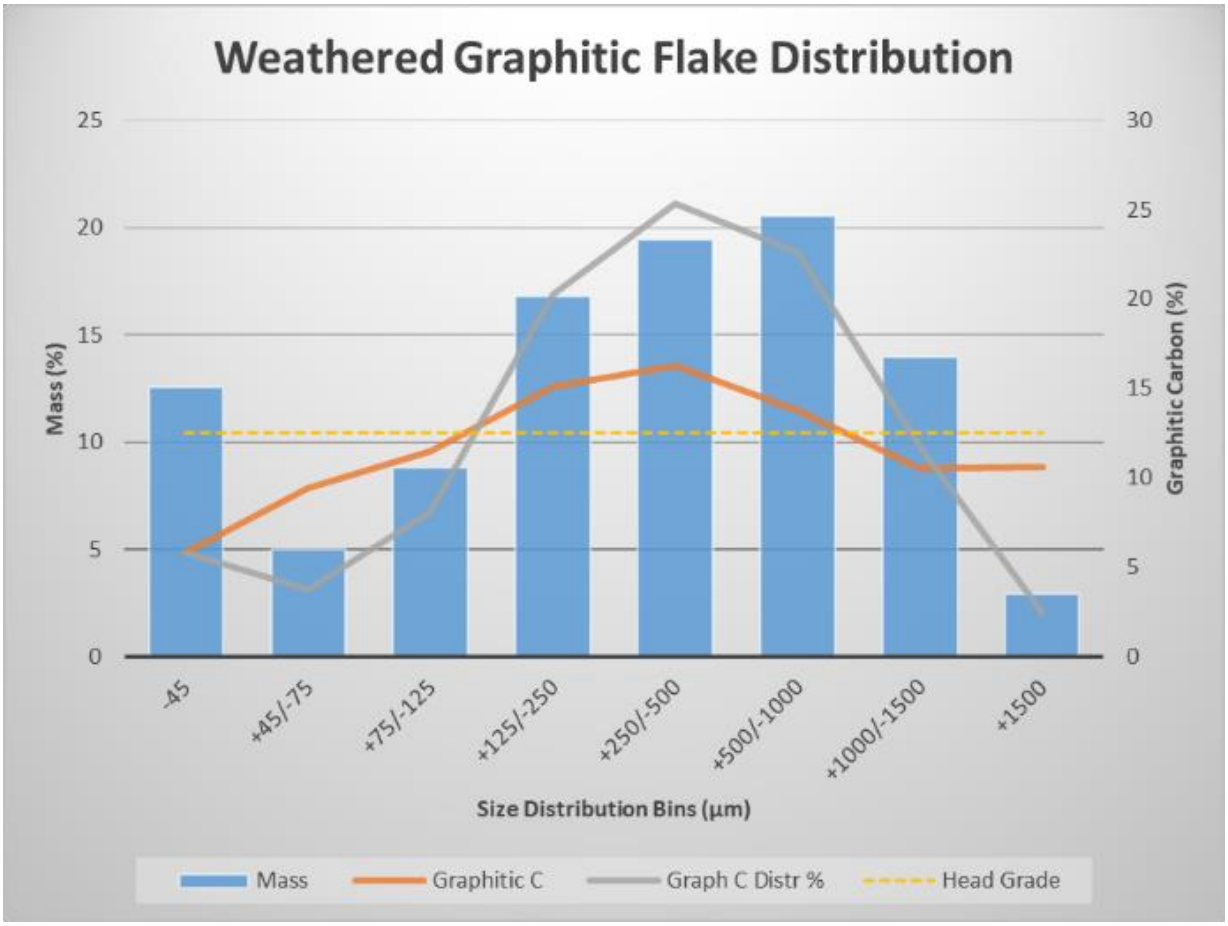

Figure 33 – Weathered graphite flake size distribution graph illustrating the graphite flake sizes with represented graphitic carbon grades.

The unweathered distribution size and grade analysis was conducted on three individual samples representing low, medium and the high grade (Figure 34). These grades were determined based on visual graphite flake concentration within the host material, assigned during the field sampling program. The graphite size distribution indicates that 60% of the total flakes are above 212 µm in size. The graphitic carbon grade of these size fractions indicates that a higher carbon grade (and graphitic carbon) occurs within the +106 µm to -425 µm size fraction (medium to jumbo size according to the market terminology). The larger flake size fractions (+425 µm) contain lower graphitic carbon grade which is most likely due to gangue minerals attached to the large flakes.

Table 10 below illustrates the size fraction distribution for the three composited samples. Figure 34 visually illustrates the size fraction mass percentage (blue bars) and graphitic carbon grades (orange line). The yellow dotted line represents the head grade of each sample. These results suggest that a potential grade upgradeability can be obtained by simply separating the flakes into size fractions, seen with the +106 µm to +425 µm grade increase relative to the head grade.

Table 10 – Three graded samples with illustrated size distribution and grade analysis.

	Mass		Graphitic Carbon		
			Grade	Distr.	Cum Distr.
Microns	g	%	%	%	
Low Grade (Head Grade 6.1%)					
-106µm	231.59	23.21	4.76	18.76	18.76
+106µm	142.01	14.23	7.68	18.56	37.32
+212µm	256.2	25.67	8.24	35.93	73.25
+425µm	76.26	7.64	6.08	7.89	81.14
+850µm	96.5	9.67	4.42	7.26	88.40
+1180µm	195.39	19.58	3.49	11.60	100.00
Total	997.95	100.00	5.89	100.00	
Medium Grade (Head Grade 8.98%)					
-106µm	270.5	26.06	5.73	16.92	16.92
+106µm	177.38	17.09	8.91	17.25	34.16
+212µm	209.91	20.22	11.6	26.57	60.74
+425µm	165.22	15.92	11.9	21.46	82.19
+850µm	73.45	7.08	9.39	7.53	89.72
+1180µm	141.44	13.63	6.66	10.28	100.00
Total	1037.90	100.00	8.83	100.00	
High Grade (Head Grade 12.5%)					
-106µm	205.05	20.43	10.7	17.46	17.46
+106µm	134.53	13.40	16.5	17.67	35.13
+212µm	185.73	18.51	17.6	26.01	61.14
+425µm	208.54	20.78	11.4	18.92	80.06
+850µm	97.28	9.69	10.7	8.28	88.34
+1180µm	172.54	17.19	8.49	11.66	100.00
Total	1003.67	100.00	12.52	100.00	

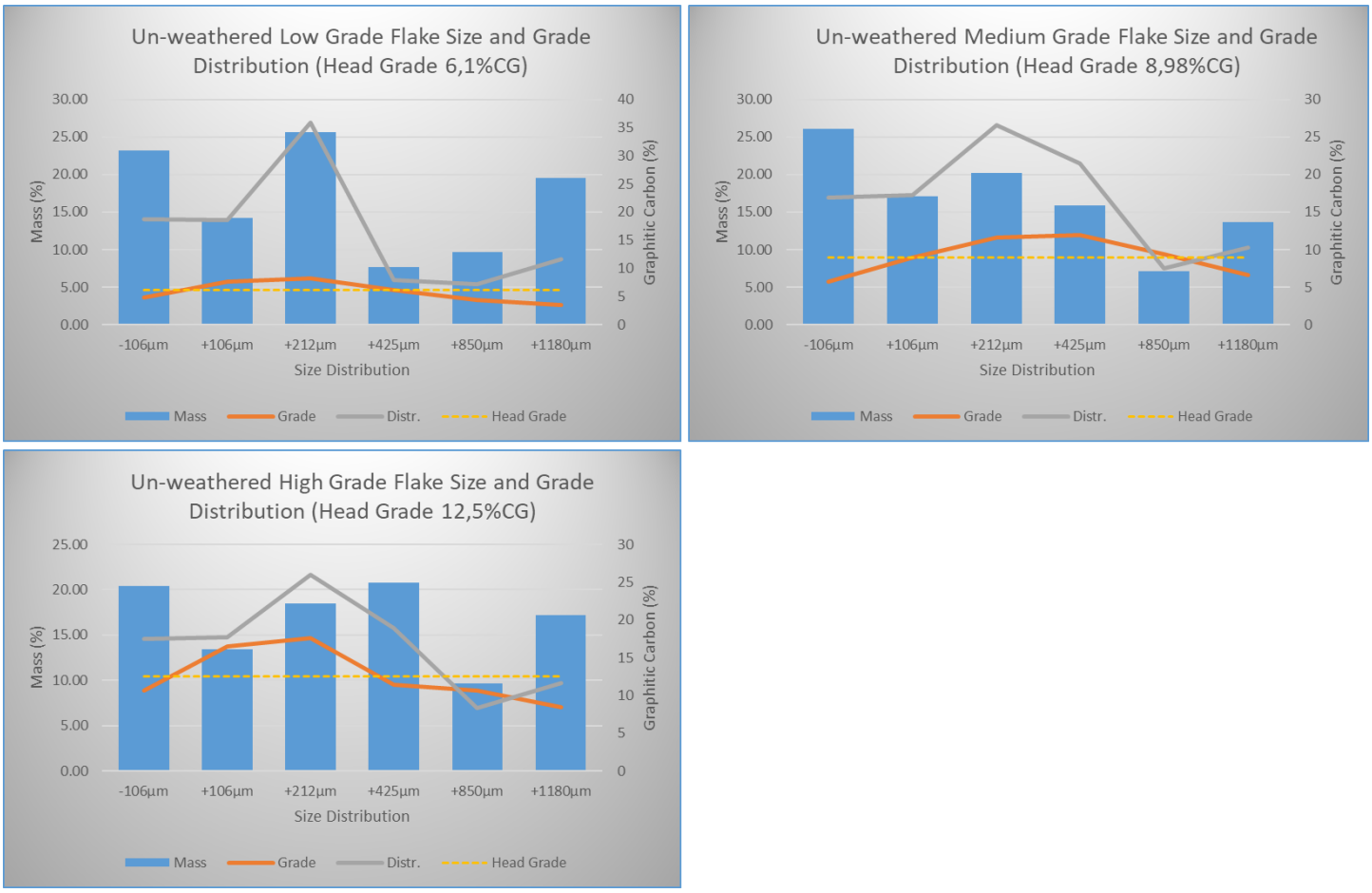

Figure 34 – Unweathered graphite flake and grade distribution graphs for low, medium, and high-grade graphite lithologies. The blue bars represent the sample mass plotted on the primary axes (Left). The line graphs (Grade, Distr, and Head Grade) represents the concentrations reported in percentage plotted on the secondary axes (Right)

III. Mineralogy and flake liberation (Weathered and unweathered material)

Mineralogical studies were conducted on the unweathered and weathered samples collected during the drilling and trenching stage. The first test was conducted by SGS using XRD analysis on the low, medium and high-grade samples. The main mineral assemblages consisted of quartz, biotite, plagioclase and graphite with trace amounts of calcite, garnet, amphibole and chlorite.

Table 11 - Mineralogical XRD studies conducted on low, medium and high-grade samples

Minerals	M6152 (Low Grade)	M6204 (Medium Grade)	M6244 (High Grade)
Quartz	25 - 50%	25 - 50%	25 - 50%
Mica (Biotite)	15 - 25%	15 - 25%	15 - 25%
Plagioclase	25 - 50%	5 - 15%	15 - 25%
Graphite	5 - 15%	5 - 15%	5 - 15%
Calcite	Tr	Tr	Tr
Garnet	Tr	-	-
Amphibolite	-	Tr	-
Chlorite	-	-	Tr

The samples separated according to the graphite flake size distribution bins discussed in section II were used to identify the associated gangue minerals and individual flake liberalization index for both the weathered and unweathered samples using an electron microscope. The method included visually identifying the graphite and gangue minerals form the unweathered (Figure 35) and weathered material (Figure 36) after the crushing and screening processes.

The graphite size distribution for both the weathered and unweathered material remained relatively uniform. The liberalization study however revealed different gangue mineral characteristics for the weathered and unweathered material. The unweathered gangue material associated with the graphite flakes generally consisted of mica (biotite), sulphides (pyrite) and quartz grains. Crushing of the un-weathered material liberated the graphite flakes from the quartzite but left the micas and sulphides still attached. Further crushing, grinding or chemical liberalization techniques will be required to liberate the graphite flakes from these gangue minerals.

The Electron microscope study on the weathered material revealed a different mineral assemblage consisting of quartz, kaolinite, goethite, micas and graphite. Crushing liberated the graphite flakes from the quartz grains but left kaolinite, goethite and micas still attached. This suggests that additional mechanical or chemical metallurgical processing techniques are required to liberate the graphite flakes.

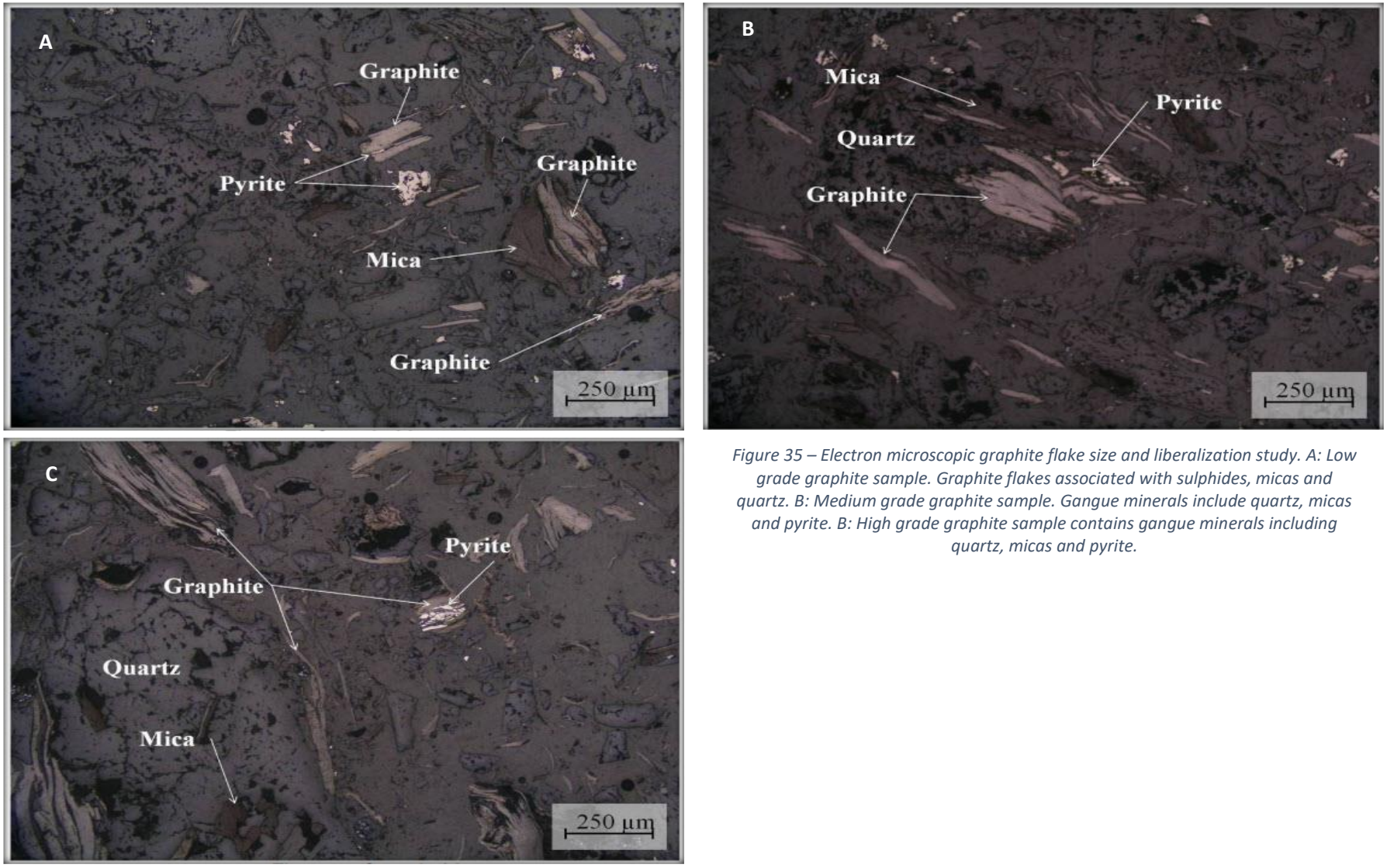

Figure 35 – Electron microscopic graphite flake size and liberalization study. A: Low grade graphite sample. Graphite flakes associated with sulphides, micas and quartz. B: Medium grade graphite sample. Gangue minerals include quartz, micas and pyrite. B: High grade graphite sample contains gangue minerals including quartz, micas and pyrite.

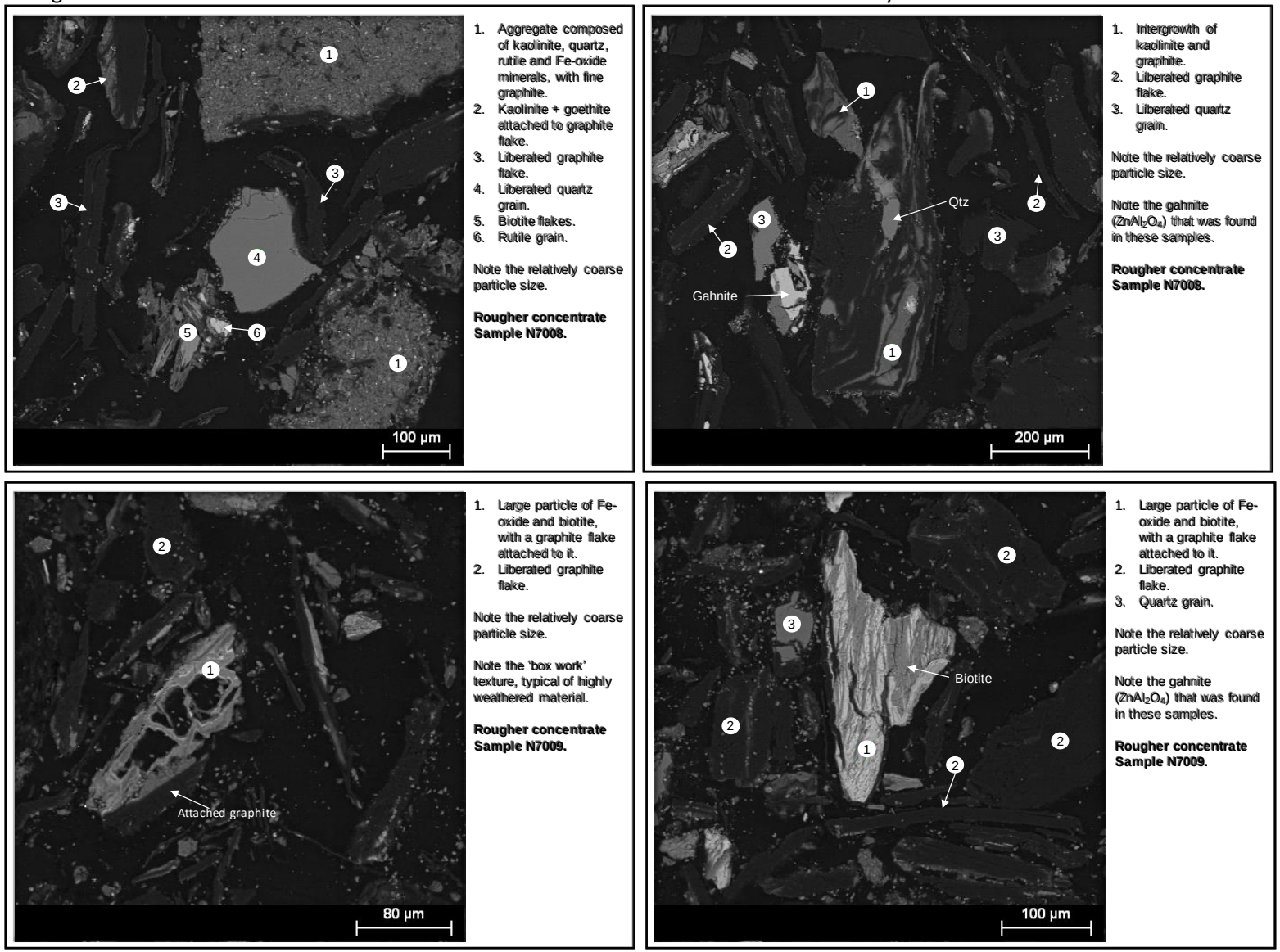

Figure 36 – Electron microscope graphite flake size and liberalization study conducted on concentrate material produced during the upgradeability analyses of the weathered trench material indicating liberated graphite flakes as well as gangue material still attached to the graphite flakes.

IV. Flotation upgradability study (weathered material)

Two sets of flotation testing were conducted on the weathered graphite material collected during the reconnaissance mapping and trenching programs. The samples were split according to size fractions as was discussed in the previous sections. Each size fraction was then subjected to flotation processing in order to determine whether the graphite material could be upgraded to industrial standards. Thus, the primary focus of this these studies was to determine if the graphite can be recovered within the industry grade standards and what process will be required to achieve a marketable graphite product.

The first set of flotation upgradability tests was conducted by SGS Laboratories in South Africa on weathered samples collected during the mapping reconnaissance program. The flotation process was performed on six 1 kg composite samples which were crushed to 1.7 mm and wet screened into four size fractions (53 µm, 53 - 300 µm, 300 - 710 µm, and +71 µm). Three tests were performed on these samples in order to determine one:

1. the bulk rougher recovery of the graphite mineral
2. the base-line cleaner grade without milling
3. the upgrade potential with milling of the concentrate

The first flotation test was performed with the aim of establishing the bulk rougher recovery of the graphite mineral, as well as establishing the relative grain size of recoverable minerals. The results indicated a collective recovery of 75% at a graphitic carbon grade of 73.9% with the +710 µm size fraction producing above collective average graphitic carbon and best recovery results (Table 12).

Table 12 – Weathered samples upgradeability flotation test 1: Rougher Concentrate (SGS)

				Grade	Recovery
Product	Time	Mass	Mass	Graphitic C	Graphitic C
	(min)	(g)	(%)	(%)	(%)
+710 µm		12.4	1.3	78.9	8.69
-710+300 µm		70.8	7.3	76.5	48.06
-300+53 µm		28.5	2.9	72.1	18.24
-53 µm		3.7	0.4	22.8	0.75
Rougher Conc.	5	115.4	11.9	73.9	75.73
Rougher Tail		851.8	88.1	3.2	24.27
Head Assayed				10.8	

The second flotation test was performed by excluding a milling stage within the flotation process circuit. The aim was to provide a baseline indicative cleaner grade without milling of the concentrate but increasing the collector dosage and residence time. The concentrate was then subjected to a single

cleaner stage. The results indicated an overall increase in the rougher concentrate grade to a collective 89.2% recovery graded at 86.1% graphitic carbon (Table 13). This stage was conducted without milling the rougher concentrate.

Table 13 – Weathered samples upgradeability flotation test 2: Upgrade potential without milling. (SGS)

				Grade	Recovery
Product	Time	Mass	Mass	Graphitic C	Graphitic C
	(min)	(g)	(%)	(%)	(%)
Cl Conc. 1		59.8	6.1	86.2	45.3
Cl Conc. 2		51.7	5.2	85.85	39
Cl Conc. 3		6.5	0.7	87.09	5
Total Cleaner Conc.	3	118	12	86.1	89.2
Cleaner Tail		35.2	3.6	12	3.7
Rougher Tail	5	832.1	84.5	0.97	7.1
Head Assayed				10.8	

The third upgradeability test conducted by SGS utilized the same parameters as in test 2 but included a milling stage prior to the cleaning stage. The product of this milling stage was subjected to two cleaning stages using sodium silicates. However, this extra milling stage did not increase the graphitic carbon grades and provided a collective recovery of 55.1% with a grade of 84.0% graphitic carbon.

Table 14 – Weathered sample upgradability flotation test 3: Upgrade potential with milling of the concentrate. (SGS)

Product	**Time**	**Mass (g)**	**Mass (%)**	**Grade**	**Recovery**
	(Min)			**Graphitic C (%)**	**Graphitic C (%)**
RCl Conc. 1		52.4	4.9	82.90	32.2
RCl Conc. 2		36.2	3.4	85.60	23.0
Total Re-Cleaner Conc.	3	88.6	8.3	84.00	55.1
RECLT		91.8	8.6	52.40	35.6
Cleaner Conc.	3	180.4	16.9	67.92	90.8
Cleaner Tail		33.0	3.1	7.67	1.9
Rougher Conc.	5	213.4	20.0	59.43	93.9
-53 µm		10.1	0.9	17.40	1.3
Rougher Tail		845.2	79.1	0.97	6.1
Head Calc		1068.7	100.0	12.63	100.0
Head Assayed				10.80	

The second study was performed by SJT MetMin Services on the weathered material collected during the trenching program. The study consisted of 4 tests with different parameters (Table 15). The tests could unfortunately not reproduce the results as seen in the previous tests conducted by SGS with the best results obtained during test 4 with a recovery of 73.8% at a graphitic carbon grade of 75.2% which is well below the industrial grade standards. The most likely cause of the low recovery and grades was sighted as being due to the mineralogy and poor liberalization of the graphite flakes. The solution to this problem will most likely involve further crushing and/or milling stages in order to liberate the graphite flakes.

Table 15 - Second Upgradeability study procedures and parameters. (SJT MetMin)

Test Number	Stages	Reagent Dosage	Residence Time	Additional
Test 1	1 Rougher Stage	200 g/t paraffin and 100 g/t MIBC	collected over a 3-minute residence time	Frother added when floatation ceased
Test 2	Desliming and 1 Rougher stage	200 g/t paraffin and 100 g/t MIBC	collected over 1, 3, 7, and 15-minute intervals (cumulative)	Frother added when floatation ceased
Test 3	2 minutes of Milling and 1 Rougher stage	150 g/t paraffin and 50 g/t MIBC (inter-stage reagent addition)	collected over 1, 3, 7, 15, and 30-minute intervals (cumulative)	Frother added when floatation ceased
Test 4	2 minutes of Milling, 1 Rougher stage, and 2 Cleaner Stages	150 g/t paraffin and 50 g/t MIBC (inter-stage reagent addition)	Rougher Float (30-minute), Stage 1 cleaner (5-minute), Stage 2 cleaner (3-minute),	Frother added when floatation ceased

4.8.7 Exploration Potential

The data obtained from the exploration work conducted to date does not warrant the reporting of resources within the inferred, indicated or measured category. This is due to the level of confidence obtained from the geological data and the complicated structural nature of the graphite mineralised body. This does not mean that the size and grade of the mineralised body cannot be quantified to some extent. The method used to quantify this graphite mineralisation was reported as a function of a range estimation whereby the tons and grades are reported as a lower and upper range rather than a specific number. By reporting the mineralisation potential, the possible investors are made aware

of the potential margin of error which can be reduced by increasing the mineralisation potential into a resource classification by means of further exploration programs conducted in the future.

Available data indicates that the weathered profile extends at depth from 20 m to 60 m below surface, depending on the topography. The specific gravity (SG) used for tonnage estimations was determined based on the Archimedes principle which integrates the weight of samples under normal atmospheric conditions as well as the weight within a known density medium, which in this case was water. The values obtained from these samples returned average SGs of 2.69 and 2.02 for unweathered and weathered samples respectively. A surface mineralisation area was calculated by importing the mapping and geophysical data into a software program (MICROMINE^{TM}). The surface mapping, trenching and drilling programs indicated that the mineralisation occurs within bands as thin graphite bearing gneisses with barren gneiss diluting the overall unit. This dilution factor was quantified by calculating the total graphite intersecting lengths versus the barren gneiss lengths mapped during the trenching (See section 4.8.3). The average graphite intersecting length for each identified graphite mineralised units quantified to 54%, suggesting that 46% of the length consisted of barren units. This dilution factor was used in the volume calculations for the mineralised potential range analysis with a range of depths used, based on the drilling data (Section 4.8.4).

Table 16 – Mineralisation potential range analysis indicating the possible size of the graphite mineralised body. SG 0-20m = 2.02; SG 20-60m = 2.69. Average grade of weathered material (0-20m) = 6.08 %GC; Average grade of un-weathered material (20-60m) = 8.01 %GC.

Geophysical Target	Surface Area (m^2)	Dilution Factor	Depth	Volume (mil m^3)	Tonnes (Mt)	Tonnage (Mt) (Lower Range) -25%	Tonnage (Mt) (Upper Range) +25%	Grade (%GC)
Target 1	4,686,038.00	54%	0-20	51.0	102.0	76.5	127.5	5.47-6.69
			0-40	101.0	238.0	178.5	297.5	6.27-7.67
			0-60	152.0	375.0	281.3	468.8	6.54-8.00
Target 2	3,699,706.00	54%	0-20	40.0	81.0	60.8	101.3	5.47-6.69
			0-40	80.0	188.0	141.0	235.0	6.27-7.67
			0-60	120.0	296.0	222.0	370.0	6.54-8.00

The two main target areas, as identified by the geophysical study (Section 4.8.2), were estimated to a depth of 20, 40, and 60 meters which represent the weathered (free-dig) and unweathered tonnage estimation (Table 16). The average graphitic carbon head grades as discussed in section 4.8.6.I were used to quantify the in-situ mineralisation potential. The grades obtained from the weathered pit samples collected during the reconnaissance program contain higher grades (Mean 10.71 %GC) than the weathered trench samples (Mean 6.08%GC). These grades do not however represent the weathered section as selective sampling could have upgraded the mean head grades. Thus, the decision was made to discard the weathered pit samples' grade estimation and instead use the mean

weathered trench grades within the mineralisation range calculations. This decision was based on the confidence level by which each sample represents the weathered unit.

The range method implemented (Table 16) used the volumes and grades obtained during the exploration programs and applied a buffering range to each. The grade range was estimated by calculating a 10% buffer of the selected mean grades reported for both the weathered (6.08%GC) and unweathered (8.01%GC) samples. A 25% buffering was used to calculate the volumes obtained from the mapping, trenching and geophysical results with the weathered and unweathered SG used to calculate the tonnages.

By applying three proposed depths, the following tonnage and grade ranges could be estimated for both targets 1 and 2 (Table 16):

- 0 – 20 m depth:
    - Lower tonnage range - **137.3 million tons (76.5 Mt + 60.8 Mt)**
    - Upper tonnage range - **228.8 million tonnes (127.5 Mt + 101.3 Mt)**
    - Grade range of - **5.47 to 6.69 % GC**
- 0 – 40 m depth:
    - Lower tonnage range – **319.5 million tons (178.5 Mt + 141.0 Mt)**
    - Upper tonnage range – **532.5 million tonnes (297.5 Mt + 235.0 Mt)**
    - Grade range of - **6.27 to 7.67% GC**
- 0 – 60 m depth:
    - Lower tonnage range – **503.3 million tons (281.3 Mt + 222.0 Mt)**
    - Upper tonnage range – **838.8 million tonnes (468.8 Mt + 370.0 Mt)**
    - Grade range of - **6.54 to 8.00% GC**

However, these estimations only estimate the graphite mineralisation potential for 2 out of the possible 4 main targets as well as a number of smaller regional “satellite” targets/anomalies.

5 ECONOMIC AND FINANCIAL ANALYSIS OF GRAPHITE PROJECTS

The growing global demand for graphite used in lithium-ion batteries has created a new development and investment potential for this industrial mineral. Although this renewed interest in graphite has spearheaded many exploration initiatives over the last decade, the economics, risks and uncertainties have provided a new maze to navigate for resource developers and investors. The following section will provide the reader with the basic financial analysis collected from exploration projects (See appendix for list of companies and projects used in this assessment) currently ranged from pre-feasibility studies to bankable/definitive feasibility studies. This economic assessment can be used to evaluate an exploration project based on the financial and economic factors of peer projects, thus establishing whether a project has a competitive potential within the graphite market.

The financial models only focus on the core aspects such as the initial and sustaining capital costs, operational costs associated with the mining, processing and screening, and the revenue based on the products sold. Taxes and royalties has been excluded to be able to evaluate each project based on measurable parameters.

5.1 Capital Expenses

The capital cost was divided into two criteria namely an initial capital cost and a sustaining capital cost. The initial capital cost is largely based on the operation size and the infrastructure required to produce the desired yearly concentrate. This amount included the construction cost, plant and mining equipment, processing facilities, tailing storage, cash float for mining activities that will not produce products and a percentage contingency which reflects the level of project development and certainty. The on-going or sustaining capital cost is estimated on a yearly base and predicts the amount of capital needed to maintain the equipment acquired from the initial capital expenses in order to sustain a productive operation.

5.2 Operational Expenses

The operational cost includes all expenses related to the extraction of 1 ton of graphite concentrate. The estimates include mining, processing, tailings management, site service and administration. The estimation takes into account steady-state operating conditions based on each optimised run-of-mine feed rate and final production rate.

5.3 Revenue

The revenue created by the mining and processing can be obtained from at least four product criteria based on the graphite flake size and graphitic carbon purity with higher price ranges with an increase in these categories (See section 3.1). Thus, the revenue calculated for each project utilizes the graphite

flake size distribution as estimated by metallurgical studies during the reserve estimation. Each project thus contains a unique blend of graphite concentrate product from which a basket price can be estimated that will provide its revenue throughout the Life-of-Mine. Table 17 illustrates the product categories used during the financial model for each project.

Table 17 – Graphite concentrate criteria used in the financial model.

Flake Size (Mesh)	Flake Size (microns)	Industrial Term	Price Base Case (USD per ton)	Price Lower Case (USD per ton)	Price Upper Case (USD per ton)
+50	+300 µm	Jumbo	1500	1100	1700
-50 to +80	-300 to +180 µm	Large	950	550	1150
-80 to +150	-180 to +75 µm	Medium – Small	900	500	1000
+150	-75 µm	Amorphous	700	400	800

5.4 Project Financial Models

The financial model and economic analysis included information supplied by various companies currently within different stages of developing graphite projects across the globe. The financial models only focusses on the economic aspect related to the extraction of a range of graphite product with values greater than 93% graphitic carbon with a recovery greater than 90%. One of the primary focusses of this analysis is to identify a possible trend related to proposed annual graphite concentrate production (Table 18). Due to the different the geographical locations of these projects the logistical value related to product transport was not considered. Taxes and royalties are also excluded from the financial models.

The initial capital expenses required to develop a project is determined by two criteria namely a determinable factor which includes the proposed project size, and undeterminable factors such as the project location and proximal predeveloped infrastructure available. Figure 37 illustrates the capital required to develop each project. This graph indicates that the initial capital does increase with the proposed project production size but also includes factors that can increase or significantly decrease the required capital needed. The trendline indicates that the initial capital needed greatly increase with project sizes ranging from an annual graphite production of 15 000t to 100 000t. This increase in the capital needed decreases and will almost plateau with project sizes greater than 100 000t concentrate per year. The same trend is observed for the on-going or for sustaining the capital needed (Figure 38).

The operational expenses included all cost associated with the extraction and processing of the graphite concentrate. In detailed financial analysis this cost also included the cost associated with transport as negotiated with the buyer or client. The operation cost of extracting graphite concentrate is estimated between USD 300 to USD 500 per ton with the bankable- and definitive- feasibility studies reporting operation costs of USD 300 and USD 400 per ton respectively. Figure 39 illustrates the operation cost per ton of graphite concentrate and suggests that the overall trend increases with an increase in project size. This increase is not however significant and averages between USD300 to USD400 per ton of graphite concentrate. The yearly operation cost reflects a more significant increase (Figure 40). This trend occurs due to the specific mining equipment used in the different project sizes in order to reduce the operation cost in larger run-of-mine projects.

By combining the capital and operational expenses over a LOM of 22 years, a yearly combined Capex and Opex can be calculated. This enables a visual comparison of each project related to its size (Figure 41).

The revenue of each project was calculated based on its graphite size category as estimated based on metallurgical analysis. This resulted in each project containing a unique product range which can be summarized based on the calculated basket value (Table 18). The LOM used to calculate the Net Present Value (NPV) was at 22 years at a discount rate or 8%. The calculated NPV indicated an increase in value with an increase in project size. The Internal Rate of Return (IRR) is however a function of the initial and ongoing expenses and operational cost versus the revenue and only measures the increase in value of the capital invested.

The final financial analysis conducted was aimed at establishing a yearly expense (Initial & on-going Capital + Opex) and possible revenue scenarios in order to establish a “Golden Zone” by which graphite projects can be evaluated. The fixed categories include a product of >95% graphitic carbon with a recovery of >92% and the graphite price and categories as stipulated in Table 17. This resulted in a range of possible revenue income streams with the maximum income obtained from a 100% Jumbo product and a minimum income obtained from a 100% amorphous product at a range of annual production. The yearly combined capital and operation cost was then superimposed within the possible revenue streams in order to obtain an indication as to the economic viability of a proposed project based on its yearly graphite concentrate production size (Figure 42).

Table 18 – Financial models of graphite projects ranging in size from 16 000 t concentrate per year to 313 000 t concentrate per year. Abbreviations: PEA = Preliminary Economic Assessment; PFS = Pre-Feasibility Study; FS = Feasibility Study; DFS = Definitive Feasibility Study; BFS = Bankable Feasibility Study; NPV = Net Present Value; IRR = Internal Rate of Return. Note: Graphite projects level of study as of Aug 2017, see appendix for list of companies and technical reports and dates used.

Graphite Project	Molo Deposit (NextSource Material)	Lindi Deposit (Walkabout Resources)	Lac Guéret Deposit (Mason Graphite)	Namangale Deposit (Volt Resources)	Nachu Deposit (Magnis Resources)	Balama Deposit (Syrah Resources)
Concentrate (tpa)	**16,000**	**40,000**	**50,000**	**170,000**	**220,000**	**313,000**
Level of Study	FS	DFS	PEA	PFS	BFS	FS
Mining Method	Open Pit	Open Pit	Open Pit	Open Pit	Open Pit	Open Pit
Mining and Processing	Mining, Mechanical Separation (Crushing and Grinding), Flotation, Drying, Screening, Bagging					
Base of Operations	Madagascar	Tanzania	Canada	Tanzania	Tanzania	Mozambique
Reported Life-of-Mine	30	22	22	22	22	42
Initial Capital (Mil USD)	18.00	39.00	130.00	173.00	269.00	144.00
On-Going/Sustaining Capital (Mil USD per Year)	0.08	5.59	0.49	5.00	4.68	7.10
Operation Expenses (USD per ton Graphite Concentrate)	300.00	300.00	400.00	500.00	400.00	300.00
Operation Expenses (Mil USD per Year)	4.80	12.00	20.00	85.00	88.00	93.90
Revenue Basket Price (USD/t)	1,009.89	1,224.96	965.81	1,072.90	1,136.42	894.44
Revenue (Mil USD per Year)	16.16	49.00	48.29	182.39	250.01	279.96
IRR	124%	81%	28%	50%	60%	112%
NPV (Mil USD)	92.00	269.00	181.00	680.00	1,324.00	1,961.00
Payback Period (Years)	1	2	5	3	2	1

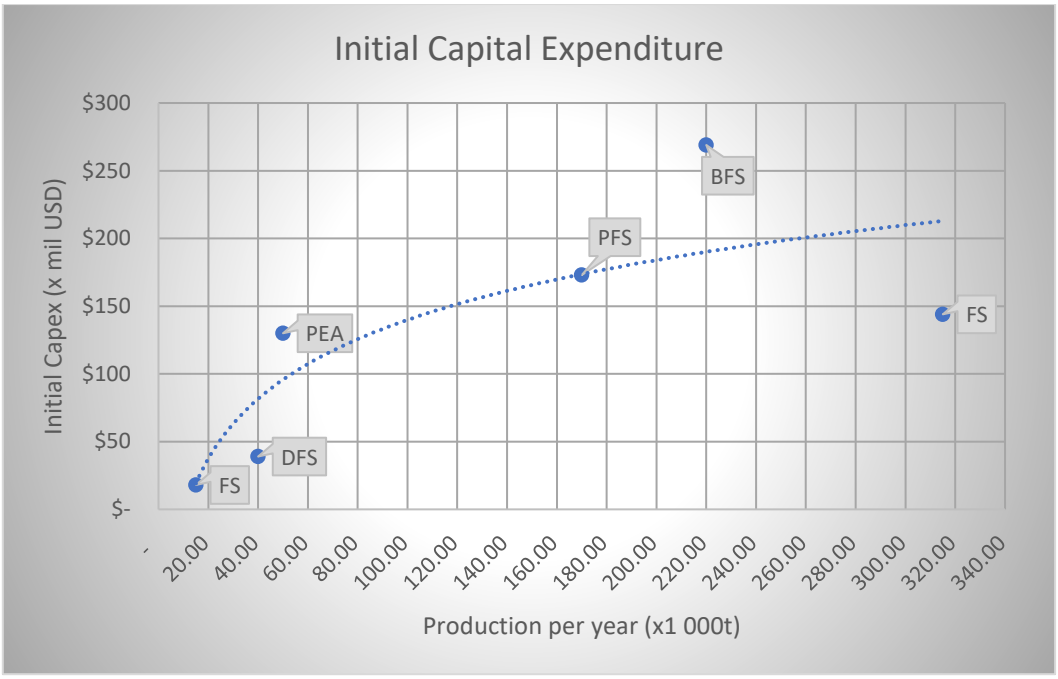

Figure 37 – The initial capital expenses required to construct a productive operation based on the desired graphite concentrate produced per year. Initial capital included construction cost, plant and mining equipment cost, and mining activities which will not produce product (pre-mining stripping or box cuts). Includes contingency based on the level of certainty with pre-feasibility studies containing a larger percentage contingency than definitive/bankable feasibility studies. PEA = Preliminary Economic Assessment; PFS = Pre-Feasibility Study; FS = Feasibility Study; DFS = Definitive Feasibility Study; BFS = Bankable Feasibility Study (Project development and certainty level based as described by project owner)

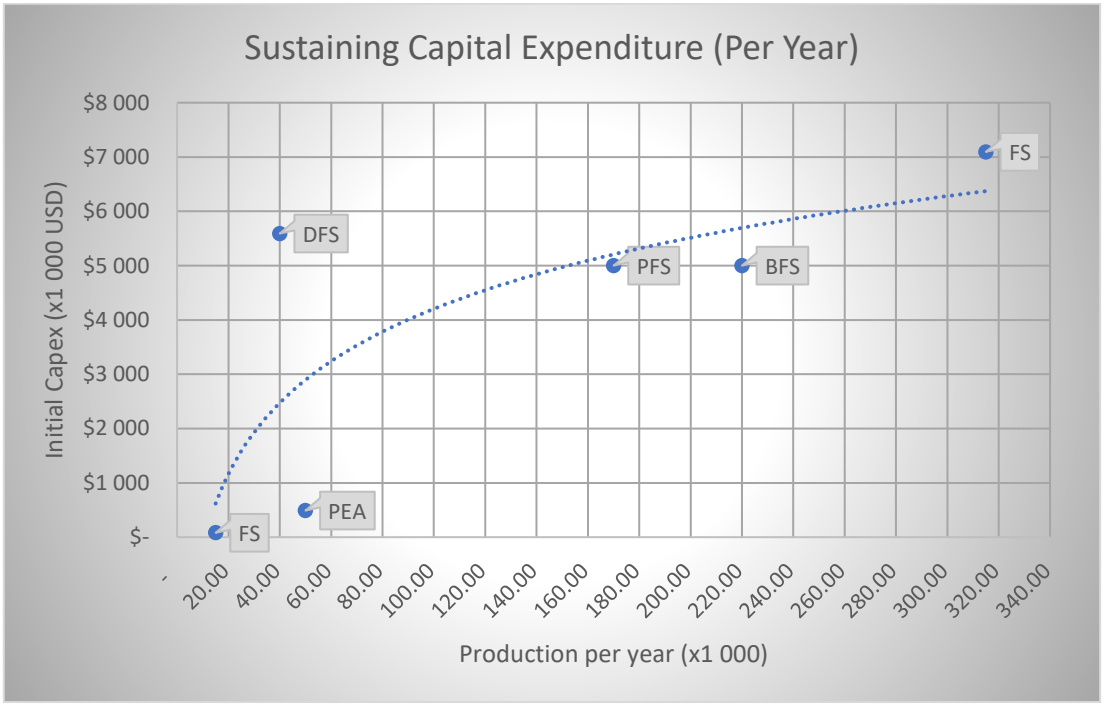

Figure 38 – On-going or sustaining capital per year required to maintain productive operations. PEA = Preliminary Economic Assessment; PFS = Pre-Feasibility Study; FS = Feasibility Study; DFS = Definitive Feasibility Study; BFS = Bankable Feasibility Study (Project development and certainty level based as described by project owner)

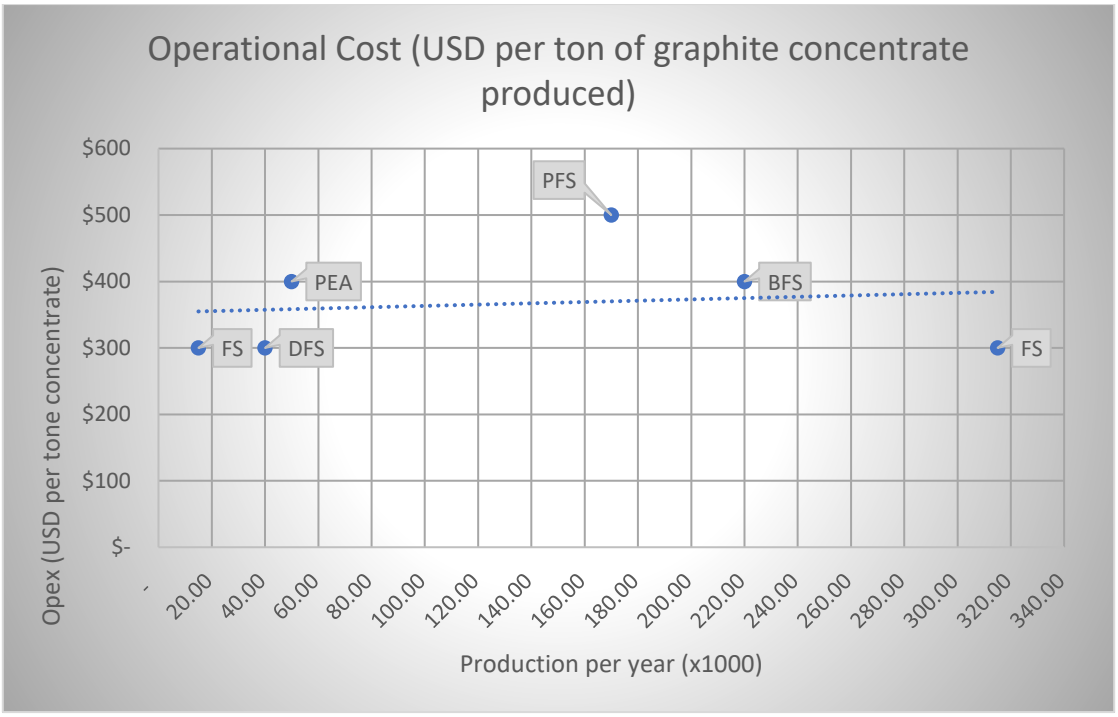

Figure 39 – Operating cost. Mining, processing, and administration cost involved in processing 1 ton of graphite concentrate.

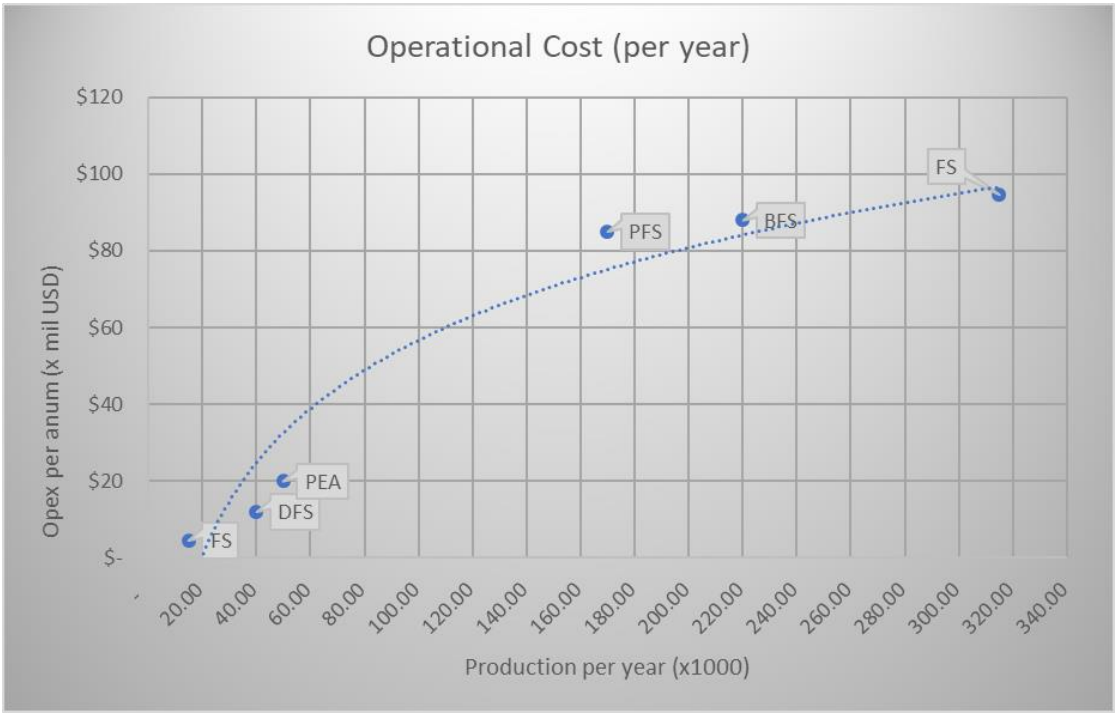

Figure 40 – Operating cost per years concentrate production.

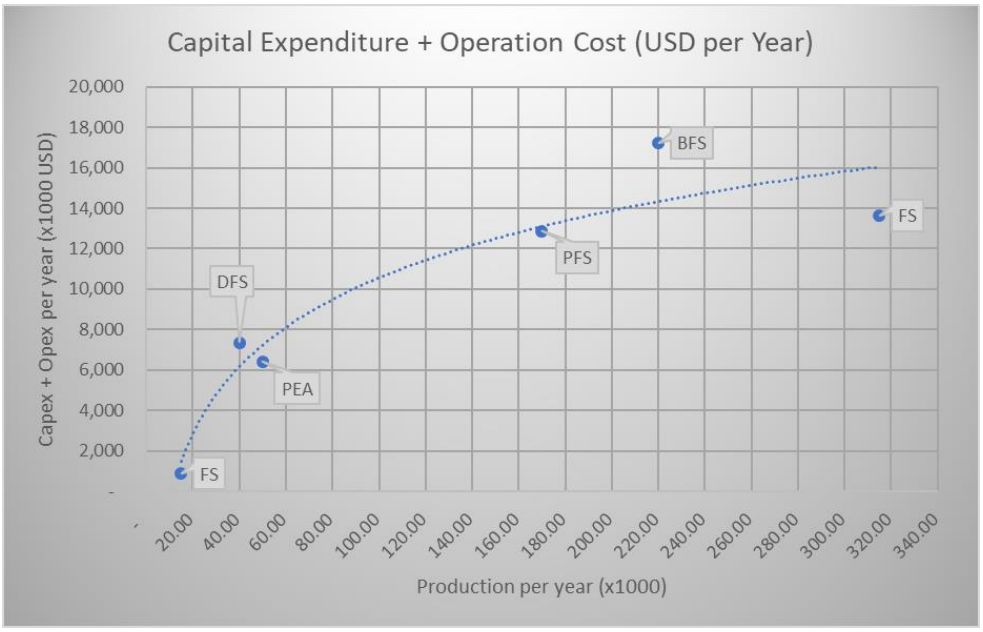

Figure 41 – Calculated yearly capital and operation expenses versus project size.

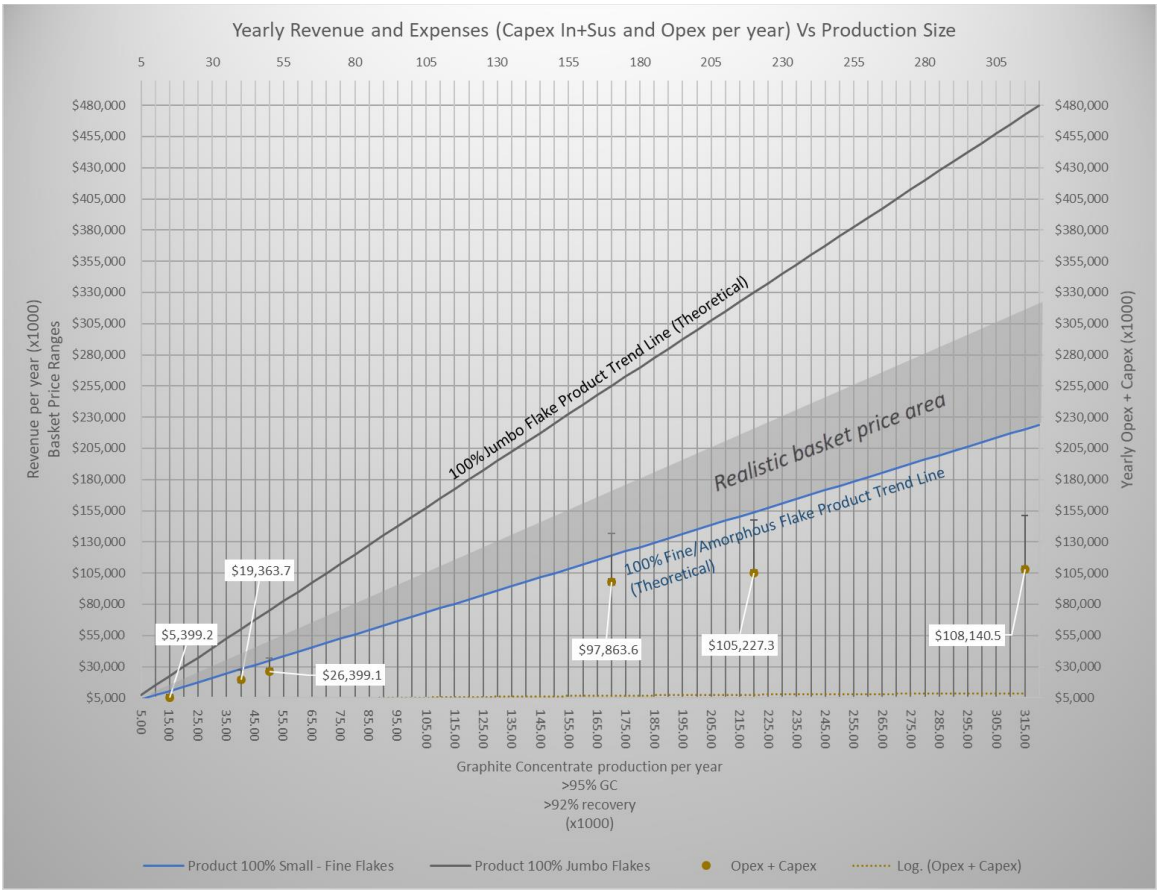

Figure 42 – Capex and Opex vs Revenue diagram illustrating the "Golden Zone" of graphite operations. Solid lines indicate the possible maximum and minimum revenue based on the different product size categories. The curved dashed line indicates the best fit overall Capex and Opex value with an increase in the project size. Error bars indicates a 40% increase in the Capex and Opex in order to visualize a possible increase due to tax, royalties (for illustrative purposes). Revenue based on Jumbo Flakes trading at USD 1,500 per ton concentrate & Small/Amorphous flakes trading at USD 700 per ton concentrate. Medium to large graphite flake concentrate products cost per ton assumed to trade at prices greater than USD 700 and less than USD1,500. Price effectively a function of market trend.

6 GRAPHITE PROJECT DEVELOPMENT AND MANAGEMENT

Developing a graphite exploration project from the initial targeting process to field scoping, and finally defining resources and reserves is a costly exercise accompanied by large risks. Managing these risks and effectively limiting the exposure to financial mismanagement can be accomplished by developing an exploration project development framework and implementing a decision point planning diagram. Figure 43 illustrates a basic project development framework from the conceptual target generation exercises, through to the final project development into a Definitive Feasibility Study (DFS).

The initial target generation phase consists of the development of a mineral deposition theory based on known geological features and similar or proximal mineralisation occurrences. This mineralisation theory then needs to be tested in the form of a scoping study. This phase of the project development, verifies the possible occurrence of a mineralisation body and determines whether the initial data supports an economic potential which will thus justify further development. On completion of the scoping phase, and the possible identification of a potentially economic mineralisation body, the management team can elect to continue delineating the mineral resource by progressing to the project development phase and Mineral Resource Estimation (MRE) phase. This phase consists of delineating an indicated to measured resource by means of drilling, trenching and metallurgical studies. By applying economic factors such as Capital requirement (CAPEX), Operational expenditure (OPEX) and the possible revenue generated, these resources can be converted to ore reserves.

The risks associated with developing an exploration project and progressing through the project development framework (Figure 43) can be quantified by developing a decision point planning tree (Figure 44). By developing such a diagram, the possible risks and rewards can be quantified for each decision, leaving a “road map” indicating whether or when a project should be abandoned or developed. The graph is based on a set of decision points with chance events that quantify the possibility of success or failure. Each decision point can either be implemented or skipped based on a specific circumstance or choice made by the management team. The chance that a decision leads to a positive or negative outcome can be estimated based on previous decisions or outcomes.

As the project develops and choices are made, the Net Present Value of a specific project can be quantified by means of a Cost-based Approach (Lilford and Minnitt, 2002). This method of valuating a project uses the cost of exploration and applies a multiplying factor based on the results of the specific exploration program. These multiplying factors are termed Multiples of Exploration Expenses (MME) and Prospectivity Enhancement Multiplier (PEM), first described by Lawrence (1994). The multiplying factors are listed in Table 19 below.

Table 19 – Cost Based Approach exploration valuation method with Prospectivity Enhancement Multipliers.

Multiplier	Exploration Results
< 0.5	Little to no encouraging results from extensive exploration. Past work has downgraded prospectivity significantly. Future exploration expenditure not warranted.
x 0.5 -1.0	Poor results, future exploration unlikely.
x 1.0 -1.3	Explorational potential has been maintained but not enhanced from regional potential. Additional geology, geochemical and /or geophysical work to investigate target warranted.
x 1.3 -1.5	Exploration potential has been slightly enhanced, with some findings of a positive nature.
x 1.3 – 1.5	Exploration results (geological mapping, geochemistry and geophysics) have enhanced prospectivity. Direct evidence of an interesting target or targets.
x 1.5 - 2.0	Lease contains a defined drill target or targets, based on strong geological, geophysical and/or geochemical evidence/models. Scout drilling with interesting intersections of mineralisation.
x 2.0 – 2.5	Mineralisation has been intersected by detailed drilling of defined targets. Follow-up work likely to define a maiden resource.
x 2.5 – 3.0	Initial mineral resource estimated. Further exploration expected to increase the size and quality of known resource.
x 3.0 – 4.0	Indicated mineral resource estimated. May form basis for scoping or prefeasibility study. Further exploration very likely to increase the size and quality of known resource.
x 4.0 – 5.0	Have already found a substantial resource at higher levels of confidence (that is likely to lead to a mine). May be ready to undergo definitive feasibility study.
>5.0	Exceptional discovery (size & grade) for low exploration expenditure.

By estimating a possible Net Present Value (NPV) by means of Cost-based Approach using the Multiples of Exploration Expenses (MEE) and Prospectivity Enhancement Multiplier (PEM) and assigning these to the possible positive and negative outcome of each decision, an Expected Monetary Value (EMV) can be calculated.

This EMV suggests the amount that can be made based on the expected cost, NPV and probability of success and can form the platform for the choices made by the project management team on whether to proceed with a project or whether to abandon the project, for example:

Figure 44 **Scenario "a"** – The initial target generation program cost the company theoretically US$100,000. The next decision is whether to proceed with a mapping program which has an 80% chance to produce positive results and which is estimated to cost US$1.5M. This produced an Expected Monetary Value (EMV) of US$0.006M with the company electing not to proceed with the mapping but rather with a geophysical program with a EMV of US$-0.6M. The geophysical program unfortunately delivered negative results based on an estimated 50% chance to produce positive. This decision led to a final NPV of 0.31M whilst producing a negative cashflow of US$-3.1M.

Figure 44 **Scenario "b"** – In this scenario the company elected to proceed with the mapping program with an EMV of US$0.62M. Although the mapping program produced negative results, the company elected to skip the geophysical phase and proceed to the initial drilling and metallurgical study phase. The EMV of this decision was estimated at US$-2.55M. This suggests that based on the previous decision and outcome, and skipping the geophysical program, the probability of the company losing cash is relatively high.

Figure 44 **Scenario "c"** – The decision being made at this stage of a project is based on the positive outcome of both the mapping and geophysical programs. Based on these outcomes and the probability of producing positive results, the EMV of the decision to proceed to the initial drilling and metallurgical test is estimated at US$22.51M. This suggests that the chance to increase the project value by implementing the drilling and metallurgical program is relatively high a should be executed.

Understanding the geological and economic factors associated with graphite and the relationship between the commodity and the everchanging global market, can help to identify exploration projects or investment opportunities which hold a possible advantage in a highly competitive market. Developing a graphite exploration program into a mine requires the exploration and management team to identify and target a possible marketable commodity that is both realistic and flexible with the market trends. This requires a keen understanding of graphite's characteristics and the marketable future it has, especially with the everchanging technology industry. By understanding the commodity and identifying a product, the exploration team can start developing targetable areas based on graphite's geological features. The exploration project development can then be guided by goal focussed, result orientated mileposts by means of project management. This will aid in maximising productivity whilst minimizing possible budget mismanagement.

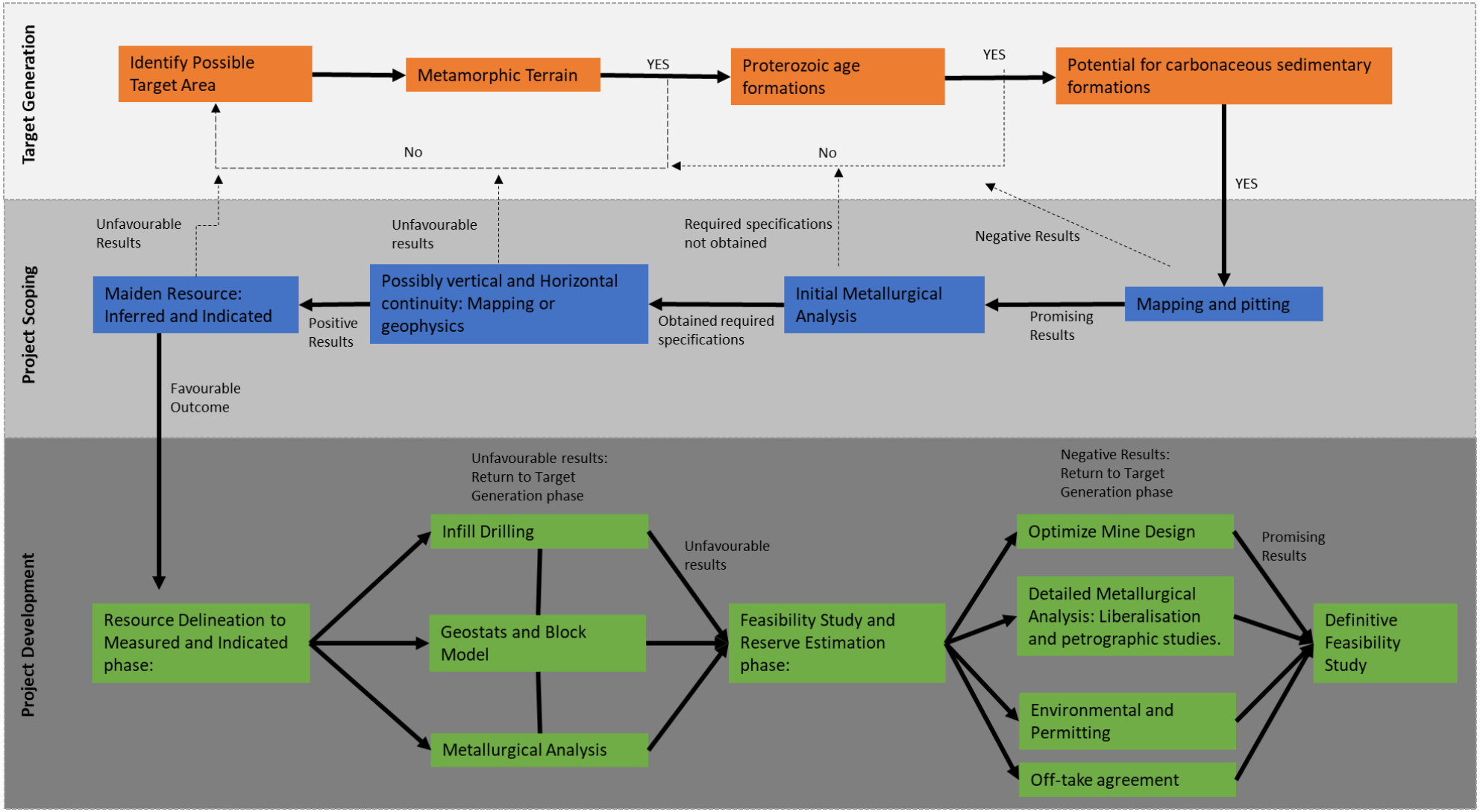

Figure 43 – Graphite Project Development framework. Development of a project from the initial project targeting, project scoping, to final definitive feasibility study.

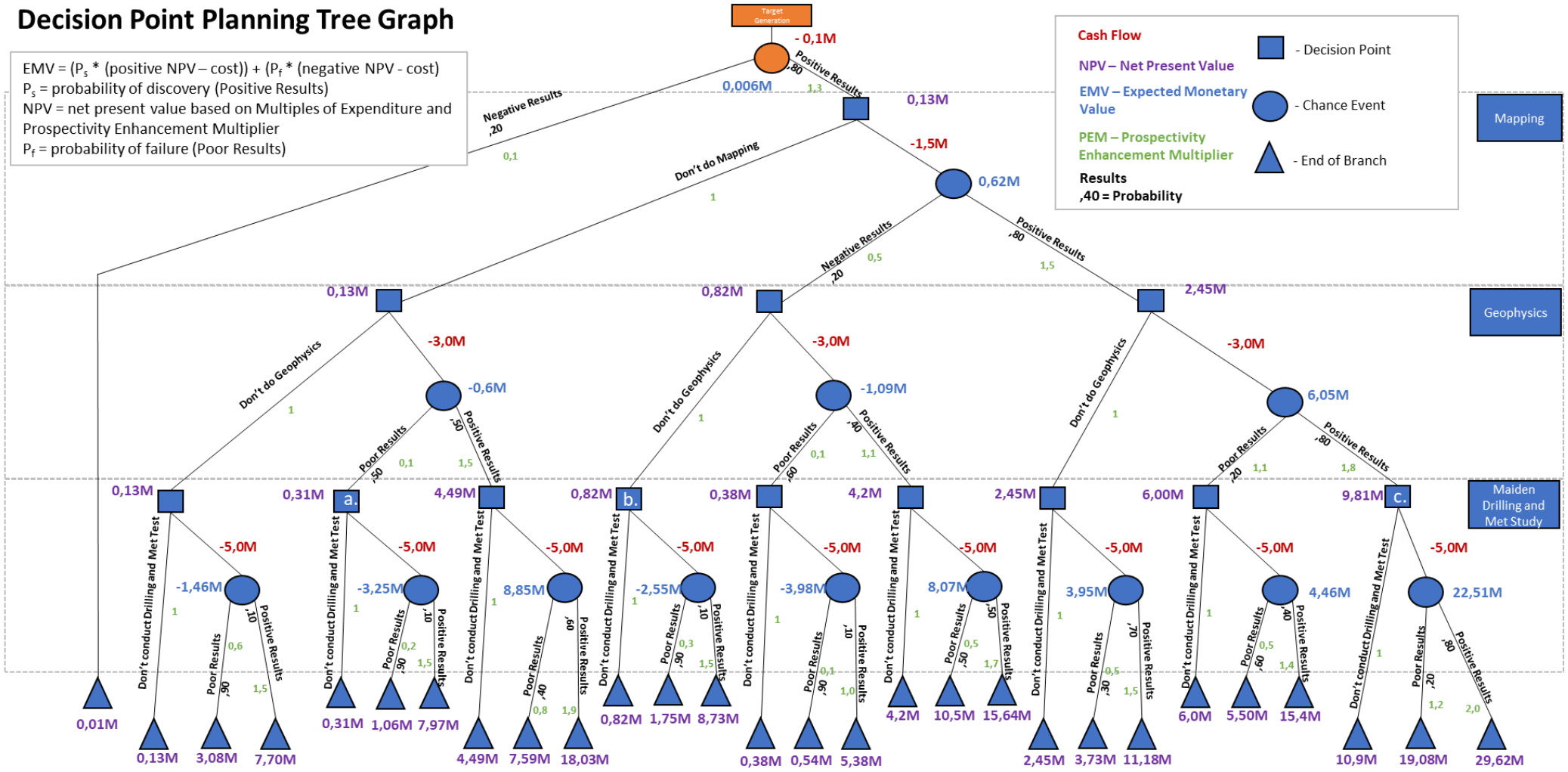

Figure 44 – Example of a decision planning tree based on the decision and possible outcome related to the Project Scoping Phase (Figure 43). Net Present Value (NPV) calculated based on the Cost Approach using the Multiples of Expenditure and Prospectivity Enhancement Multipliers.

7 DISCUSSION

Successfully developing any exploration project is dependent on a number of pillars, each signifying a different principle that must be addressed in order for the exploration project to develop into a producing mine. These pillars include 1) the geology and associated mineralisation environment, 2) understanding the market trends and predicting the future demand, 3) delineating mineral resource by determining the RPEEE, 4) comparing the exploration project with peer deposits in order to determine a competitiveness factor and 5) developing the project based on a goal orientated, results driven plan.

The formation of graphite requires a complex sequence of geological and biological components to merge in the perfect conditions which promote the preservation of carbonaceous sediments, metamorphism of carbon to graphite and the erosion of the rock formation to present day surface. Identifying these potential graphite mineralised environments is thus possible by identifying geological areas which had a high sedimentation rate and were deposited during a period in the earth's history that was lush with biological activity. Adequate time is also needed for these sedimentary deposits to undergo diagenesis followed by high-grade pressure and temperature metamorphism which promoted carbonization and eventually graphitization. Combining these factors suggests that the perfect period for the deposition of carbonaceous sediments occurred during the formation of Gondwana. This period involved a high sedimentation rates within the Phanerozoic bio-diversity boom (Barnosky *et al.*, 2011), and orogenic events that could produce high grade metamorphic conditions. Figure 45 below illustrates a simplified global map with orogenic belts which adhere to the criteria listed above.

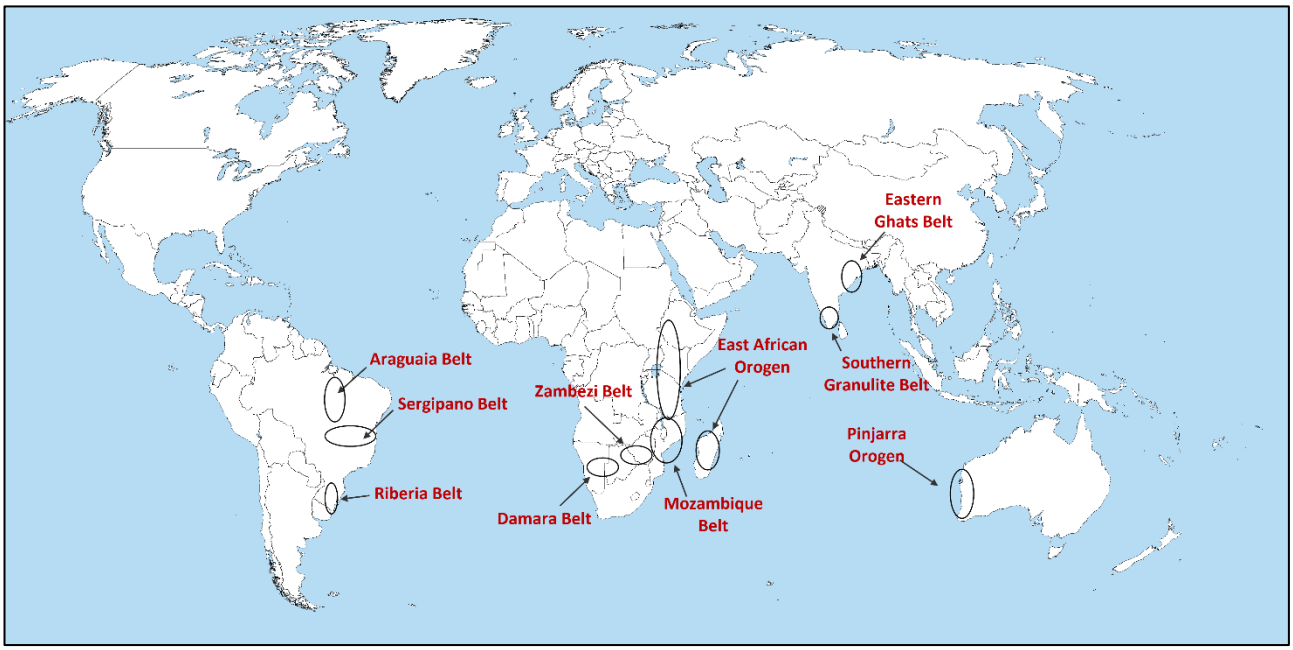

Figure 45 - Global map indicating highly prospective belts with metamorphic sediments related to the phanerozoic eon. Modified from Merdith et al.(2017).

The economic component of graphite exploration consists of both the market trends - referring to the supply and demand, and whether the minerals can be extracted economically - and the finances associated with a producing mine. The ability of an exploration project to develop from initial exploration to a mining project is dependent on how these factors affect the project and how they can be managed.

The refractory industry dominated the global graphite demand consuming approximately 54% of the graphite supply in 2014 (Shaw, 2015). The health of this industry is proportional to the global economic development with the GDP serving as a good measuring stick. Economists predict that the global GDP is likely to increase by 5% year on year (Hykawy and Chudnovsky, 2014). This prediction suggests that the global graphite demand can also follow the same trend. The increase of the refractory industry is not however the primary cause of the graphite frenzy observed in the last decade which can rather be attributed to the development of the battery industry. The need to develop an effective energy storage battery propelled the future demand for numerous critical and industrial metals and minerals, graphite being one of the primary sought after commodities which some economists predicting will increase in demand by up to 520% if specific parameters are met, such as for instance a 100% EV market (Jeff Desjardins, 2017). If we create two scenarios, one where the 100% EV market is reached within 20 years, and the second within 40 years, then approximately 6.2Mt of graphite will be needed by either 2037 or 2057. This demand increase opened the market for new graphite sources. Four identified projects, all currently at an advanced stage of development, can collectively supply the graphite market with approximately 432,900 tons of graphite concentrate per year by the end of 2018. Based on the two scenarios mentioned and an exponential growth in graphite demand, what these four companies can supply will sufficiently quench the global graphite demand until 2022 (20-year scenario) or 2027 (40-year scenario). Although these scenarios are still hypothetical, understanding the market requirements and behaviour can aid in developing an exploration project. By studying the graphite market and identifying possible products such as an 85 – 95 % GC product used in the refractory industry compared to a 95 – 99% product which targets the battery industry, can aid in understanding the metallurgical requirements needed and can greatly affect the management of the exploration project.

The geological criteria mentioned above along with the market trends were used to identify and target a possible graphite mineralisation body with the aim of delineating a mineralisation resource that can supply the market with a 95 – 99% GC product, thus targeting the Li-ion battery industry. This resulted in the initiation of the scoping study for the Orom Graphite project.

The Orom Graphite project followed the project development framework (Figure 43) with the initial target generation study consisting of historical data collection. This historical data confirmed the presence of graphite mineralisation within gneiss lithologies (Morton, 1969). The regional geological study confirmed

that the Orom Graphite project is located within the East African orogenic belt. This orogen is one of many suture zones formed from the amalgamation of numerous cratons and shields into a supercontinent, known as Gondwana, during the late-Proterozoic to early-Phanerozoic era. The formation of this orogeny started with the convergence of the Sao Francisco Congo craton and the SLAMIN terrain (Modern-day Eritrea, Somalia, Ethiopia, Seychelles, Madagascar, India and Sri Lankan) resulting in the closing of the Mozambique Ocean dated approximately 750 – 820Ma (Meert, 2003). According to Meert (2003) convergence occurred along the equator with plate tectonics migrating towards lower latitudes during the final collisional event. This mid to low latitude position possibly provided the favourable climate needed for a thriving biological community.

The collisional event provided amphibolite to granulite metamorphic conditions required for the carbonization and graphitization of the organic carbon material. The lithological units observed at the Orom Graphite project consisted of both amphibolite and granulite rock assemblages (Figure 21 A-C) with augen gneisses identified in numerous places (Figure 21 D). These rock formations wrap around a large granitic intrusion referred to as the Orom mountain which towers an estimated 1 000 m over the landscape. The relatively undeformed (post-orogenic) nature of the intrusive Orom Mountain and associated granites scattered around the area most likely provided a local thermal increase during regional retrograde metamorphism. This is a visual observation and can be verified by conducting chemical analysis and constructing P-T-t paths from the chemical zonation patterns associated with garnet growth. The regional metamorphic conditions provided the required environment for the formation of crystalline flake graphite deposits, whereas the temperature influx associated with the post-orogenic granitic intrusion provided the required conditions for the formation of high grade vein type graphite deposits

The exploration results obtained from the mapping, pitting, trenching and geophysical programs delineated vertical and lateral continuity of the graphitic gneiss member. Based on these results, a total of 4 primary anomalies were identified, with numerous smaller anomalies scattered within the project area. Two of the primary anomalies were investigated and exploration range analysis indicated a possible tonnage and grade range as listed below:

- 0 – 20 m depth:
    - Lower tonnage range - **137.3 million tons (76.5 Mt + 60.8 Mt)**
    - Upper tonnage range - **228.8 million tonnes (127.5 Mt + 101.3 Mt)**
    - Grade range of - **5.47 to 6.69 % GC**
- 0 – 40 m depth:
    - Lower tonnage range – **319.5 million tons (178.5 Mt + 141.0 Mt)**
    - Upper tonnage range – **532.5 million tonnes (297.5 Mt + 235.0 Mt)**

    - Grade range of - **6.27 to 7.67% GC**
- 0 – 60 m depth:
    - Lower tonnage range – **503.3 million tons (281.3 Mt + 222.0 Mt)**
    - Upper tonnage range – **838.8 million tonnes (468.8 Mt + 370.0 Mt)**
    - Grade range of - **6.54 to 8.00% GC**

One of the factors which can have a major influence on every exploration project is the competitiveness of the project in question. The habit of evaluating and valuating exploration projects against peer deposits does not form part of the geological delineating section but is rather used as a bar for economic competitiveness and will, depending on the exploration company's strategy, be used as a marketing platform. By comparing the Orom graphite deposit to other global graphite exploration projects currently under different exploration stages will determine its competitiveness and to some extent, the probability of the project's success.

The projects mentioned and investigated in Section 3.3 and Chapter 5 ranged from pre-feasibility to bankable feasibility stages, with some reporting indicated to measured resources as well as probable to prove reserves. The Orom graphite deposit is however still in the scoping study to preliminary economic assessment stage. However, this does not mean that the Orom graphite project cannot be compared to these more advanced graphite projects; it should be evaluated in order to determine if the Orom project will be competitive if proved feasible. The criteria for this comparison included tonnage, grad, and metallurgical recovery.

The tonnage and grade of a project are two of the factors determining the range of possible mine production sizes and LOM which can have an effect on both investors and the graphite market. This can increase the competitiveness of a project, especially within the graphite market which is generally driven by private capital and supplier-buyer negotiations and contracts. Figure 46 and Figure 47 illustrate the grade, tonnage and graphite flake size comparison between the known graphite projects and the Orom Graphite project. This suggests that if a mineralisation resource can be defined during the MRE phase then the Orom Graphite project has the potential to be the third largest known deposit with above average grades. The possible large graphite resource suggests that the future sustainability of the project can extend well into the future. However, the grade suggests that the cost of extracting graphite per ton will not be one of the competitive factors distinguishing the Orom Graphite project from its peers.

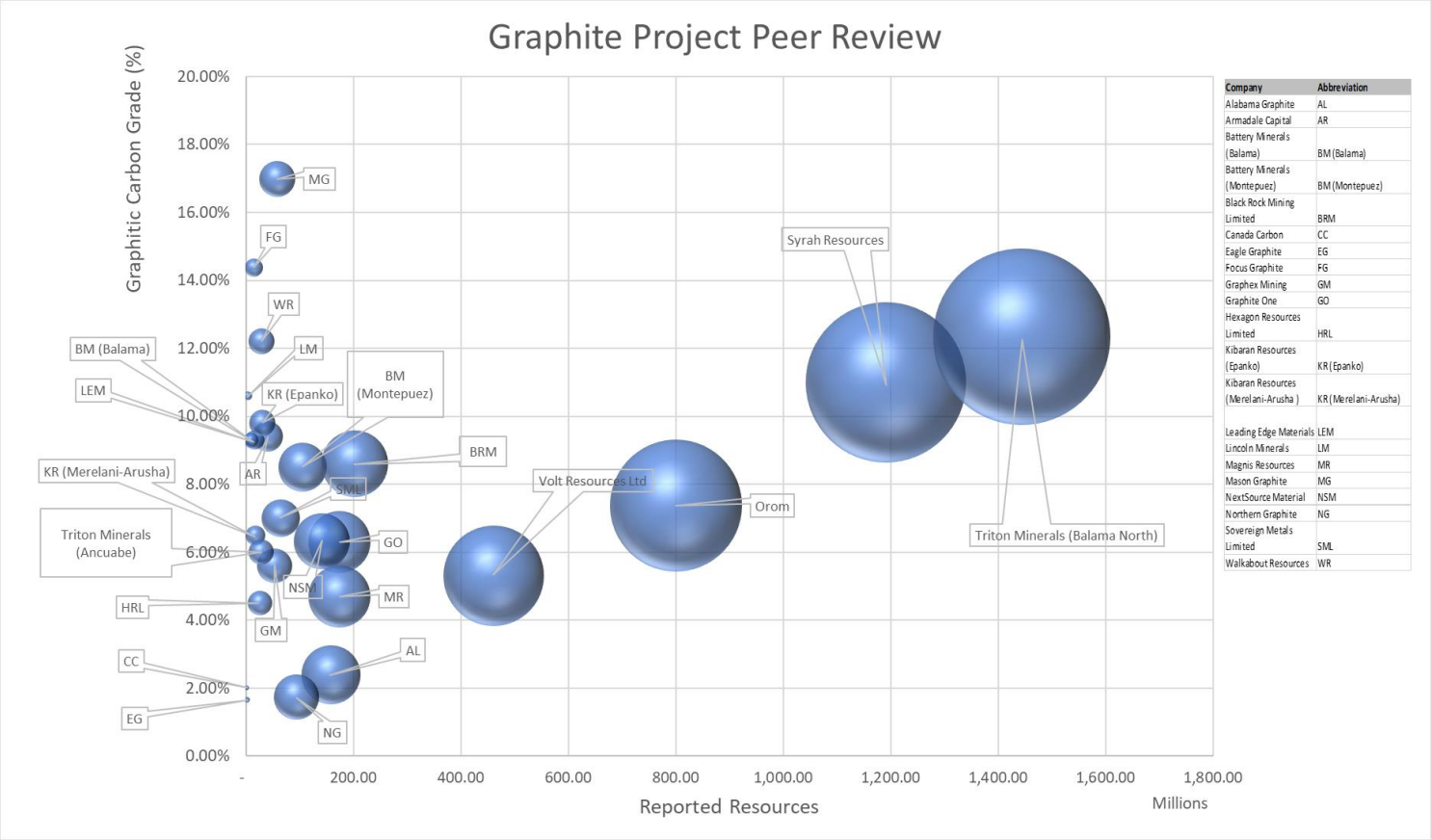

Figure 46 – Graphite project peer comparison based on reported resources vs graphitic carbon grades.

The competitiveness of each of these projects is not only a function of the tonnage and grade but also a function of the complete costs involved in extracting graphite concentrate. These costs can influence the financial models of each project and are divided into capital and operational costs, revenue, as well as taxes and royalties.

Capital cost is divided into the initial and sustaining capital cost. Initial capital cost is required to develop the project into a productive mine, whereas sustaining capital cost is required to keep the operation productive. The capital cost will vary depending on the proposed production size and infrastructure required to develop the project. Thus, projects located in poorly developed counties with little infrastructure will need to invest more capital than projects being developed in countries with well-maintained infrastructure. The Operational cost is the cost associated with the mining and processing of a quantity of ore product. Most of the operational cost reported for a number of graphite projects fluctuated between US$300 to US$500 per ton of graphite concentrate. This amount will vary depending on the mining method proposed as the cost associated with hard-rock mining is higher than the cost of a free-dig operation. The logistical cost of transporting the graphite concentrate to the agreed destination can vary considerably with cost being proportional to the distance to port.

The revenue generated by each project is dependent on the graphite flake size and graphitic carbon concentrations. Each project contains a specific flake size distribution, with larger flakes providing more revenue to the collective/basket price.

Mining Tax can vary considerably from project to project and is specified on the mining legislation of the county of operations. Countries with a mining friendly approach have a lower tax rate or can implement a tax-cut during the first years of operations. Although the tax rates are usually fixed, politically unstable countries can quickly change these rates, which adds significant risk to any project.

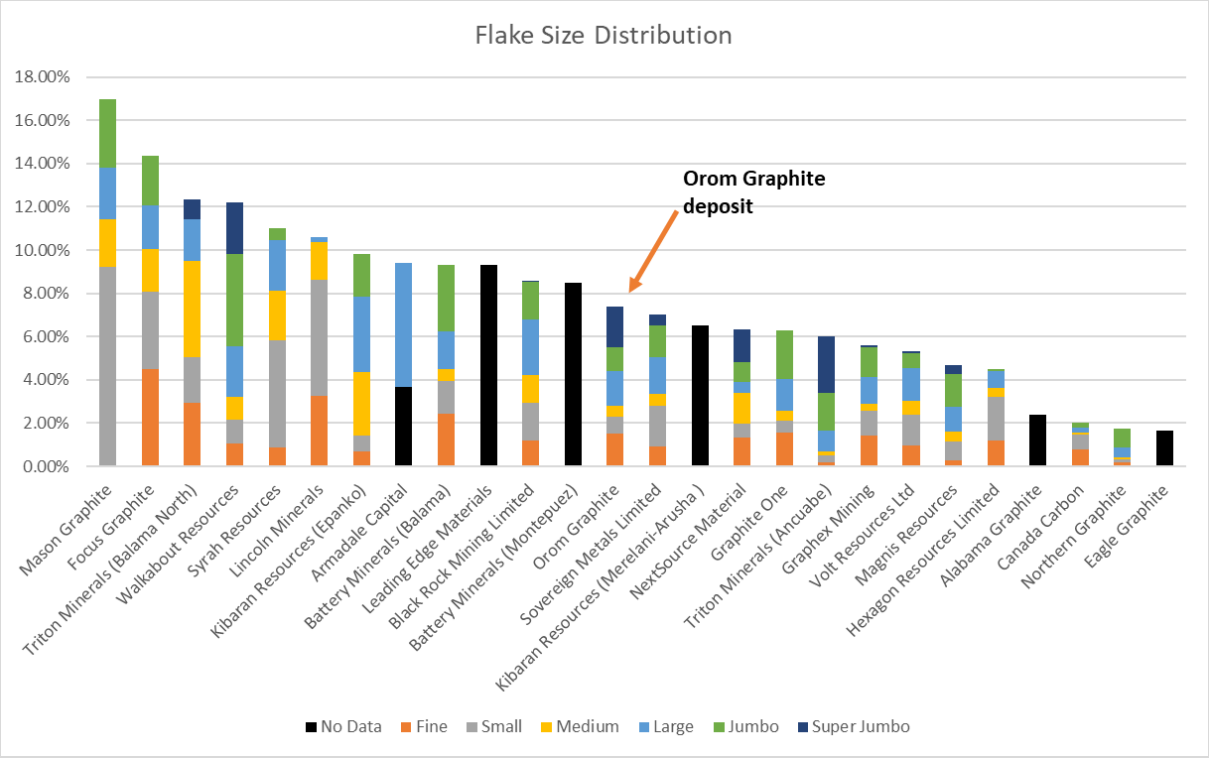

Figure 47 - Graphitic carbon grade distribution of numerous developed projects. The graphitic carbon grades of the Orom project plots at the lower half portion of the known graphite projects.

Although the current geological data indicates that the Orom Graphite project has the potential to become a competitive global graphite supplier, metallurgical studies could not produce a marketable product for the battery industry. The metallurgical studies included samples from both the weathered and unweathered material with the best results producing an 86.1% GC grade product at an 89% recovery. Additional processing circuits were proposed by the metallurgist in an attempt to increase the product grade to 95% GC. This will however require additional funds as a bulk sample is needed.

The unfavourable metallurgical results prohibit the project from progressing into the MRE phase of the project development framework. Therefore, a decision must be made on whether to conduct the second

metallurgical study or to abandon the project completely. Both these decisions bear large risks which needs to be addressed when making a choice. This can be accomplished by means of implementing a decision tree which calculates the Expected Monetary Value (EMV) of each decision based on the chance of success or failure. Figure 48 below illustrates the decisions implemented within the scoping project phase of the Orom Graphite project. The primary function of the decision tree is to quantify the risk associated with proceeding with the second metallurgical tests. Prior to the first metallurgical tests, the project NPV amounted to a theoretical US$12.47M. The EMV calculated for conducting the first metallurgical study amounted to a possible US$17.66M based on a 60% chance of success. The results of the metallurgical tests did not produce the desired outcome and consequently decreased the NPV of US$6.49M. The metallurgical analysis method has since been questioned by the management team and the possibility of conducting a second metallurgical test on a representative bulk sample has been proposed. Based on the previous results, the chance of obtaining a favourable result has been estimated at 35%, increasing the NPV from US$6.46M to US$14.8M. There is however a 65% chance to decreasing the NPV based on an unfavourable result from US$6.49M to US$3.6M. The EMV calculated for this decision amounted to US$6.73M, with the total costs adding up to US$5.7M if the second metallurgical test is conducted. This leaves the management team with two options: Option One: do not conduct the second metallurgical study and be assured of a NPV of US$6.49M; Option Two: conduct the second metallurgical study with slight statistical increase in value (EMV of US$6.73M) with a 35% chance of decreasing the NPV to US$3.60M.

The Orom Graphite project is currently within the scoping study stage and will require additional years for a mineral resource and eventually a reserve to be defined. This makes it unlikely that the project will advance to a mining stage within the next 4 to 10 years as numerous peer projects can already produce graphite concentrate within the next year. At this stage, the level of project development also makes it impossible to quantify the capital cost required to initiate the infrastructure and mining development. The location of the project is not favourable as it is within a poorly developed area of northern Uganda with the closest sea-port located some 1 500km in Malindi – Kenya, and the container port located some 1 400km in Mombasa, Kenya. This will increase the logistical cost of the project dramatically compared to possible similar sized projects in Tanzania and Mozambique.

.

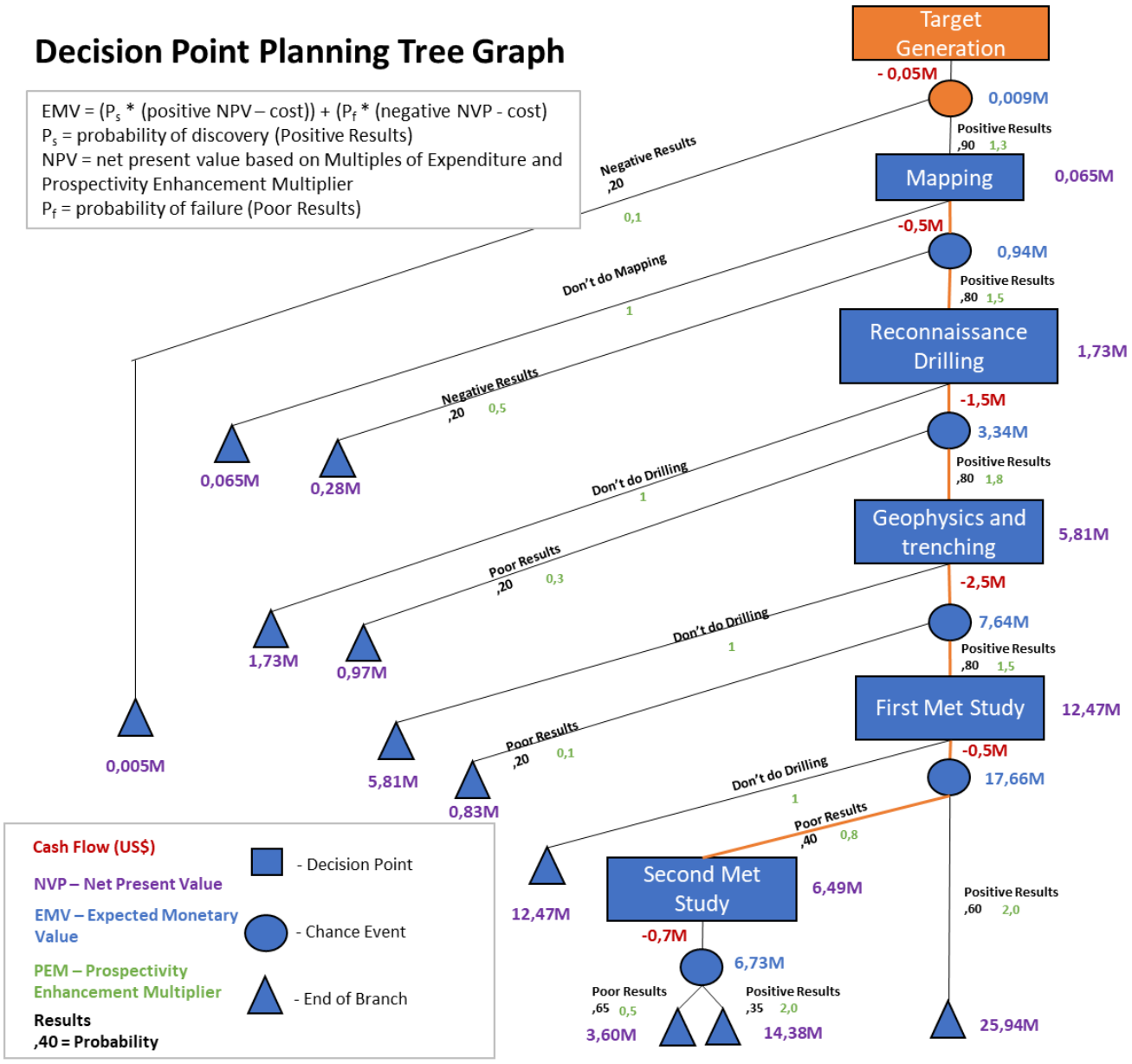

Figure 48 – Orom Graphite project decision tree. NPV calculated using the cost-based approach with prospectivity enhancement multipliers. The cost of each program is a speculative value for illustrative purposes.

8 CONCLUSIONS

The success in developing an exploration project is not measured in whether a project develops from the target generation stage through to an economical producing mine but is rather measured in whether the conclusion reached is obtained in the most cost-effective manner whilst minimizing risk and capitalizing on the results. Initiating and developing an exploration project requires key components to be understood and implemented. These components include the geology and mineralisation morphology, the specific commodity's role in the market and the market's trends, and an effective and productive project management based on risk and results.

The Orom Graphite project followed this basic exploration project development framework. The initial target generation study phase focussed on identifying whether graphite mineralisation can occur within the project area. The key geological components required included a terrane with a paleo-sedimentary origin dated not older than the early Phanerozoic era and with an amphibolite to granulite grade metamorphic overprint.

The scoping phase focussed on valuating the project based on the market demands and establishing whether the project can deliver the targeted market factors which will aid in developing the Reasonable Prospects for Eventual Economic Extraction (RPEEE) required to declare a mineral resource and eventually an ore reserve. One of the components determining if the Orom Graphite project comply to the RPEEE, includes proving that a marketable product can be produced from the mineralised material. The two marketable products were identified and include an 85 to 95% GC product used in the refractory industry, as well as a 95 to 99% GC product used in the battery industry. The market studies identified that the battery industry is currently experiencing abnormal growth and will eventually dwarf associated graphite industries. The metallurgical beneficiation tests conducted on the Orom Graphite samples could not produce the desired marketable product. However, the unfavourable results do not mean that the project is dead and further metallurgical studies were proposed. The decision to abandon the project at the current level or to continue with the proposed metallurgical studies include risks of overspending on a project that might not produce the desired market product. By identifying the risks and quantifying the possibility of success (35%) or failure (65%), the decision can be made based on the present Net Present Value (NPV = 6.49M USD) and Expected Monetary Value (EMV = 6.73M USD). This suggests that the risks outweigh the rewards and that the chance of producing a final NPV of 3.6M USD outweighs the chance of a successful result, that is the production a possible NPV of 13.38M USD (Cost at this point will be 5.75M USD) (Figure 48).

Peer graphite project comparisons confirmed that the project has a competitive nature with a large resource potential and above average grades. However, the economic factors will play a vital role in determining whether the financial aspects of the project are competitive as the project is located in a poorly developed area of landlocked Uganda. This will greatly affect the initial capital cost required to construct basic infrastructure, as well as increase the operational cost due the increased logistical cost. Based on these conclusions, the Orom Graphite project contains a potential to quantify a large graphite resource at average grade. The project location is favourable with respect to graphite mineralised geology but unfavourable with respect to economic factors. A marketable product could not be produced with the current metallurgical tests and requires additional studies. The consequences of the additional metallurgical study producing unfavourable results will devaluate the project's NPV to 3.6M USD, effectively overspending with 2.15M USD (NPV-Cost). The project is currently valuated at a NPV of 6.49M USD with the total expenditure amounting to 1.05M USD. The chance that the Orom Graphite project will produce graphite within the next 10 years is highly unlikely.

REFERENCES

'About Spherical Graphite' (no date). Available at: http://northerngraphite.com/wp-content/uploads/2016/02/SPG-Summary-2.pdf.

Ansari, A. H. and Alamdar, K. (2009) 'Reduction to the Pole of Magnetic Anomalies Using Analytic Signal', *World Applied Sciences Journal*, 7(4), pp. 405–409. Available at: https://pdfs.semanticscholar.org/0c68/ba1ed775ac6c2007504e41f5db3e68f3b5ed.pdf (Accessed: 4 February 2018).

Arthur, M. and Sageman, B. (1994) 'Marine Black Shales: Depositional Mechanisms and Enviroments of Ancient Deposits', *Annual Review of Earth and Planetary Sciences*, 22, pp. 499–551.

Baldock, J. W. *et al.* (1969) *Explanation of the geology of sheet 25 (Labwor Hills)*. Entebbe.

Baranov, V. and Naudy, H. (1964) 'NUMERICAL CALCULATION OF THE FORMULA OF REDUCTION TO THE MAGNETIC POLE', *GEOPHYSICS*. Society of Exploration Geophysicists, 29(1), pp. 67–79. doi: 10.1190/1.1439334.

Barnosky, A. D. *et al.* (2011) 'Has the Earth's sixth mass extinction already arrived?', *Nature*. Nature Publishing Group, 471(7336), pp. 51–57. doi: 10.1038/nature09678.

Basson, E. (2017) *World Steel In Figures 2017*. Available at: https://www.worldsteel.org/en/dam/jcr:0474d208-9108-4927-ace8-4ac5445c5df8/World+Steel+in+Figures+2017.pdf (Accessed: 2 August 2017).

Berry, L. and Ruxton, B. . (1959) 'Notes on weathering zones ad soils on granitic rocks in two Tropical Regions', *Journal of Soil Science*. Blackwell Publishing Ltd, 10(1), pp. 54–63. doi: 10.1111/j.1365-2389.1959.tb00665.x.

Bliss, J. D. and Sutphin, D, M. (1992) *Grade and Tonnage Model of Amorphous Graphite: Model 18k*, *U.S. Geological Survey*.

Bundy, F. P. *et al.* (1996) 'The Pressure-Temperature phase and transformation diagram for carbon: Updated through 1994.', *Carbon*, 34(2), pp. 141–153. Available at: https://ac.els-cdn.com/0008622396001704/1-s2.0-0008622396001704-main.pdf?_tid=874657f7-2772-42d6-ac89-55c41b8c1dcf&acdnat=1520763308_ddcf1551e4dd5116af6a7f350c1f601c (Accessed: 11 March 2018).

Buseck, P. R. and Beyssac, O. (2014) 'From organic matter to graphite: Graphitization', *Elements*, 10(6), pp. 421–426.

Carley, S. *et al.* (2011) 'Energy-based economic development', *Renewable and Sustainable Energy Reviews*. Pergamon, 15(1), pp. 282–295. doi: 10.1016/J.RSER.2010.08.006.

Cawley, A. (1962) *Napak, Sheet 35, N.A. 36, KIII*. Entebbe.

Climate Rom: Temperature, Climograph, Climate table for Rom - Climate-Data.org (no date). Available at: https://en.climate-data.org/location/786502/ (Accessed: 27 December 2017).

Collins, A. S. and Pisarevsky, S. A. (2005) 'Amalgamating eastern Gondwana : The evolution of the Circum-Indian Orogens', 71, pp. 229–270. doi: 10.1016/j.earscirev.2005.02.004.

Collins, A. S., Razakamanana, T. and Windley, B. F. (2000) 'Neoproterozoic extensional detachment in central Madagascar: Implications for the collapse of the Eastern Africa Orogen', *Geol. Mag.*, 137, pp. 39–51.

Dentith, M. and Mudge, S. . (2014) *Geophysics for the mineral exploraiton geoscientist*. Cambridge university Press.

Evans, R. B. (1965) *Notes on a brief visit to Rom N.E. Acholi*.

Ferry, J. and Baumgartner, L. (1987) 'Thermodynamic models of molecular fluids at the elevated pressures and temperatures of crustal metamorphism', *Reviews in Mineralogy and Geochemistry*, 17(1), pp. 323–365. Available at: http://0-rimg.geoscienceworld.org.wam.seals.ac.za/content/17/1/323.short (Accessed: 11 August 2017).

Grantham, G. H., Maboko, M. and Eglington, B. M. (2003) 'A review of the evolution of the Mozambique Belt and implications for the amalgamation and dispersal of Rodinia and Gondwana', *Geological Society, London, Special Publication*, 206, pp. 401–425. doi: 10.1144/GSL.SP.2003.206.01.19.

Grew, E, S. (1974) 'Carbonaceous Material in some metamorphic rocks of New England and Other Areas', *The Journal of Geology*, 82(1), pp. 50–73.

Grothoff, J. M. (2015) 'Battery Storage for Renewables : Market Status and Technology Outlook', *Irena - International Renewable Energy Agency*, (January), p. 60.

Guiraud, R. *et al.* (2005) 'Phanerozoic geological evolution of Northern and Central Africa: An overview', *Journal of African Earth Sciences*, 43(1–3), pp. 83–143.

Hahn-Weinheimer, P. and Hirner, A. (1981) 'Isotopic evidence for the origin of graphite', *Geochemical Journal*, 15(1), pp. 9–15.

Hawkes, H. E. and Webb, J. S. (1962) *Geochemistry in mineral exploration.* New York.

Hykawy, J. and Chudnovsky, T. (2014) *INDUSTRY REPORT Graphite INITIATING SECTOR COVERAGE A Stress Test on Future Graphite Pricing*.

Jeff Desjardins (2017) *The Massive Impact of EV's on Commodities in One Chart*, *Visual Capitalist*. Available at: http://www.visualcapitalist.com/massive-impact-evs-commodities/ (Accessed: 7 October 2017).

Kramer-miller, B. (2015) 'Investing In Graphite Part 1 : Supply / Demand Overview'.

Lawrence, G. M. (1994) *Due Diligence in Business Transactions*. Volume 2. Law Journal Seminars-Press. Available at: https://books.google.com.na/books/about/Due_Diligence_in_Business_Transactions.html?id=1DW0nQAACAAJ&redir_esc=y (Accessed: 4 February 2018).

Lilford, R. C. . and Minnitt, E. V. (2002) 'A comparative study of valuation methodologies for mineral developments.', *Journal of the Southern African Institute of Mining and Metallurgy*. South African Institute of Mining and Metallurgy, 102(7), pp. 369–384. Available at: https://0-journals.co.za.wam.seals.ac.za/content/saimm/105/1/AJA0038223X_2989 (Accessed: 4 February 2018).

MacGregor, J. P. (1962) *Explanation of the Geology of Sheet 10 (Kaobong)*. Entebbe.

Meert, J. G. (2003) *A synopsis of events related to the assembly of the eastern Gondwana*, *Tectonophysics*.

Meert, J. G. and Lieberman, B. S. (2008) 'The Neoproterozoic assembly of Gondwana and its relationship to the Ediacaran – Cambrian radiation', *Gondwana Research*, 14, pp. 5–21. doi: 10.1016/j.gr.2007.06.007.

Merdith, A. S. *et al.* (2017) 'A full-plate global reconstruction of the Neoproterozoic', *Gondwana Research*. Elsevier, 50, pp. 84–134. doi: 10.1016/J.GR.2017.04.001.

Moore, K. (2016) *Have All The Big Deposits Been Discovered?*, *Resource World Magazine*. Available at: http://resourceworld.com/index.php/gold-big-deposits-discovered/ (Accessed: 14 March 2018).

Morton, W. H. (1969) *Mineralisation in the Rom Mountain Graphitic Gneisses*. Entebbe.

Nash, W. A. (1964) *Preliminary report - northwest Karamoja sheet 9/III, 17/I and 17/II. Geological Survey unpublished report WAn/1: Canadian Technical Assistance project report no.5*.

Nash, W. A. (1966) *Report on the Rom Mountain zinc anomaly. Unpublished report on file XEP/Rom.*

Nichols, G. (2009) *Sedimentology and Stratigraphy*. Second Edi, *Journal of Chemical Information and Modeling*. Second Edi. Wiley-Blackwell.

Oldon, D. W. (2017) *USGS Minerals information*, *U.S. Geological Survey, Mineral Commodity Summaries.* Available at: http://minerals.usgs.gov/ (Accessed: 2 August 2017).

Olson, D. W. (no date) *USGS Minerals Information: Graphite*. Available at: https://minerals.usgs.gov/minerals/pubs/commodity/graphite/ (Accessed: 20 December 2017).

Pasteris, J. D. (1999) 'Causes of the uniformly high crystallinity of graphite in large epigenetic deposits', *Journal of Metamorphic Geology*, 17, pp. 779–787.

Punchuk, K. (2017) *Physical Geology*. Second Ada. Simple Book Production. Available at: https://physicalgeology.pressbooks.com/.

Rapp, M. *et al.* (2016) 'Spheroidisation of Graphite as Anode Material for Li-Ion Batteries Spheroidisation Process and Material Texture and Morphology', in *International Meeting on Lithium Batteries*. Chicago. Available at: https://ecs.confex.com/ecs/imlb2016/webprogram/Paper76389.html.

Scogings, A. (2016) 'Global graphite market set for change'. Australie's Paydirt, pp. 42–43.

Scogings, A. and Chesters, J. (2014) 'Graphite The Six Steps to Striking Success.pdf'. Industrial Minerals.

Scogings, A., Chesters, J. and Shaw, B. (2015) *Rank and file : Assessing graphite projects on credentials*, *Graphite*. Available at: http://www.csaglobal.com/wp-content/uploads/2015/07/Pg-50-55-Graphite-success-08_15_proof_5.pdf.

Shaw, S. (2015) *Roskill's Natural & Synthetic Graphite: Global Industry Markets and Outlook.* 9th Editio, *Roskill Information Services*. 9th Editio. Available at: https://roskill.com/wp/wp-content/uploads/2015/10/Suzanne_Shaw_Roskill_UNITECR.pdf.

Shiraishi, K. *et al.* (1994) 'Cambrian Orogenic Belt in Eastern Antarctica and Sri Lanka: Implications for Gondwana Assembly', *The Journal of Geology*, 102(1), pp. 47–65.

Simandl, G. J. and Kenan, W. M. (1998a) 'Crystalline Flake Graphite', *Geological Fieldwork 1997*, pp. 1–4.

Simandl, G. J. and Kenan, W. M. (1998b) 'Microcrystalline Graphite', *Geological Fieldwork 1997*.

Simandl, G. J. and Kenan, W. M. (1998c) 'Vein graphite in metamorphic terrains', *Geological Fieldwork 1997*.

Simandl, G. J., Paradis, S. and Akam, C. (2015) *Graphite deposit types , their origin , and economic significance*, *British Columbia Geological Survey*.

Sloss, L. L. (1947) 'Environments of Limestone Deposition', D(3), pp. 109–113. doi: 10.1306/D42692C4-2B26-11D7-8648000102C1865D.

Stern, D. and Cleveland, C. J. (2004) *Energy and Economic Growth*, *Rensselaer Working Papers in Economics*. Available at: http://www.rpi.edu/dept/economics/www/workingpapers/.

Struthers, R. (2017) *Battery production more than a Tesla nightmare*, *Treetwise Reports*. Available at: https://www.streetwisereports.com/article/2017/11/28/battery-production-more-than-a-tesla-nightmare.html.

Wallace, M. W. *et al.* (2017) 'Oxygenation history of the Neoproterozoic to early Phanerozoic and the rise of land plants', *Earth and Planetary Science Letters*. Elsevier, 466, pp. 12–19. doi: 10.1016/J.EPSL.2017.02.046.

Weis, P. L., Friedman, I. and Gleason, J. P. (1981) 'The origin of epigenetic graphite: evidence from isotopes', *Geochimica et Cosmochimica Acta*, 45(12), pp. 2325–2332.

Westerhof, A. B. *et al.* (2014) 'Geology and Geodynamic Development of Uganda with Explanation of the 1:1,000,000 - Scale Geological Map.', *Geological Survey of Finland*.

Williams, C. E. (1966) *Geology of Karamoja, scale 1:250 000*. Entebbe.

Wilson, J. T. (1966) 'Did the Atlantic close and the Re-open?', *Nature*, 211, pp. 676–681.

Windley, B. F. *et al.* (1994) 'Tectonic framework of the Precambrian of Madagascar and its Gondwana connections: a review and reappraisal.', *Geol. Rundsch*, 83, pp. 642–659.

Wopenka, B. and Pasteris, J. D. (1993) 'Structural characterization of kerogens to granulite-facies graphite: applicability of Raman microprobe spectroscopy', *American Mineralogist*, 78(5–6), pp. 533–557.

APPENDIX

List of companies

Company	Data Type	Title	Effective Date
Alabama Graphite	Corporate Presentation	Alabama Graphite CORP	Apr-17
Armadale Capital	Investors Presentation	Armadale Capital PLC	Jan-17
Battery Minerals	ASX Resource Announcement	Montepuez Graphite Project Mineral Resource and Ore Reserve Estimation	Feb-17
Black Rock Mining Limited	ASX Announcement	Black Rock Mining PFS Confirms High Margin, Low Capex Potential for Mahenge Graphite Mine	Apr-17
Canada Carbon	NI43 101 PEA Technical Report	Technical Report and Preliminary Economic Assessment for the Miller Graphite and Marble Property, Grenville Township, Quebec, Canada	Mar-16
Eagle Graphite	NI43 101 Technical Report	Technical Report on the Black Crystal Graphite Property	Nov-14
Focus Graphite	NI43 101 Feasibility Study Technical Report	NI43 101 Technical Report on the Lac Knife Graphite Feasibility Study, Quebec - Canada	Aug-14
Graphex Mining	Corporate Presentation	Arlington Pre-daba	Feb-17
Graphite One	NI43 101 Technical Report	2015 Indicated and Inferred mineral resource estimation at the Graphite Creek Property, Alaska, United States	Mar-15
Hexagon Resources Limited	ASX Announcement	Pre-feasibility study confirms viability of Hexagon's Mcintosh flake graphite project	May-17
Kibaran Resources	Corporate Presentation	Updated Bankable Feasibility Study	Jun-17
Leading Edge Materials	NI43 101 Technical Report	Technical Report for the Woxna Graphite Project, Central Sweden	May-15
Lincoln Minerals	Corporate Presentation	Kookaburra Gully Graphite Mine Development	Apr-17

Magnis Resources	Corporate Presentation	Nachu BFS and Corporate Update	Mar-16
Mason Graphite	NI43 101 PEA Technical Report	Technical Report on the Preliminary Economic assessment Lac Guaret Graphite Project	Jun-16
NextSource Material	NI43 101 Technical Report	Molo Feasibility Study	Jul-17
Northern Graphite	NI43 101 Technical Report	Feasibility Study, Bissett Creek Graphite Project, Ontario, Canada	Aug-12
Sovereign Metals Limited	ASX Announcement	Malingunde: The World's Largest Reported Saprolite-Hosted Graphite Resource	Apr-17
Syrah Resources	Investors Presentation	Equity Capital Raising Presentation	Sep-17
Triton Minerals	ASX Announcement	Ancuabe Graphite Resource Increase by 87% Maiden T16 Resource Maiden Indicated Resource	Apr-17
Volt Resources Ltd	Corporate Presentation	Emerging Natural graphite supplier to global market	May-17
Walkabout Resources	Corporate Presentation	Walkabout Resources, Lindi Jumbo Graphite Project	Jun-17